

# **Modeling of particle segregation in a rotating drum**

**Marleen M.H.D. Arntz**

**Thesis committee**

**Thesis supervisors**

Prof.dr.ir. R.M. Boom

Professor of Food Process Engineering, Wageningen University

Prof.dr. W.J. Briels

Professor of Computational Biophysics, University of Twente

**Thesis co-supervisors**

Dr.ir. W.K. den Otter

Assistant professor, University of Twente

Dr. H.H. Beftink

Assistant professor Bioprocess Engineering, Wageningen University

**Other members**

Prof.dr. E. van der Linden. (Wageningen University)

Prof.dr. S. Luding (University of Twente)

Prof.dr.ir. K. van der Voort Maarschalk (University of Groningen)

Dr.ir. P.J.T. Bussmann (TNO Quality of Life, Zeist)

This research was conducted under the auspices of the Graduate School VLAG

# Modeling of particle segregation in a rotating drum

Marleen M.H.D. Arntz

## **Thesis**

submitted in fulfillment of the requirements for the degree of doctor  
at Wageningen University  
by the authority of the Rector Magnificus  
Prof. dr. M.J. Kropff,  
in the presence of the  
Thesis Committee appointed by the Academic Board  
to be defended in public  
on Wednesday 1 December 2010  
at 4 p.m. in the Aula.

Marleen M.H.D. Arntz  
Modeling of particle segregation in a rotating drum,  
156 pages.

PhD thesis, Wageningen University, The Netherlands (2010)  
With propositions and summaries in Dutch and English

ISBN: 978-90-8585-802-7





# Contents

Chapter 1	Introduction	1
Chapter 2	Granular mixing and segregation in a horizontal rotating drum: a simulation study on the impact of rotational speed and fill level	17
Chapter 3	Segregation by mass, radius and density of granular particles in a horizontal rotating drum	51
Chapter 4	Repeated segregation and energy dissipation in an axially segregated granular bed	71
Chapter 5	End walls induce axial segregation in a horizontal rotating drum	87
Chapter 6	Discussion	113
Summary		127
Samenvatting		131
List of publications		137
Nawoord		139
Curriculum vitae		143
Overview of completed training activities		145



---

# Chapter 1 Introduction



## INTRODUCTION

### **GRANULAR MIXING: COMMONLY APPLIED, BUT INSUFFICIENTLY UNDERSTOOD**

Blending of heterogeneous granular materials is a common step in many technical endeavours. In the food industries, for example, granular mixing is a common and important unit operation, which is applied during drying and sterilization of spices and herbs, in freeze drying, in the production of instant soups, and to coat snacks and candies. Notwithstanding the numerous practical applications, the understanding of the flow and mixing behaviour of granular materials is still incomplete. As a result, factories that rely on powder handling often require much longer start-up times than plants that involve only fluids. Sometimes facilities for powder production are even abandoned after the expense of many millions of dollars for want of an effective means of inducing powder flow or blending (Nelson *et al.*, 1995). A common problem during blending is unwanted particle segregation, causing process and product defects (Turner and Nakagawa, 2000; Khakhar *et al.*, 2003; Di Renzo and Di Maio, 2004). To overcome these defects, more insight in granular mixing and segregation is needed.

### **SEGREGATION: EASY TO ACHIEVE, HARD TO AVOID**

Typical granular behaviour can be illustrated by a simple household demonstration. Two salt vessels are partially filled with salt; one contains a steel hex nut, the other an equally large pushpin. If both vessels are shaken vertically, the hex nut rapidly rises to the salt surface while the pushpin sinks to the bottom of the vessel. If the vessels then are shaken horizontally, the pin will rise and the nut will sink. This outcome is paradoxical and reveals the complexity of granular (de)mixing. Both the practical importance and intriguing complexity have made granular mixing the subject of intense research over the last decades (Ottino and Khakhar, 2000). Nevertheless, the translation of the more fundamental findings into reliable predictions for practical process performance is still incomplete (Ottino and Khakhar, 2000; Jain *et al.*, 2005; Rapaport, 2007).

### **PRACTICAL CONSTRAINTS IN ACHIEVING MIXING AS NEEDED, AN EXAMPLE**

The practical incentive of this current study on solids mixing is based on the mixing of zeolite granules with spices or herbs. Nowadays, spices and herbs are sterilized with steam or with irradiation. With steam sterilization, the quality of

food degrades in the final flashing step, during which volatiles such as essential oils are lost with the steam. While irradiation would be a viable alternative, consumers disapprove of the application of radiation. Therefore, a new process is needed that sterilizes the herbs and spices but avoids quality degradation by flashing. Such a new sterilization technique may be based on the application of zeolite. Zeolite granules are mixed with product granules (spices or herbs) and adsorb water from the product; in turn, the zeolite will release adsorption heat (Figure 1), which heats up the product.

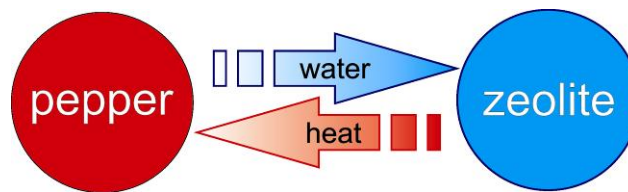


**Figure 1:** Drying and sterilization of pepper granules with zeolite.

An important requirement - already known from steam sterilization - is mixture homogeneity. This ensures that each individual product grain will be heated long enough to guarantee sterilization, yet short enough to avoid degradation by e.g. Maillard reactions. However, designing and operating a mixing operation leading quickly to a homogeneous mixture is extremely difficult and sometimes even impossible. Since we are dealing with foods, high shear rates are undesired in order to avoid attrition and breakage. Therefore, low shear mechanical agitation should be applied. However, it is not trivial that homogeneity is promoted by such operation since the mixture also meets the most important prerequisites of segregation, namely a difference in size and density. Therefore, insight in solid-solid mixing is a prerequisite for the rational design and operation of an effective process.

## GOAL OF THIS THESIS

In view of the need for better understanding and controlling of solids mixing, the work in this thesis has two closely coupled objectives. The first objective is generating a more comprehensive understanding of segregation mechanisms than available at this moment. The second objective is to provide guidelines for

mixing operations, based on the insight generated, and based on information on mixing behaviour at different rotational velocities and fill levels.

## **APPROACH**

The bed behaviour of a model system was studied by means of a model. Research focused on the analysis of the degree of mixing, during both transient and steady states. Details about the mathematical model, the system and the analyses are given below.

## **MODEL SYSTEM**

A relatively simple mixing operation is needed to limit the possible causes of segregation and obtain unambiguous results. Since a horizontal rotating drum is the simplest geometry that is still relevant for industrial practice, this was chosen as model system. For the same reasons a granular system consisting of two types of spherical particles was chosen.

## **SIMULATIONS VERSUS EXPERIMENTS**

A rough qualification of the extent of segregation in experiments is not difficult. Designing a mixer of a transparent material makes it possible to do a first analysis of segregation by visual observation of the particle bed exterior. For a full quantification of the mixing degree, however, also the inside of the bed should be analyzed. If a homogeneous mixture is wanted, bad internal mixing regions should be detected. To analyse the interior of particle beds, bed solidification methods were developed (Wightman and Muzzio, 1998; Schutyser *et al.*, 2002). After solidification, bed slices are made to investigate compositional patterns. A disadvantage of this solidification method is that the system is destroyed. The behaviour in time is hard to study and it is impossible to repeat the experiment with the exact same initial configuration. Nowadays methods like Magnetic Resonance Imaging (MRI) and Positron Emission Particle Tracking (PEPT) are available that allow non-invasive study of bed dynamics. Unfortunately, both methods have their drawbacks and are complex and expensive (Chen *et al.*, 2008). Numerical software simulations offer an attractive alternative to solidification experiments and to cumbersome MRI and PEPT techniques. Even though numerical systems are simplified compared to reality, they allow non-invasive, detailed characterisation of the complete bed, and

accurate control over all variables. Since 1980, the Discrete Element Method (DEM) is developed that allows a detailed study of the dynamics of granular mixing. DEM simulations are comparable to an extremely defined and controlled experiment with the benefit of knowing the particles position, velocity and angular velocity in time, and analyses possible. Another benefit of DEM is the possibility to vary all parameters independently, e.g. size ratios, density ratios, which makes all kinds of experiments possible

### **DISCRETE ELEMENT METHOD**

DEM (Cundall and Strack, 1997) was the first granular dynamics simulation technique published in the open literature. Due to the progress described above, new doors were opened for the research in segregation and mixing. At first mainly 2D simulations were conducted, focusing on radial segregation (see also the section on radial segregation) (Ristow, 1994; Dury and Ristow, 1997). The step to simulate 3D segregation phenomena was a significant one, since these phenomena take longer time scales to develop, and many more particles need to be simulated. Due to the development of better computers (CPUs), increasing computational power became available and a first attempt to simulate axial segregation (see also paragraph axial segregation) was made by (Shoichi, 1998). Only initial stages of axial segregation were observed. A next successful trial of simulating axial segregation was conducted by D. Rapaport (Rapaport, 2002) and (Taberlet *et al.*, 2004). In this thesis we continue this approach for an in depth study of segregation phenomena.

In the DEM method one first has to generate a representative initial configuration. For this, particles obtain their initial coordinates in the mixer from a random number generator. Subsequently, in a short DEM simulation the particles are allowed to settle on the bottom of the drum by gravity. A file containing the resulting coordinates of the settled particles is then used the initial configuration of the actual DEM simulation.

A DEM simulation, also referred to as a soft-sphere granular dynamics simulation, is a simulation in which the simulated particles are soft. This implies that particles can deform when a certain force acts on them. In this method particles are allowed to overlap slightly. From this overlap, contact forces are calculated that repulse the particles and inhibit any further overlap. Knowing the contact forces, Newton's equations of motion can be solved to obtain the new

positions and (angular) velocities of the particles in time. By calculating the trajectories of each of the individual particles in time, the global flow of the granular material is determined.

The time step used is very small to prevent large overlap of the particles, which is not realistic, and in extreme cases could lead to particles moving through other particles. In this research the time step was approximately a microsecond, in which a particle can only move a small fraction of its own diameter.

### **VISUALIZATION**

The obtained position data can be converted to a movie or snapshots (see Figure 2) e.g. with the graphics visualization package VMD (Humphrey *et al.*, 1996). The data can also be processed to extract local flow profiles or bed densities, or to calculate the mixing degree. In this study a many movies are made to convert the data file of positions and velocities to the actual bed behavior. By making use of tracer particles the path of individual particles in the bed could be followed.

### **QUANTIFICATION**

While visualization is useful and necessary, it is also important to quantify the configurational changes in time, which allows more objective evaluation and analysis of gradual changes. For this we developed a method based on the order parameter of mixing. This parameter translates the results of the interactions between particles into a value representing the overall degree of mixing. This is done with the entropy of mixing, calculated over different lattices inside the drum. By normalisation, a value between zero and one results that represents the overall-mixing degree, with zero for complete segregation, and one for ideal mixing.

### **STATE OF THE ART**

Because of the elusiveness of fundamental understanding in the field, its practical importance and intriguing complexity have made granular mixing the subject of intense research in the last decades (Ottino and Khakhar, 2000). The subsequent overview briefly describes the state of the art and describes the starting point for this thesis.

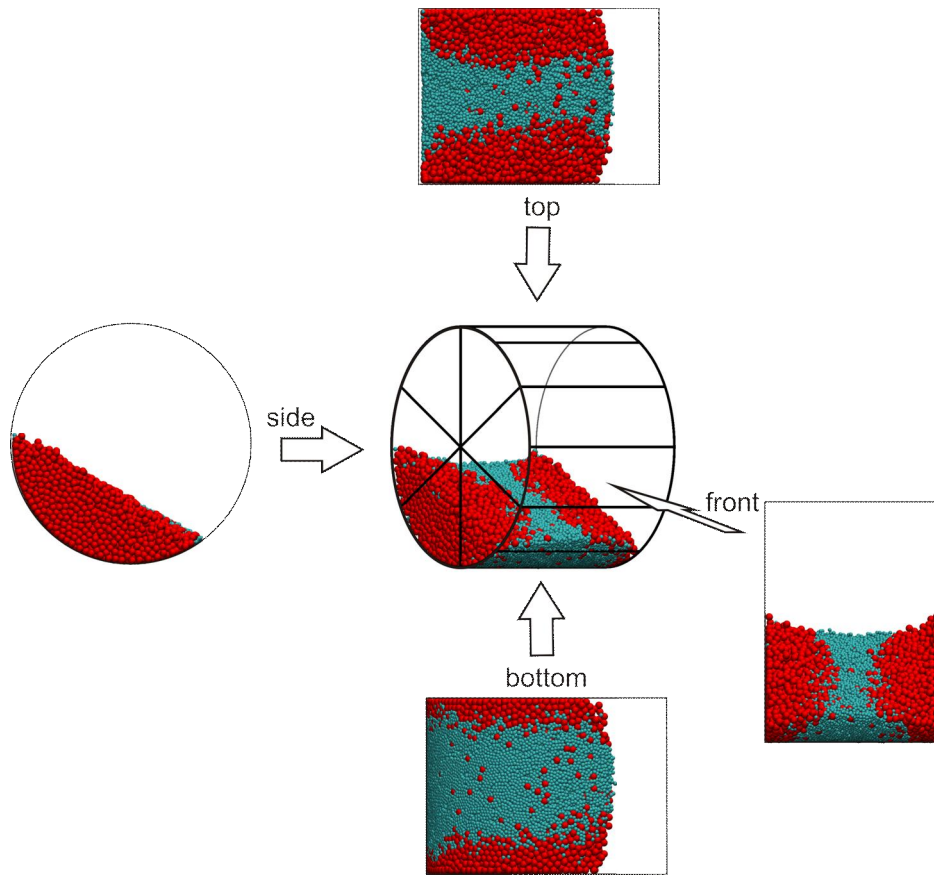


**Figure 2:** Different views of simulated horizontally rotating drum.

## **RADIAL SEGREGATION**

Depending on the rotational speed of the drum, the particle bed can be in one of the following six flow regimes, in order of increasing rotational speed;

1. sliding,
2. avalanching, also called slumping,
3. rolling,
4. cascading,
5. cataracting,
6. centrifuging.

The latter four are discussed in great detail in this thesis and are illustrated in Figure 3. The first two have been previously illustrated elsewhere (Henein *et al.*, 1983; Mellmann, 2001). Depending on the flow regime (and the drum geometry) the system can mix or segregate radially, axially, or inverted (Donald and Roseman, 1962; Nityanand *et al.*, 1986; Dury and Ristow, 1999; Ottino and Khakhar, 2000; Rapaport, 2002) (Figure 3, 4 and 5).

Radial segregation refers to the accumulation of the smaller or denser particles in a coaxial core in the beds interior, spanning the entire length of the drum (Figure 3a); Inverted segregation is the inverse of radial segregation and refers to the

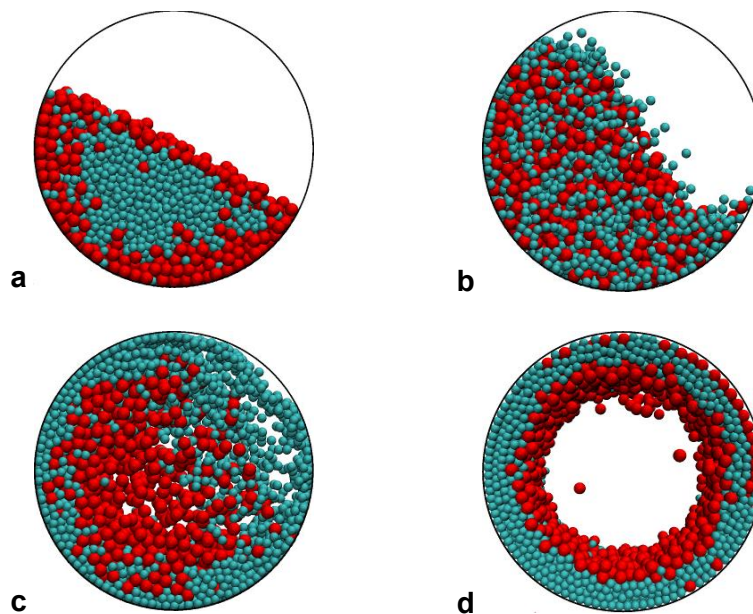


**Figure 3a:** Side view of the rolling regime, in which the bed can roughly be divided in two parts, the passive bulk, in which particles undergo solid body rotation around the cylinder axis, and the active layer, also known as the flowing layer or fluidized layer, in which the particles undergo collective linear translation down the slope of the stagnant rotating layer. The characteristic of the rolling regime is that the surface is flat. **b:** The cascading regime, in which the flowing characteristics lead to an s-shaped surface. **c:** In the cataracting regime, the flowing layer consists mainly of particles being flung into the previously void space above the bed. **d:** In the centrifuging regime, the apparent centrifugal force is larger than the apparent gravitational force through which the particles forming a stagnant layer covering the entire wall.

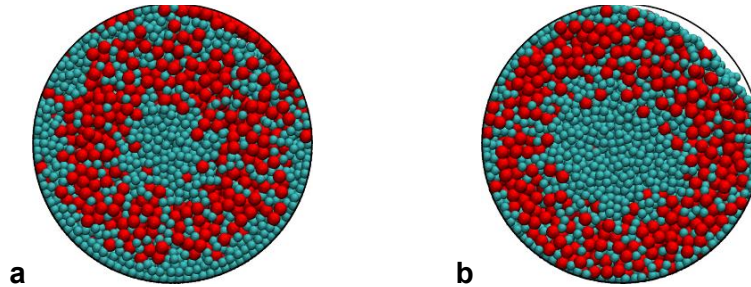


**Figure 4a, b:** Examples of less common segregation patterns with the small particles present in the core and in the periphery of the particle bed.

accumulation of larger or lower density particles in the coaxial core of the bed (Figure 3c). These segregation patterns are widely observed, but other patterns are possible, depending on specific settings (Figure 4). In some cases, complex patterns emerge when particles differ not only in size and/or density, but also in shape (McCarthy and Ottino, 1998; Ottino and Khakhar, 2000). Most research focuses on granular beds in the avalanching or rolling regime with particles that are bidisperse in size (Dury and Ristow, 1997; Chakraborty *et al.*, 2000; Thomas, 2000; Turner and Nakagawa, 2000; Ding *et al.*, 2002; Khakhar *et al.*, 2003; Hajra and Khakhar, 2004; Kawaguchi *et al.*, 2006).

Since for rational design of mixer or segregators we need to have insight in all regimes, we studied the rolling, cascading, cataracting and centrifuging regimes in chapter 2 of this thesis. Since many food systems do not only differ in size but also in density (for example zeolite and particles like pepper or coriander), we studied the interplay in size and density segregation in greater detail (chapter 3 of this thesis).

## AXIAL SEGREGATION

In a large number of experiments (Donald and Roseman, 1962; Hill *et al.*, 1997; Kuo *et al.*, 2005) and also in some simulations (Taberlet *et al.*, 2006; Rapaport, 2007), it is seen that particles which are bidisperse in size, and which show radial segregation, are also segregate axially into alternating bands of large and small particles perpendicular to the rotation axis. Axial segregation was first observed in 1939 (Oyama, 1939).

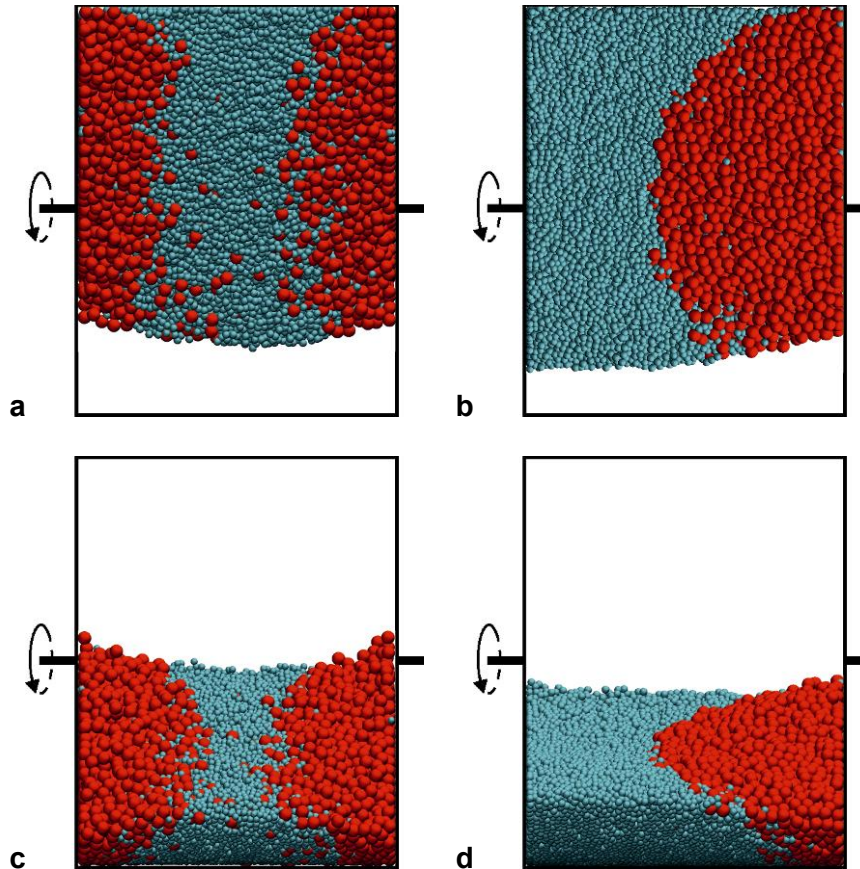


**Figure 5a:** Top view of a rotating drum displaying axial segregation into three bands. **b:** Top view of a rotating drum displaying axial segregation into two bands. **c:** Front view of a rotating drum displaying axial segregation into three bands. **d:** Front view of a rotating drum displaying axial segregation into two bands.

The fact that radial segregation always precedes axial segregation evidence of a connection between radial and axial segregation was only observed in 1997, when MRI measurements (Hill *et al.*, 1997) revealed undulations in the thickness of the radial core, which at some point break through to the surface.

Upon rotating, these undulations generally transform into pure axial segregation, with fully segregated bands perpendicular to the rotating axis. The number of bands depends on the particle properties, drum geometry (length and radius) and process parameters (fill level, angular velocity of the drum), and the initial

configuration (Taberlet *et al.*, 2006). In time, the bands tend to merge and ultimately form a system of three (Hill and Kakalios, 1994, 1995) or two bands (Chicharro *et al.*, 1997) as illustrated in Figure 5.

The formation of multiple bands and their merging into three or two bands is intriguing emergent behaviour that is not well understood. This is reflected in the number of papers dealing with the phenomenon (Donald and Roseman, 1962; Hill and Kakalios, 1994, 1995; Choo *et al.*, 1997; Hill *et al.*, 1997; Aranson and Tsimring, 1999; Kuo *et al.*, 2005; Taberlet *et al.*, 2006; Rapaport, 2007).

However, these phenomena are only obtained in relatively long drums, while practical systems, such as tumblers, usually have a length that is only 3-10 times the diameter, it is important to investigate the segregative dynamics in these the relatively short drums. Moreover, experiments on rotating bidisperse particle beds indicate that end-wall effects can initiate band formation (Hill and Kakalios, 1995; Caps *et al.*, 2003). It has been shown in monodisperse systems that the flow near the middle of the length of drums is significantly different from that near the end walls (Maneval *et al.*, 2005; Pohlman *et al.*, 2006; Chen *et al.*, 2008).

Since end wall effect are much more important in short drums compared to longer ones, it is of practical importance to study the effect of end walls on the axial segregation process, as it is one of the design parameters for these systems. For this reason in chapter 4 and 5 of this thesis end wall effects will be discussed in detail.

## OUTLINE OF THIS THESIS

**Chapter 2** is dedicated to two major operational parameters that influence mixing: the fill level and the rotational speed. Their influence on transient and steady state mixing is studied in a very short (quasi 2D) rotating drum. The effect of particle properties (size, density and roughness) on radial segregation is investigated in **chapter 3**. A new implementation of the concept of the order parameter is introduced, based on entropy calculations. The effect of end walls on the development and final configuration of the axially segregated state will be discussed in **chapter 4**. Surprising long-term oscillatory behaviour is observed,

which seems to be coupled to the limited lengths of the drums investigated. It is shown that minimization of energetic dissipation plays a role in the segregation process. In **chapter 5**, the friction between the end walls and the particles is varied, proving that the end walls have strong effect on axial segregation and on the occurrence of the long-term oscillations. In **chapter 6**, an overview of the conclusions is given and suggestions about future research on segregation are made. The chapter is concluded with a translation of the findings into the practical design and operation of mixing or segregating systems.

## REFERENCES

- Aranson, I. S. and Tsimring, L. S.** (1999). Dynamics of axial separation in long rotating drums. *Physical Review Letters* **82**(23).
- Caps, H., Michel, R., Lecocq, N. and Vandewalle, N.** (2003). Long lasting instabilities in granular mixtures. *Physica A: Statistical Mechanics and its Applications* **326**(3-4): 313-321.
- Chakraborty, S., Nott, P. R. and Prakash, J. R.** (2000). Analysis of radial segregation of granular mixtures in a rotating drum. *European Physical Journal E* **1**(4): 265-273.
- Chen, P. F., Ottino, J. M. and Lueptow, R. M.** (2008). Subsurface granular flow in rotating tumblers: A detailed computational study. *Physical Review E* **78**(2).
- Chicharro, R., Peralta-Fabi, R. and Velasco, R.** (1997). Segregation in dry granular systems. *Powders and Grains 97*. P. Behringer and J. Jenkens. Rotterdam, Balkema: 479-482.
- Choo, K., Molteni, T. C. A. and Morris, S. W.** (1997). Traveling granular segregation patterns in a long drum mixer. *Physical Review Letters* **79**(16).
- Cundall, P. A. and Strack, O. D. L.** (1997). Discrete Numerical-Model for Granular Assemblies. *Geotechnique* **29**(1): 47-65.
- Di Renzo, A. and Di Maio, F. P.** (2004). Comparison of contact-force models for the simulation of collisions in DEM-based granular flow codes. *Chemical Engineering Science* **59**(3): 525-541.
- Ding, Y. L., Forster, R., Seville, J. P. K. and Parker, D. J.** (2002). Segregation of granular flow in the transverse plane of a rolling mode rotating drum. *International Journal of Multiphase Flow* **28**(4): 635-663.
- Donald, M. and Roseman, B.** (1962). Mixing and demixing of solid particles. Part 1. Mechanisms in a horizontal drum mixer. *British Chemical Engineering* **7**: 749-752.
- Dury, C. M. and Ristow, G. H.** (1997). Radial segregation in a two-dimensional rotating drum. *Journal De Physique I* **7**(5): 737-745.
- Dury, C. M. and Ristow, G. H.** (1999). Competition of mixing and segregation in rotating cylinders. *Physics of Fluids* **11**(6): 1387-1394.
- Hajra, S. K. and Khakhar, D. V.** (2004). Sensitivity of granular segregation of mixtures in quasi-two-dimensional fluidized layers. *Physical Review E* **69**(3).

- Henein, H., Brimacombe, J. K. and Watkinson, A. P.** (1983). Experimental-Study of Transverse Bed Motion in Rotary Kilns. *Metallurgical Transactions B-Process Metallurgy* **14**(2): 191-205.
- Hill, K. M., Caprihan, A. and Kakalios, J.** (1997). Bulk segregation in rotated granular material measured by magnetic resonance imaging. *Physical Review Letters* **78**(1).
- Hill, K. M. and Kakalios, J.** (1994). Reversible Axial Segregation of Binary-Mixtures of Granular-Materials. *Physical Review E* **49**(5).
- Hill, K. M. and Kakalios, J.** (1995). Reversible Axial Segregation of Rotating Granular Media. *Physical Review E* **52**(4).
- Humphrey, W., Dalke, A. and Schulten, K.** (1996). VMD: Visual molecular dynamics. *Journal of Molecular Graphics* **14**(1): 33-38.
- Jain, N., Ottino, J. M. and Lueptow, R. M.** (2005). Regimes of segregation and mixing in combined size and density granular systems: an experimental study. *Granular Matter* **7**(2-3): 69-81.
- Kawaguchi, T., Tsutsumi, K. and Tsuji, Y.** (2006). MRI measurement of granular motion in a rotating drum. *Particle & Particle Systems Characterization* **23**(3-4): 266-271.
- Khakhar, D. V., Orpe, A. V. and Hajra, S. K.** (2003). Segregation of granular materials in rotating cylinders. *Physica a-Statistical Mechanics and Its Applications* **318**(1-2): 129-136.
- Kuo, H. P., Hsu, R. C. and Hsiao, Y. C.** (2005). Investigation of axial segregation in a rotating drum. *Powder Technology* **153**(3): 196-203.
- Maneval, J. E., Hill, K. M., Smith, B. E., Caprihan, A. and Fukushima, E.** (2005). Effects of end wall friction in rotating cylinder granular flow experiments. *Granular Matter* **7**(4): 199-202.
- McCarthy, J. J. and Ottino, J. M.** (1998). Particle dynamics simulation: a hybrid technique applied to granular mixing. *Powder Technology* **97**(2): 91-99.
- Mellmann, J.** (2001). The transverse motion of solids in rotating cylinders - forms of motion and transition behavior. *Powder Technology* **118**(3): 251-270.
- Nelson, R. D., Davies, R. and Jacob, K.** (1995). Teach 'em particle technology. *Chemical Engineering Education* **29**: 12-15.
- Nityanand, N., Manley, B. and Henein, H.** (1986). An Analysis of Radial Segregation for Different Sized Spherical Solids in Rotary Cylinders. *Metallurgical Transactions B-Process Metallurgy* **17**(2): 247-257.
- Ottino, J. M. and Khakhar, D. V.** (2000). Mixing and segregation of granular materials. *Annual Review of Fluid Mechanics* **32**: 55-91.
- Oyama, Y.** (1939). Studies on mixing of solids. *Bulletin of the Institute of Physical and Chemical Research of Japan* **5**(18): 600-639.
- Pohlman, N. A., Ottino, J. M. and Lueptow, R. M.** (2006). End-wall effects in granular tumblers: From quasi-two-dimensional flow to three-dimensional flow. *Physical Review E* **74**(3).
- Rapaport, D. C.** (2002). Simulational studies of axial granular segregation in a rotating cylinder. *Physical Review E* **65**(6).
- Rapaport, D. C.** (2007). Radial and axial segregation of granular matter in a rotating cylinder: A simulation study. *Physical Review E* **75**(3).

- Ristow, G. H.** (1994). Granular dynamics: a review about recent molecular dynamics simulations of granular materials. *Annual Reviews of Computational Physics*. D. Stauffer, World Scientific. **I**: 275-308
- Schutyser, M. A. I., Weber, F. J., Briels, W. J., Boom, R. M. and Rinzema, A.** (2002). Three-dimensional simulation of grain mixing in three different rotating drum designs for solid-state fermentation. *Biotechnology and Bioengineering* **79**(3): 284-294.
- Shoichi, S.** (1998). Molecular-dynamics simulations of granular axial segregation in a rotating cylinder. *Molecular Physical Letters B* **12**(4): 115-122.
- Taberlet, N., Losert, W. and Richard, P.** (2004). Understanding the dynamics of segregation bands of simulated granular material in a rotating drum. *Europhysics Letters* **68**(4): 522-528.
- Taberlet, N., Newey, M., Richard, P. and Losert, W.** (2006). On axial segregation in a tumbler: an experimental and numerical study. *Journal of Statistical Mechanics-Theory and Experiment*(7).
- Thomas, N.** (2000). Reverse and intermediate segregation of large beads in dry granular media. *Physical Review E* **62**(1).
- Turner, J. L. and Nakagawa, M.** (2000). Particle mixing in a nearly filled horizontal cylinder through phase inversion. *Powder Technology* **113**(1-2): 119-123.
- Wightman, C. and Muzzio, F.** (1998). Mixing of granular material in a drum mixer undergoing rotational and rocking motions - II. Segregating particles. *Powder Technology* **98**(2): 125-134.

---

---

**Chapter 2 Granular mixing and segregation in a horizontal rotating drum: a simulation study on the impact of rotational speed and fill level**

## ABSTRACT

The rich phase behaviour of granular beds of bidisperse hard spherical particles in a rotating horizontal drum has been studied by Discrete Element Method (DEM) simulations. By varying the operational parameters of the drum, i.e. fill level and velocity of rotation, we observe several flow regimes, various forms of radial segregation and mixing. This complex behaviour is summarized in two state diagrams. To delve deeper into the observed correlations between flow regime and segregation process, several analysis methods are used to investigate the local properties of the granular bed and an entropy method is used to quantify the degree of mixing. A percolation mechanism provides a qualitative explanation for most of the observed segregations. Initially blockwise segregated beds are found to mix before radial segregation sets in. The simulations at high fill fractions (>65%) show the most intense segregation.

The contents of this chapter have been published as:

**M.M.H.D. Arntz, W.K. den Otter, H.H. Beftink, P.J.T. Bussmann, W.J. Briels and R.M. Boom** (2008) Granular mixing and segregation in a horizontal rotating drum: a simulation study on the impact of rotational speed and fill level. *AIChE Journal*, 54: 3133-3146

---

---

## INTRODUCTION

Granule mixing is a common and important unit operation in the food industry. It is for example applied during drying and sterilization of spices and herbs, in freeze drying, in the production of instant soups, and to coat snacks and candies. The fundamental phenomena in granule mixing are still poorly understood, making it difficult to a priori predict the effectiveness of mixing processes. Operations aimed at mixing polydisperse granules may even result in segregation. Although granular mixing has been the subject of research for some time (Cleary, 1998b, a; Cleary *et al.*, 1998; Ottino and Khakhar, 2000), the translation of the more fundamental findings into predictions for practical processes is still sketchy. In addition, the range of parameter values studied so far is rather limited. From this perspective, we here report an extensive numerical study of mixing and segregation in a bed of bidisperse granules in a rotating horizontal drum, which is the simplest geometry relevant in industrial practice.

Simulations of granular materials are based on either discrete elements or continuum models. The discrete element methods (DEM) combine semi-empirical models for the interparticle interactions with the equations of motion from classical mechanics to simulate the explicit paths of all granules in the drum, thus yielding realistic predictions of the mixing process. This approach is very demanding computationally, which strongly limits the number of granules and the number of revolutions in a simulation. Continuum models dispense with the discrete particles and can therefore be scaled up more easily. But the constitutive relations that serve as the foundation for continuum modelling are difficult to come by, and often only applicable to specific systems and conditions. Here we have chosen for DEM simulations, since in this approach the phenomena emerging in the simulations are expected to be the least affected by the details and approximations of the simulation model.

In this chapter, DEM simulations are presented of the mixing of bidisperse, nearly incompressible, spherical granules in a rotating horizontal drum, with the aim to analyse the mixing and segregation behaviour of cohesionless particles, such as spices and herbs. Even in this simple system, several segregation processes are known to occur: radial segregation (Nityanand *et al.*, 1986; Boateng and Barr, 1996; Dury and Ristow, 1997, 1999; Ottino and Khakhar,

2000), inverted segregation (Nityanand *et al.*, 1986; Turner and Nakagawa, 2000), axial segregation (Donald and Roseman, 1962; Hill *et al.*, 1997; Ottino and Khakhar, 2000; Rapaport, 2002), radial streaking (Khakhar *et al.*, 2001a; Khakhar *et al.*, 2001b; Khakhar *et al.*, 2003; Hill *et al.*, 2004; Jain *et al.*, 2005b, a), double radial segregation (Turner and Nakagawa, 2000; Khakhar *et al.*, 2003; Hajra and Khakhar, 2004) and formation of unmixed cores (Cleary, 1998b, a; Cleary *et al.*, 1998; Eskin and Kalman, 2000a). To limit their number, we have chosen to follow Dury and Ristow (Dury and Ristow, 1999) by focusing on quasi-2D systems, meaning that the drum has a limited depth to suppress axial transport and thus axial segregation. The two types of particles differ in size, which at identical specific gravities implies that they also differ in mass, while the particles are identical in all other respects. Of primary interest in this study are the fill level and the rotational velocity of the drum, as it is our objective to analyse how these two easily tuneable operational parameters determine the mixing and segregation process.

Mixing and segregation in a rotating drum is believed to take place predominantly in the topmost tilted layer of the granular bed, where the particles move, individually or collectively, from one side of the drum downhill to the opposite site. Six regimes of particle flow in this flowing layer have been identified (Henein *et al.*, 1983a, b; Mellmann, 2001), namely the sliding, avalanching a.k.a. slumping, rolling, cascading, cataracting and centrifuging regimes. Industrial mixing operations are typically performed in the rolling or cascading regime, and sometimes in the cataracting regime, while the sliding regime is avoided for its poor mixing behaviour. Previous DEM studies cover a limited range of fill levels and rotational velocities, and consequently only the avalanching and rolling regimes have been observed in simulations. By considerably extending the ranges of these two operational parameters, we have been able to study the cascading, cataracting and centrifuging regimes as well. These three regimes will therefore be discussed in more detail than the rolling regime. Simulations in the latter regime are included to validate our model against previous studies, and to complete the emerging physical picture.

The simulations presented here are analysed using a series of methods to further the understanding of the observed mixing and segregation processes, and the roles played herein by the fill factor and the angular velocity of the drum. Quantitative data on the degree of mixing, both in the steady state and as a

function of time, are obtained by an entropy-based characterization method. Density maps and velocity vector maps are used to analyse the tilted flowing layer on top of the bed. Velocity-difference vector maps are helpful in the identification of the specific regions where the small and large particles are being separated. A state diagram depicting the dependence of the flow regime on the fill level and angular velocity shows a remarkable agreement with the state diagrams collected previously for monodisperse systems. The steady state degree of mixing is also plotted as a function of these two operational parameters. From this detailed analysis the general picture appears that a percolation mechanism, i.e. small particles falling through the voids in the flowing layer, is responsible for translating the flow regime into a steady state segregation pattern.

This chapter is organised as follows: In the section Model description and characterization of mixing the simulation model and the aforementioned analysis methods are introduced briefly. The simulation results are presented and discussed in the section Results and discussion, followed by a summary of the main conclusions in the section Conclusions.

## MODEL DESCRIPTION AND CHARACTERIZATION OF MIXING

### DISCRETE ELEMENT MODELLING (DEM)

To model time-dependent particle positions in a rotating drum, a discrete element model (DEM) is used (Cundall and Strack, 1997; Hoomans, 2000; Schutyser *et al.*, 2002). Particles are assumed to be spherical, interacting only by contact forces both normal and tangential to their touching surfaces. The normal force exerted on sphere  $i$  by sphere  $j$ , see Figure 1, is described using a linear spring & dashpot model:

$$\mathbf{F}_{ij}^n = -k_n \delta_{ij} \hat{\mathbf{n}}_{ij} - \eta_n \mathbf{v}_{ij}^n, \quad [1]$$

with  $k_n$  the elastic stiffness of the particles. The apparent overlap width  $\delta_{ij}$  of two colliding particles is calculated as

$$\delta_{ij} = (R_i + R_j) - |\mathbf{r}_i - \mathbf{r}_j|, \quad [2]$$

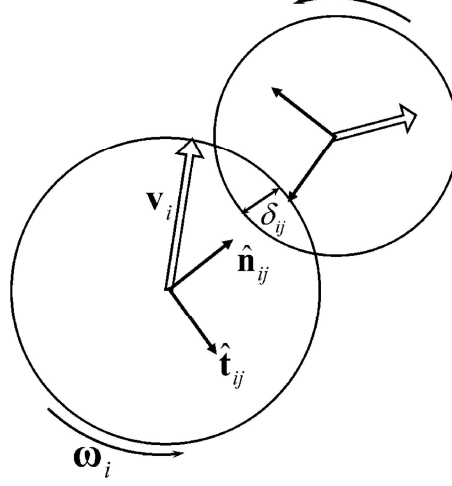


**Figure 1:** A collision of two granular particles, illustrating the notation introduced previously.

with  $R_i$  and  $R_j$  the radii, and  $\mathbf{r}_i$  and  $\mathbf{r}_j$  the position vectors of particles  $i$  and  $j$ , respectively. The normal unit vector  $\hat{\mathbf{n}}_{ij}$  is directed from the centre of particle  $i$  to the centre of particle  $j$  (Figure 1).

$$\hat{\mathbf{n}}_{ij} = (\mathbf{r}_j - \mathbf{r}_i) / |\mathbf{r}_j - \mathbf{r}_i|. \quad [3]$$

Their relative velocity along this normal is given by

$$\mathbf{v}_{ij}^n = (\mathbf{v}_i - \mathbf{v}_j) \cdot \hat{\mathbf{n}}_{ij} \hat{\mathbf{n}}_{ij} \quad [4]$$

in which  $\mathbf{v}_i$  and  $\mathbf{v}_j$  are the velocities of particles  $i$  and  $j$  respectively. The normal damping coefficient  $\eta_n$  is related to the energy restitution coefficient  $e_v$  of particle collisions by

$$\eta_n = 2m_{\text{red}} \ln(e_v) / \tau, \quad [5]$$

where  $m_{\text{red}} = m_i m_j / (m_i + m_j)$  is the reduced mass and,  $m_i$  and  $m_j$  are the masses of particles  $i$  and  $j$ . The collision time or contact time

$$\tau = \pi / \sqrt{(k_n / m_{\text{red}}) - (\eta_n / (2m_{\text{red}}))^2} \quad [6]$$

can be solved exactly from the above equations of motion (Schäfer *et al.*, 1996).

In the description of the tangential friction force one has to distinguish between the sticking and the sliding regime. In Schäfers' approximation (Schäfer *et al.*, 1996) of the Coulombic friction model the tangential force in the sticking regime reads as

$$\mathbf{F}_{ij}^t = -\eta_t \mathbf{v}_{ij}^t, \quad [7]$$

in which  $\eta_t$  is the viscous friction coefficient. The tangential velocity difference at the point of contact is given by

$$\mathbf{v}_{ij}^t = (\mathbf{v}_i - \mathbf{v}_j) - \mathbf{v}_{ij}^n + (R_i \boldsymbol{\omega}_i + R_j \boldsymbol{\omega}_j) \times \hat{\mathbf{n}}_{ij} \quad [8]$$

where  $\boldsymbol{\omega}_i$  and  $\boldsymbol{\omega}_j$  are the angular velocities of particles  $i$  and  $j$ , respectively. The maximum attainable friction force in the sticking regime, which is also the friction force in the sliding regime, reads as

$$\mathbf{F}_{ij}^t = -\mu |\mathbf{F}_{ij}^n| \hat{\mathbf{t}}_{ij} \quad [9]$$

with  $\mu$  the Coulombic friction coefficient and

$$\hat{\mathbf{t}}_{ij} = \mathbf{v}_{ij}^t / |\mathbf{v}_{ij}^t| \quad [10]$$

the unit vector in the direction of the tangential velocity. Note that Schäfer's approximation (Schäfer *et al.*, 1996) circumvents the discontinuity in the Coulomb model by allowing the particles to slide very slowly in the sticking regime. Both normal and tangential cease when the particles are not in contact anymore, i.e. for  $\delta_{ij} < 0$ .

The interactions of particles with the drum walls are of the same form as the particle-particle interactions in equations 1, 7 and 9, where distances and velocity differences are now calculated relative to the contact point(s) with the walls. The cylindrical drum wall of radius  $R_d$  and length  $L$  is oriented with its rotation axis along the  $y$ -axis and is closed by flat circular walls at either end, see Figure 2. The origin of our coordinate system coincides with the centre of the drum. A gravitational force pulls along the negative  $z$ -direction.

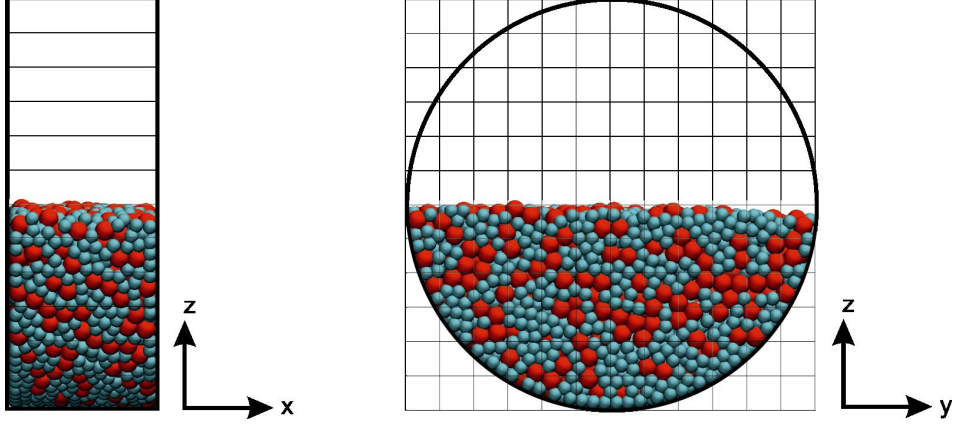


**Figure 2:** Front view (left) and side view (right) illustrating the relative dimensions of the drum and the two particle radii. The fill level is 50% in all simulations. The grid of thin lines mark the cell dimensions used in the calculation of the order parameter.

The total force  $\mathbf{F}_i^{\text{tot}}$  on particle  $i$  is obtained by summation of all forces with respect to that particular particle, including contact forces exerted by the drum walls and gravity. One may then solve the particles motion by numerically integrating Newton's second law of motion

$$d^2\mathbf{r}_i/dt^2 = \mathbf{F}_i^{\text{tot}}/m_i. \quad [11]$$

The rotation of particles is taken into account by calculating the total torque  $\mathbf{T}_i^{\text{tot}}$  on each particle and integrating the equation of motion

$$d\boldsymbol{\omega}_i/dt = \mathbf{T}_i^{\text{tot}}/I_i = R_i \sum_j \hat{\mathbf{n}}_{ij} \times \mathbf{F}_{ij}^t / I_i, \quad [12]$$

where the moment of inertia of the spherical particle  $i$  is given by  $I_i = 2m_i R_i^2/5$ . The equations of motion are integrated using the half-step 'leap-frog' scheme (Allen and Tildesley, 1987) with a fixed time step  $\Delta t$ . The time step in this integration should be sufficiently small to accurately integrate the equations of motion. Using Schäfer's criterion (Schäfer *et al.*, 1996) one arrives at  $\Delta t = 0.01\tau$ , but we find that an even smaller time step of  $0.0025\tau$  is needed to ensure numerical accuracy.

The simulation parameters employed in this study are presented in Table 1, along with the parameters of the similar models by Dury and Ristow (Dury and Ristow, 1999) and by Schutyser *et al.* (Schutyser *et al.*, 2001). The starting configurations of our simulations were created by placing particles randomly in the drum, avoiding overlap, followed by a short simulation to condense the bed under the influence of gravity. By initially placing small particles on the right side ( $x > 0$ ) and large particles on the left side ( $x < 0$ ) of the drum, we arrived at the block-wise segregated starting configuration of Figure 3, snapshot A. After all particles had settled, their velocities were set to zero before setting the drum in motion.

**Table 1:** Simulation parameters in this work and two related studies.

Description (unit)	This work	Dury Ristow (1999)	Schutyser et. al. (2002)
Radius particle $a$ , $r_a$ (mm)	1.0	1.0	4.9
Radius particle $b$ , $r_b$ (mm)	1.5	1.5	-
Total volume fraction $a/b$	1	1	monodisperse
Number ratio $N_a/N_b$	3.375/1	3.375/1	monodisperse
Specific gravity $\rho$ ( $\text{kg m}^{-3}$ )	2500	2500	2900
Restitution coefficient particle-particle $e_v$ (-)	0.831	0.831	0.1
Restitution coefficient particle-wall $e_v$ (-)	0.9	0.9	0.1
Dynamic interparticle friction coefficient $\mu$ (-)	0.5	0.19	0.5
Dynamic particle-wall friction coefficient $\mu$ (-)	1.5	0.6	1.5
Viscous interparticle friction coefficient $\eta_t$ ( $\text{kg s}^{-1}$ )	1.0	-	1.0
Viscous particle-wall friction coefficient $\eta_t$ ( $\text{kg s}^{-1}$ )	3.0	-	3.0
Stiffness coefficient $k_n$ ( $\text{Nm}^{-1}$ )	125	60000	125
Time step $\Delta t$ (s)	$2 \cdot 10^{-6}$	variable	$2 \cdot 10^{-5}$
Fill level (%)	variable	variable	variable
Rotation speed drum $\omega$ ( $\text{rad s}^{-1}$ )	variable	variable	variable
Drum length $L$ (mm)	25	25	220
Drum radius $R$ (mm)	35	35	350

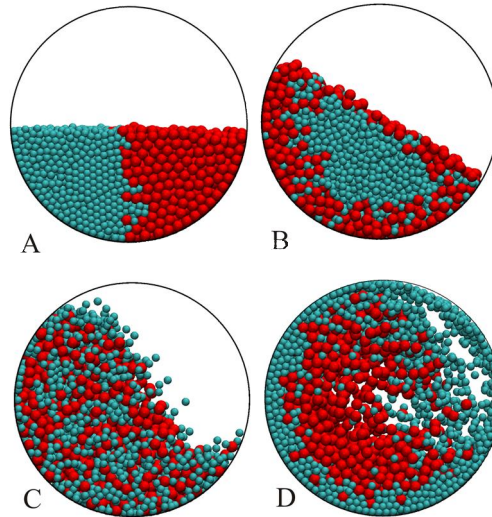


**Figure 3:** Four snapshots depicting cross-sections of half-filled drums at various angular velocities of the drum, with the large (small) particles drawn in dark (light) gray. The four pictures correspond to the four marked points in Figure 4, showing (A) the blockwise segregated starting configuration, (B) a radially segregated drum in the rolling regime, (C) a well mixed bed in the cascading regime and (D) an inverse segregated drum in the cataracting regime.

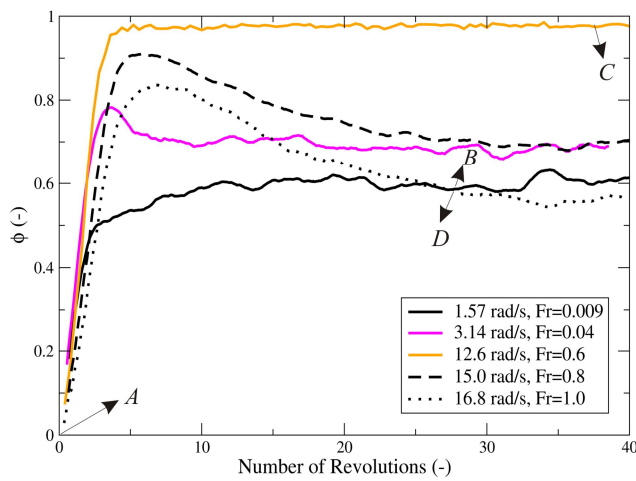


**Figure 4:** The degree of mixing, as calculated by the entropy method discussed in section 2.2, plotted against the number of drum revolutions at five angular velocities. The simulations start with a blockwise segregated drum, at 50% fill level. Snapshots of the bed at the four marked points are presented in Figure 3.

---

**METHODS OF ANALYSIS**
***Characterization of mixing***

To quantify the time dependent degree of mixing or segregation, an adaptation of the method developed by Schutyser (Schutyser *et al.*, 2001; Schutyser *et al.*, 2002) was used. The method is straightforward, suitable for any reactor geometry and has a convenient interpretation. In this method a grid of  $n_x \times n_y \times n_z$  cells is defined, in general, where in the current drum geometry  $n_x$  is chosen equal to  $n_z$  and  $n_y=1$ , see Figure 2. For every time step the local entropy  $s(\mathbf{k})$  in each grid cell  $\mathbf{k}=(k_x, k_y, k_z)$  is calculated using Boltzmann's expression

$$s(\mathbf{k}) = x_a(\mathbf{k}) \ln x_a(\mathbf{k}) + x_b(\mathbf{k}) \ln x_b(\mathbf{k}), \quad [13]$$

where  $x_x(\mathbf{k})$  is the number fraction of particles of type  $x$  in cell  $\mathbf{k}$ . The local entropy is defined to be zero if the cell contains no particles, or particles of one type only. The local entropies are then weighted by the number of particles in that cell,  $n(\mathbf{k})$ , to yield the global entropy at time  $t$ ,

$$S(t) = \frac{1}{N} \sum_{\mathbf{k}} s(\mathbf{k}, t) n(\mathbf{k}, t), \quad [14]$$

where  $N = \sum_{\mathbf{k}} n(\mathbf{k})$  is the conserved total number of particles. The global entropy is finally normalized, relative to the average global entropies  $S_{\text{mix}}$  of perfectly mixed and  $S_{\text{seg}}$  of perfectly segregated systems, to determine the mixing parameter

$$\phi(t) = (S(t) - S_{\text{seg}}) / (S_{\text{mix}} - S_{\text{seg}}). \quad [15]$$

The global entropies of the two reference states are calculated by running the above procedure on sets of randomly created homogeneously mixed and fully segregated systems. This normalization procedure leads to a conveniently scaled mixing parameter, with  $\phi=1$  for a mixed system and  $\phi=0$  for a fully segregated system. In contrast to several earlier methods (Metcalf *et al.*, 1995; Dury and Ristow, 1997) the current method is readily applied to different types of segregation. For small cubic grid cells,  $\{n_x, n_y, n_z\} > 1$ , the method detects any kind of segregation; using bar-like cells aligned along the cylinder axis,  $\{n_x, n_z\} > 1$  and  $n_y=1$ , makes the method specific for radial segregation; slices

perpendicular to the cylinder axis,  $n_x=n_z=1$  and  $n_y>1$ , render the technique sensitive to axial segregation. We emphasize that this mixing parameter is not meant as an exhaustive characterisation of the ordering in the system. For example, a radially segregated state with a core of small particles will have approximately the same mixing parameter as the inverted segregated state with a core of large particles (Figure 3 and Figure 4). After visual inspection of snapshots and movies made from the simulations with the VMD package (Humphrey *et al.*, 1996), we defined a system as ‘mixed’ at  $\phi > 0.9$  and as ‘segregated’ at  $\phi < 0.65$ , with intermediate values indicating a partially segregated state.

To evaluate the influence of the grid dimensions on the mixing parameter, we calculated  $\phi$  for one simulation using a variety of grid sizes. As Table 2 shows, grids containing  $10^2$  to  $28^2$  cells yield nearly identical mixing parameters of  $0.57 \pm 0.03$  in the steady state. Grids of less than  $10^2$  cells yield a spurious rise of the mixing parameter, indicating that they are too coarse to capture the segregated structure. For grids with more than  $28 \times 28$  cells, the cells do not contain sufficient particles to be representative and the entropy of the well-mixed state  $S_{\text{mix}}$  deviates too much from the theoretical value of  $-0.54$ . Moreover, the widths of these cells are smaller than the diameter of the bigger particle. In this article we have chosen for a grid of  $12 \times 12$  cells.

To establish the reproducibility of our simulations results and to estimate the confidence interval of the mixing parameter, changing the seed of the random number generator, yet macroscopically identical block-wise segregated configurations created a dozen microscopically distinct. The simulations started from these configurations display very similar dynamics, with inter-simulation fluctuations in  $\phi(t)$  characterised by a standard deviation of about 0.03 at any time  $t$  after the start of the simulation. It appears, therefore, that the evolution on the macroscopic level is rather insensitive to the microscopic details, and hence the process is sufficiently repeatable to be of practical relevance. We will consider configurations to be equivalently mixed if their mixing parameters differ by less than 0.03.

**Table 2:** Influence of the number of grid cells on the mixing parameter  $\phi$  in the steady state of a simulation with fill level 50%,  $\omega=1.57\text{rad/s}$  and other parameters as in Table 1. The entropies  $S_{seg}$  and  $S_{mix}$  are obtained by averaging over sets of randomly produced segregated and mixed configurations, respectively, under identical conditions.

Nr of cells $n_x \times n_z$	Cell size (mm)	Nr of particles per cell	$\phi$	$S_{seg}$	$S_{mix}$
16	18	491	0.77	-0.09	-0.54
36	12	233	0.67	-0.08	-0.54
64	9	143	0.64	-0.07	-0.53
100	7	98	0.60	-0.06	-0.53
144	6	70	0.58	-0.06	-0.53
196	5	51	0.58	-0.06	-0.53
256	4	41	0.57	-0.05	-0.52
324	4	32	0.56	-0.05	-0.52
400	4	26	0.56	-0.05	-0.52
484	3	22	0.56	-0.05	-0.51
576	3	19	0.55	-0.05	-0.51
784	3	14	0.54	-0.04	-0.50
1296	2	9	0.52	-0.04	-0.46

\* Entropy after 35 revolutions

### ***Bed expansion***

Bed density plots give impressions of the global and local expansions of the bed and the distribution of voids during mixing and segregation. The drum is divided into  $28 \times 28$  cells along the  $xz$  plane and the occupied volume per cell is averaged over the last 10 revolutions of the simulations. These values are then normalized by the accessible volumes of the cells, to account for the restrictions posed by the hard walls. Density plots in which only one type of particle is taken into account (not shown) clearly illustrate the radial cores of small particles for low rotational speeds and of large particles for high angular velocities of the drum. Because of the quasi-2D geometry of the drum, we do not observe any appreciable axial segregation in analogues density plots along the  $xy$  and  $yz$  planes (not shown).

### ***Local velocities***

Velocity vector plots are made with the same grid cells, using a mass-weighted average of the particle velocities in the  $x$  and  $z$  directions. These plots clearly

illustrate where the motion of the granular bed deviates from a solid body rotation around the axis of the drum. The net segregation/mixing flux is nicely visualized as the difference between the local average velocities of large and small particles. These velocity difference plots are made for homogeneously mixed systems, in which the averaging covers only a short time span before significant de-mixing sets in. For clarity, grid cells containing merely one type of particles are omitted in the difference plots. To study the effect of dispersion by random collisions (also called random collision diffusivity), we have also calculated the standard deviations of the  $x$  and  $z$  velocity components of the particles, per particle type and per cell.

### **MODEL VALIDATION**

The results for a rotational speed of a quarter revolution per second, corresponding to the rolling regime, compare very well against the results obtained by Dury and Ristow (Dury and Ristow, 1999) under similar conditions, although we use different expressions for the interparticle and particle-wall friction forces (results by visual inspection; not shown). We therefore conclude that the corrections for rolling friction and adjustment of the particle-wall friction applied by Dury and Ristow are of limited influence to the evolution of the bed.

A number of general observations on the rolling regime, which the bidisperse system shares with the monodisperse systems of Nakagawa (Nakagawa *et al.*, 1993), are illustrated in Figure 5. We see that the bed can roughly be divided in two parts, see Figure 5B: the passive bulk in which particles undergo solid body rotation around the cylinder axis and the active layer in which the particles undergo collective linear translation due to the sliding motion. In the latter layer the particles also experience a diffusional/random motion relative to each other, resulting from interparticle collisions (Figure 5A). The bed density increases moving along the surface normal from the free surface of the bed down to the passive bulk, see Figure 5A. The velocity parallel to the free surface varies along the flowing layer with a maximum approximately halfway down the slope, see Figure 5B, where the layer thickness and the diffusional motion also reach a maximum, see Figure 5A and Figure 6A. Similar results have been obtained in experiments on bidisperse and monodisperse systems (Nakagawa *et al.*, 1993), strengthening our confidence in the model.

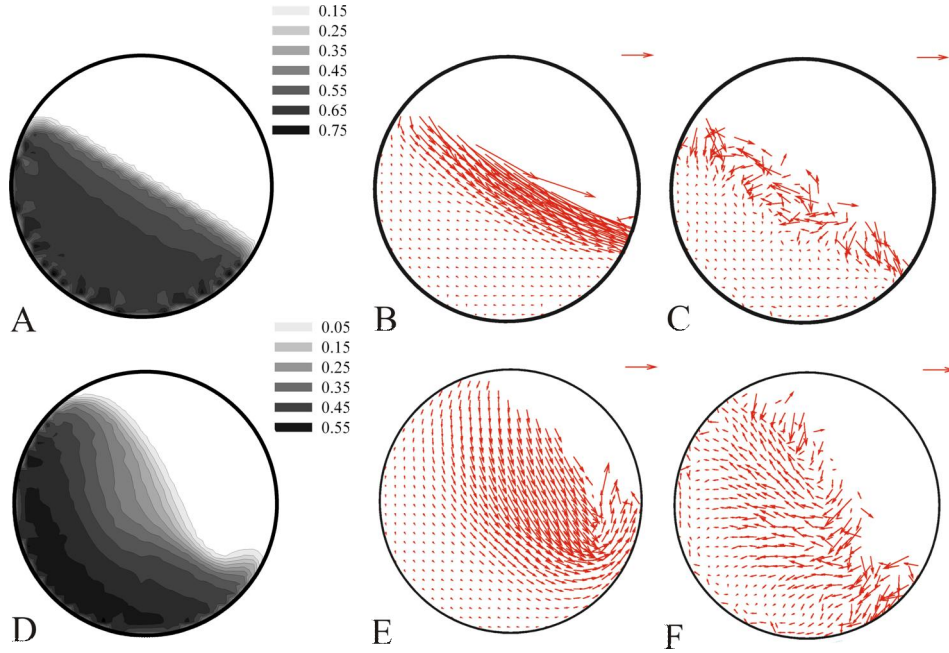


**Figure 5:** Analysis of the bed properties in a rotating drum at 50% fill level, for angular velocities in the rolling regime (1.57 rad/s ; plots **A**, **B** and **C**) and the cascading regime (12.56 rad/s; plots **D**, **E** and **F**). From left to right: the local density of the bed (plots **A** and **D**), the average velocity of the particles relative to a rigid body rotation ( $\mathbf{v}_i - \boldsymbol{\omega}_d \times \mathbf{r}_i$ ; plots **B** and **E**, with the reference vectors in the top right corner representing 0.1 and 0.8 m/s respectively), and the segregational velocity difference between small and large particles ( $\mathbf{v}_a - \mathbf{v}_b$ ; plots **C** and **F** with the reference vectors in the top right corner indicating 0.01 and 0.03 m/s, respectively).

In previous studies, it has been assumed that the Froude number unequivocally characterizes the flow regimes,

$$Fr = \omega_d^2 (R_d - r_x) / g, \quad [16]$$

with  $\omega_d$  the angular velocity of the drum and  $g$  the gravity acceleration. To validate this assumption, three simulations were performed at  $Fr = 0.14$ ,  $0.56$  and  $0.8$  by varying the rotational speed of the drum at fixed standard acceleration of  $g = 9.81 \text{ m/s}^2$ . Three additional simulations were performed at identical  $Fr$  values by varying the gravitational acceleration at a constant rotational speed of a quarter revolution per second.

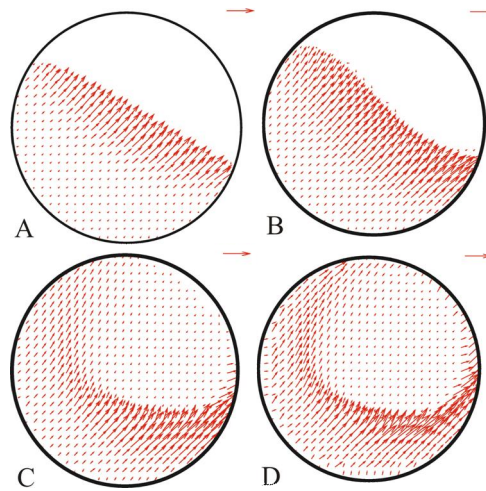


**Figure 6:** Vector plots of the standard deviations in the particle velocities, for 50% filled drums in a steady state at (A) 1.57 rad/s, (B) 6.28 rad/s, (C) 16 rad/s and (D) 18 rad/s. The x and z components of the vectors represent the standard deviations in the local particle velocities along the x and z directions, respectively. The reference vectors in the four plots correspond to 1/80, 1/60, 1/35 and 1/50 m/s respectively.

In Figure 7 we see small differences between each pair of mixing parameter curves at identical  $Fr$ , especially in the first five revolutions at the largest  $Fr$  value. Apparently, the process dynamics at high  $Fr$  values are not completely characterized by this dimensionless number, but since this effect is small it is disregarded and  $Fr$  will be used in this study as the parameter determining the flow regime.

## RESULTS AND DISCUSSION

In this section the results of our simulations are presented and discussed. The two operational parameters of the system, namely the angular velocity and the fill level, have been varied systematically to study their impact on (the evolution of) the mixing/segregation process; all other system parameters are kept fixed as stated in Table 1. The first subsection describes the effect of the drum velocity for a half filled drum, the next subsection analyses the influence of the fill level at constant angular velocity, and in the third subsection both parameters are varied systematically to scan the parameter space.

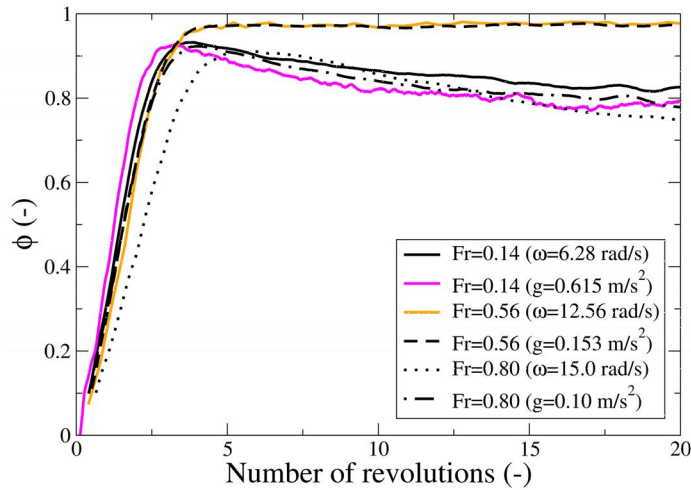


**Figure 7:** The order parameter as a function of time, illustrating the effect of the Froude number on the mixing dynamics of the half-filled drum. The Froude number was varied either by changing the angular velocity of the drum (at  $g=9.81 \text{ m/s}^2$ ) or by changing the gravitational acceleration (at  $\omega=1.57 \text{ rad/s}$ ).

### ROTATIONAL VELOCITY

The angular velocity of the drum is an important operational parameter. We first study its influence on the segregation and flow regimes in the steady state, followed by a discussion of how the various flow regimes may explain the evolutions of the distinct segregated states.

### STEADY STATE

The steady state mixing parameter  $\phi$  of a half-filled drum in the steady state, i.e. after 30 revolutions, is depicted in Figure 8 as a function of the Froude number. The degree of mixing first increases with the rotational speed, exhibits a broad maximum, and then rapidly decreases again. Visual inspection of the simulations reveals that these three regimes roughly coincide with three different ordering regimes and with three different flow regimes; the latter are identified using the criteria of Mellman (Mellman, 2001). At relatively low rotational speeds radial segregation takes place ( $10^{-4} < Fr < 0.023$ ; region RS in Figure 8), while the flow profile is characteristic of the rolling regime ( $10^{-4} < Fr < 0.035$ ; region RO in Figure 8). At intermediate speeds the system mixes relatively well ( $0.25 < Fr < 0.68$ ; region MX in Figure 8). The flow profiles observed in this regime are indicative of cascading ( $0.12 < Fr < 0.46$ ; region CS in Figure 8), with a gradual

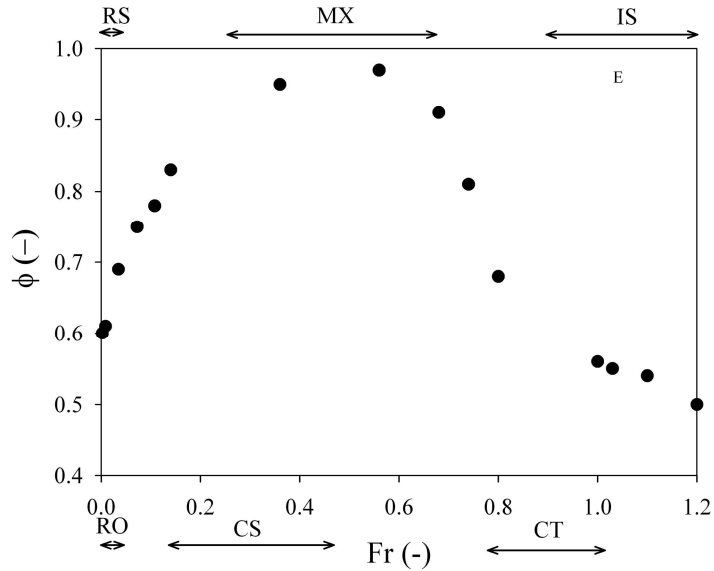


**Figure 8:** The mixing parameter  $\phi$  of the steady state in half-filled drums with various rotational velocities, plotted against the corresponding dimensionless Froude number. The ranges of different flow regimes are marked at the bottom, with “RO” denoting rolling, “CS” for cascading and “CT” for cataracting. At even higher Froude numbers,  $1.0 < Fr < 2.23$ , the cataracting-centrifuging regime is observed, finally progressing into a centrifuging regime for  $Fr > 2.23$ . The ordering regimes are highlighted at the top, with “RS” for radial segregation, “MX” for mixing and “IS” for inverted segregation.

transition to cataracting ( $0.46 < Fr < 0.68$ ). At high rotational speeds inverted segregation sets in ( $0.85 < Fr < 1.4$ ; region IS in Figure 8), coinciding with the cataracting profile ( $0.77 < Fr < 1.0$ ; region CT in Figure 7) and the transition flow profile between cataracting and centrifuging flow ( $1.0 < Fr < 2.23$ ). Please note that this latter system may not completely have reached steady state yet due to its slow re-ordering dynamics. With increasing angular velocity the centrifuging regime ( $Fr > 2.23$ ; not shown in Figure 8) is established. In this regime the whole system is stagnant with the centrifuging particles forming a layer covering the entire wall. The observed relation between the flowing regime and the segregation/mixing process will be investigated further in the next section.

---

## SEGREGATION PROCESSES

In this paragraph we focus on the formation process of the steady states for the different flow regimes.

### *Rolling*

In the rolling regime, segregation is believed to proceed by selective percolation of the smaller particles through the flowing layer (Savage and Lun, 1988). Due to the motion of the particles rolling down the inclined surface (Figure 5B), the top layer has expanded (Figure 5A), resulting in a relatively high porosity in comparison to the bulk of the bed. By virtue of their size, small particles have a higher chance of falling downwards through a pore than the large particles. This leads to a difference in average velocities between the small and large particles in the flowing layer as illustrated in Figure 5C. This segregation is visible throughout the flowing layer by the downward pointing arrows, except for a thinly populated top layer without systematic segregation. From Figure 5B it can be seen that the passive bulk of the bed mainly rotates uniformly with the drum, and therefore no segregation or mixing takes place in this part of the bed (see also Figure 6A).

### *Cascading*

Increasing the rotational speed of the drum to the cascading regime leads to an increase in the thickness of the flowing layer (Figure 5D). This expansion, especially in the top left part of the flowing layer, implies the presence of many large voids, which makes the percolation mechanism less selective on the particle size, see Figure 5F, and causes mixing of the particles. The transient part of the mixing curve is independent of the drum velocity within the cascading regime, from 5 to 12 rad/s, while the plateau value gradually increases with the rotational velocity of the drum.

At this point, it is interesting to temporarily eliminate the steric effects from the simulations. We therefore briefly focus on a *monodisperse* system with particles of the smaller type. The particles are assigned a colour depending on their initial positions in the drum, thus creating a block-wise start configuration. We observe that with increasing rotational speeds of the drum, up to 5 rad/s, fewer drum rotations are needed to obtain a mixed state, see Figure 9. In the cascading regime, ranging from 5 to 12.56 rad/s, however, the mixing profile  $\phi$  is

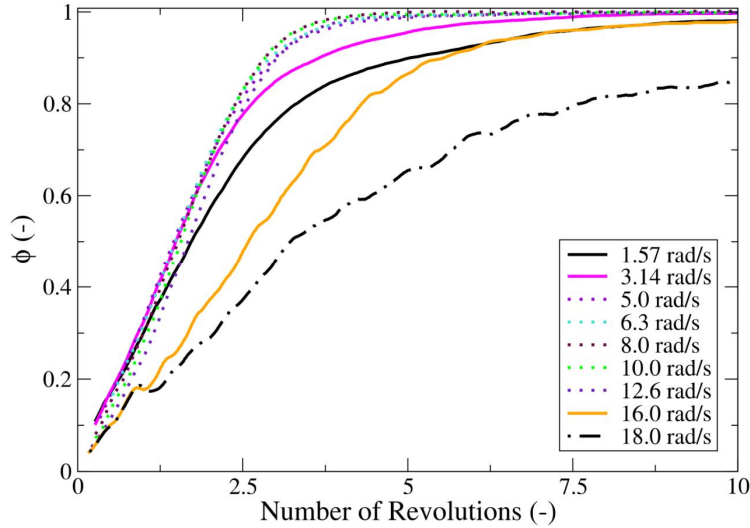


**Figure 9:** The mixing behaviour of a 50% filled monodisperse system containing equal amounts of red and blue particles in a block-wise segregated starting configuration, for various angular velocities of the drum. Note that the curves for  $\Omega = 5$  to 12.6 rad/s are identical to within about 0.03.

independent of the angular velocity. This constant profile coalesces with the mixing curve of the bidisperse system at  $\omega=12.56$  rad/s, suggesting that the mixing process has become insensitive to the particle sizes at this particular velocity and fill level. At even higher angular velocities the system requires increasingly more revolutions to reach its steady state. We now discontinue the discussion of the monodisperse system, and return to the regular system with *bidisperse* particles.

### ***Cataracting***

In the cataracting regime the flowing layer is characterized by particles from the bed being flung into the previously void space above the bed (Mellmann, 2001), as shown in Figure 9 a through c. The flowing layer can now be subdivided into three distinct regions. From left to right, we first pass a region where particles are thrown into free space by the high velocities acquired in the bed. The particles nearest the drum wall have the highest velocities, reach the highest altitude and are thrown the furthest. Next comes a region where the velocities are too low to throw the particles, and instead the particles roll down the steeply inclined

flowing layer, see Figure 9a-b. This rolling motion is also evident from Figure 10a, where the distribution of the average angular velocity component  $\omega_{i,y}$  parallel to the drum axis is depicted. In the third region of the flowing layer, at the bottom right of the drum, the rolling and flying particles meet again to settle into a densely packed bed for the next revolution. After a number of revolutions a steady state of inverted segregation is reached, with the small particles concentrated on the outside and the large particles on the inside of the drum.

It has been argued (Eskin and Kalman, 2000b; Turner and Nakagawa, 2000) that the key to inverted segregation lies in two mass-related phenomena: gravity causing particles to fall down and inertia giving rise to centrifugal effects. The former dominates at the low angular drum velocities in the rolling and cascading regimes, where regular radial segregation or mixing is observed, while the latter takes precedence at the higher drum velocities in and beyond the cataracting-

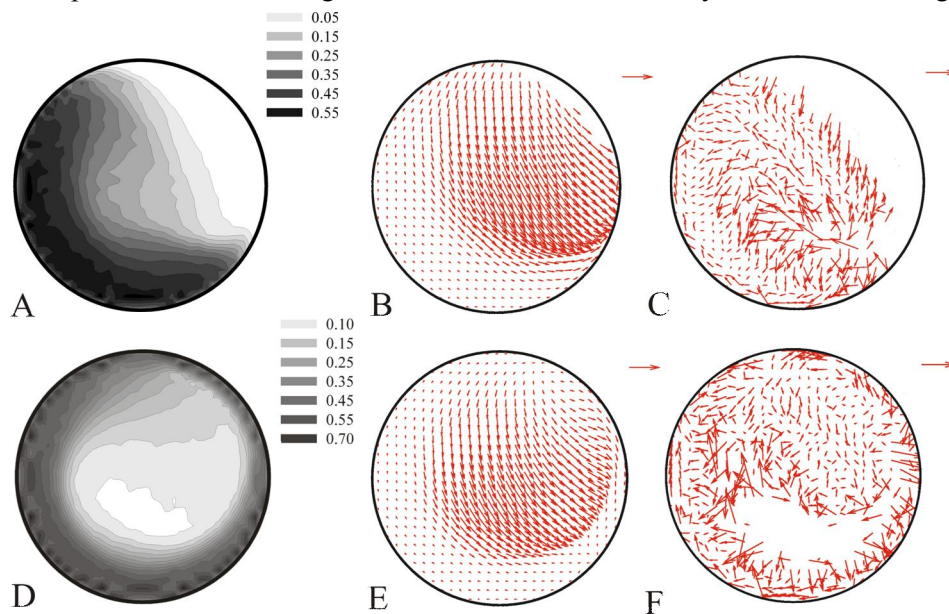


**Figure 10:** Analysis of the bed properties in rotating half full drums in the cataracting regime (15 rad/s ; plots **A**, **B** and **C**) and the cataracting-centrifuging regime (19 rad/s; plots **D**, **E** and **F**), showing the density (**A** and **D**), relative velocity (with the reference arrows in the top right corner representing 0.73 and 0.76 m/s, respectively) and velocity difference (**C** and **F** with the reference arrows in the top right corner indicating 0.024 and 0.019 m/s, respectively). See the caption of figure 5 for more details.

centrifuging regime, which display inverted segregation. A balance between the two is reached at  $Fr=1$  (see also equation 16), corresponding with the critical angular velocity  $\omega_c$  at which the outermost layer of particles starts to centrifuge. The particle radius dependence of  $\omega_c$  instigated (Turner and Nakagawa, 2000) to suggest that inverted segregation arises because the centrifugal effects are slightly stronger for the smaller particles than for the larger particles. In the current system these critical angular velocities are  $\omega_{c,a}=16.99$  rad/s and  $\omega_{c,b}=17.11$  rad/s, suggesting that the difference is probably too small to explain inverted segregation. We furthermore note that inverted segregation is already observed at 15.5 rad/s ( $Fr = 0.85$ ), well below the critical angular drum velocity of either particle.

For new insights into the physics of the segregation process we return to the distributions depicted in Figure 10. The velocity difference plot of Figure 10C shows a pronounced region of separation activities near the bottom and bottom right of the drum, where the smaller particles are moving down relative to the large particles. This region roughly coincides with the settling region in the above discussion of the flowing layer, and with a low-density region in Figure 10A. It appears therefore that inverted segregation is caused by small particles percolating through the voids in an expanded bed, i.e. the same mechanism also underlying regular radial segregation. The main difference between the two segregation processes is the location of the percolation region. In the rolling regime the percolation takes place along the entire length of the flowing layer, i.e. the full width of the drum, with the smaller particles sinking down until they reach the denser central core of small particles. In the cataracting regime the percolation occurs mainly at the right side of the drum, where the small particles sinking down quickly reach the drum wall. We believe, therefore, that a single mechanism explains both regular and inverted segregation.

### ***Cataracting-centrifuging***

The cataracting-centrifuging regime has similar characteristics to the cataracting regime, see Figure 10D through F and Figure 11B, with the main difference that some particles stack into one or more closely packed centrifuging layers covering the entire wall, while the remaining particles still form a bed in the cataracting regime. Combining Figure 10D and 10F, one sees that percolation of the smaller particles is now predominantly taking place at the right and bottom side of the

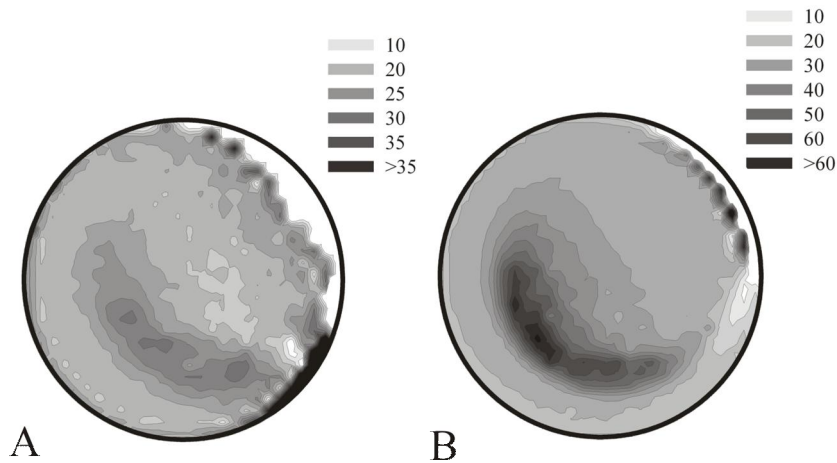


**Figure 11:** Distribution of the axial ( $y$ ) component of the angular velocities of the particles for drum angular velocities of 15 rad/s (left) and 19 rad/s (right). Note that the particles in the regions of low density,  $<0.05$  volume fraction near the top right for 15 rad/s and just below the centre at 19 rad/s, are spinning with the highest angular velocities.

drum, but the relatively high particle density in this region makes it a tedious process, and hence inverted segregation is established only very gradually. This again suggests that the main mechanism of inverted segregation is percolation, rather than the difference in critical rotational speed. At increasing angular drum velocities the fraction of particles in centrifuging layers increases, these layers become denser and more immobilised, making percolation an increasingly unlikely process. The reduced transport in this regime is also seen in the monodisperse system (Figure 9). Higher angular drum velocities effectively immobilise the particles, trapping the system in a state of incomplete inverted segregation.

### ***Initial mixing***

The percolation mechanism may also explain the transient dynamics of the mixing parameter, whose typical development can be seen in 3. Starting from a block-wise segregated configuration with  $\phi = 0$ , the mixing parameter passes through a maximum before reaching a steady state. From visualising numerous simulations, the general picture emerges that the block-wise segregated bed is always being mixed thoroughly in the first couple of revolutions of the drum. A

less-dense flowing layer containing a mix of particles gradually develops at the top of the bed, before the percolation mechanism becomes effective and starts segregating the particles in the flowing layer according to their radii. The transient peak in the mixing parameter curves reflects this sequence of events. In the rolling and cascading regimes the initial mixing process proceeds more vigorous at higher rotational speeds, while the lower density of the flowing layer makes the percolation process less discriminative to particle size, thus causing the higher transient peak of the mixing parameter. At all velocities beyond the rolling regime, the decay from the peak maximum to the steady state plateau increases with the drum velocity. Swapping the large and small particles in the block-wise segregated starting configuration (or rotating the drum in the opposite direction) does not change the outlined mechanism.

For angular drum velocities in the cataracting regime and beyond, an additional effect starts contributing to the initial mixing of the particles. Due to the limited traction between the drum wall and the granular bed, it takes some time before the particles in the dense bottom of the bed have adjusted to the instantaneously introduced angular velocity of the drum, i.e. till  $\mathbf{v}_i \approx \boldsymbol{\omega}_d \times \mathbf{r}_i$ . This transient regime characterized by pronounced slippage at the wall, which will be more pronounced and longer lived at higher angular drum velocities, appears to contribute to the mixing of the particles. Consequently, it might be possible to improve the degree of mixing by prolonging this slip regime. To validate these statements, we simulate two drums whose rotational velocities of 6.28 rad/s and 15 rad/s respectively are alternated after every  $w$  revolutions, with  $w$  ranging from 1.5 to 6. In the case of a drum velocity of one revolution per second, the effects of periodic rotation reversals are rather limited as can be seen from Figure 12. Noticeable deviations from the clock-wise rotating reference system are only observed under frequent reversals, for  $w=1.5$  and 2.5, which are found to slow down the mixing behaviour. Yet, after a dozen revolutions (ignoring the rotation direction) all alternating systems have converged to the same steady state as the reference system. The effects of alternating rotation directions are more pronounced at the higher drum velocity of 15 rad/s, see Figure 13, where the steady state degree of mixing steadily increases with the alternation frequency. Note that the mixing parameter still passes through a maximum, after 5 to 10 revolutions, before a gradual decrease sets in. Extending these simulations to nearly 70 revolutions confirms that the steady states have been reached, and

hence that the higher degree of mixing at lower  $w$  is not caused by a temporarily slowing down of the segregation.

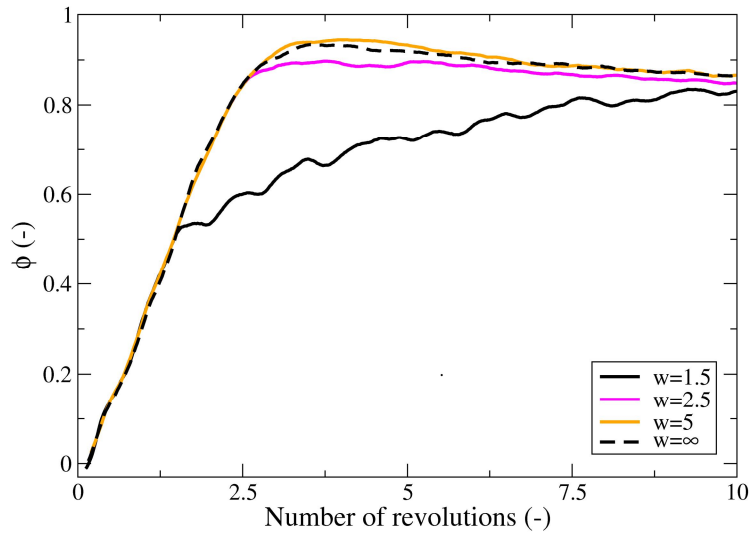


**Figure 12:** Reversing the rotational direction of the drum every  $w$  revolutions, in half-filled drums rotating at  $\pm 6.28$  rad/s, affects the evolution of the order parameter while the steady state remains essentially unaltered.

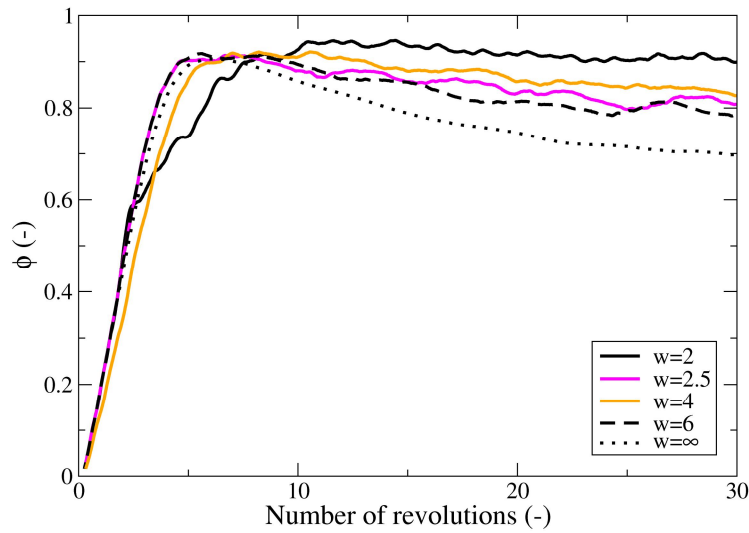


**Figure 13:** Reversing the rotational direction of the drum every  $w$  revolutions, in half-filled drums rotating at  $\pm 15$  rad/s, intensifies the steady state degree of mixing.

### FILL LEVEL

Besides the angular velocity of the drum, the fill level of the drum offers a second easily controlled experimental parameter in the mixing or segregation of granular matter. Figure 14 presents the evolutions of mixing parameters in simulations with fill levels ranging from 25% to 80%, in a drum rotating at 1.57 rad/s. The initial parts of these curves are similar to the results presented by (Dury and Ristow, 1997), who simulated only the first 5 to 8 revolutions. At the low fill fraction of 25% the particle bed is forced to turn over quicker than the drum, resulting in vigorous motions that keep the bed in a mixed state (Ottino and Khakhar, 2000). Higher fill fractions of about 50% see a less active bed, a decrease in the mixing velocity and a lower final mixing parameter. These two curves are approximated reasonably well by an exponential saturating function,  $\phi(t) = \phi_{\infty} (1 - e^{-t/t_c})$ , with  $t_c$  the characteristic relaxation time and  $\phi_{\infty}$  the steady state mixing parameter (Dury and Ristow, 1999). As discussed before: while the blockwise segregated bed is being mixed during the first couple of drum revolutions, a gradual build-up of a mixed flowing layer activates the percolation mechanism which in turn results in the exponential approach of the steady state.

The above sequence of events changes at the highest fill fractions ( $\geq 69\%$ ). Since the initial mixing process is most effective near the top layer of the bed, which

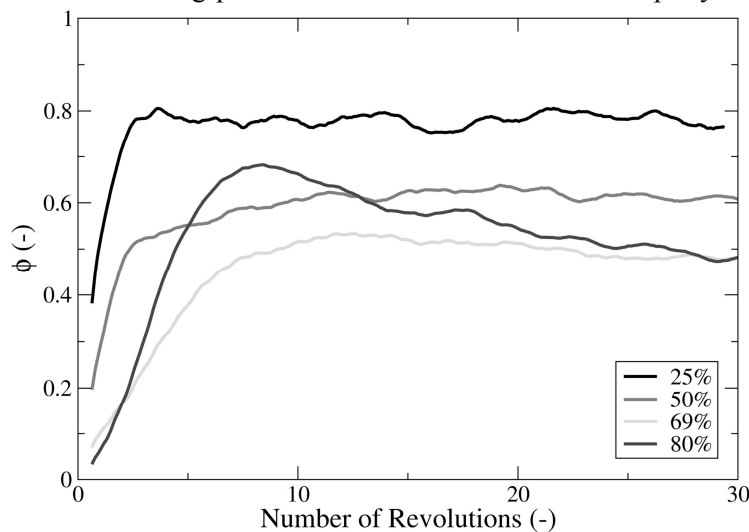


**Figure 14:** Development of the mixing parameter in drums of various fill levels, all rotating at 1.57 rad/s.

now constitutes a relatively small fraction of the total bed, it is becoming difficult to mix the entire bed. After several revolutions the outside region of the bed is reasonably mixed, while the centre of the drum is still in its pristine condition. This unmixed core continues to perform solid body rotations, while the outside region is gradually segregating. Once in a while a large particle drifts away from the core and slowly moves towards the drum wall over many revolutions. Consequently, the unmixed core gradually disappears due to the small residual frictional forces within the bulk of the bed. The mixing curves at these high fill levels show a pronounced local maximum after about 8 revolutions, see the curve for 80% fill level in Figure 14, coinciding with the mixed outside region, followed by a slow decrease due to segregation of the outside region and the even slower disappearance of the unmixed core. These curves can therefore not be fitted adequately by a single exponential relaxation function. Although it is not clear whether a steady state has been reached after the simulated 30 revolutions, the plot strongly suggests that the final degree of mixing  $\phi_\infty$  at 80% fill level will be at least as low as for a 69% fill level. This conclusion is at variance with the prediction by (Dury and Ristow, 1999) that the optimum degree of segregation is obtained at a fill level of about 65%, which was based on extrapolations of their short simulations using the above saturation function.

#### **ROTATIONAL SPEED AND FILL LEVEL**

As discussed in the preceding two subsections, both the velocity of rotation and the fill level of the drum affect the dynamics and the mixing or segregation of the granular bed. To investigate their combined impacts on these processes, we have performed approximately 50 simulations with angular velocities ranging from 1.57 rad/s to 28 rad/s and fill fractions between 25% and 92%. Each run typically lasted for 35 to 50 revolutions, allowing the systems sufficient time to reach their steady states. The results of these simulations are collected in Figure 15. The left state diagram in Figure 15 shows the flow regime as a function of the Froude number and the fill factor.

Mellmann (Mellmann, 2001) extensively discusses the state diagrams of monodisperse systems, comparing theoretical models with experimental findings on near-monodisperse gravel, limestone and sand for fill levels up to 50%. The experimental state diagrams are qualitatively very similar, and also show a remarkable resemblance to our simulation results on bidisperse systems. It appears, therefore, that the global structure of the state diagram is rather

insensitive to the size distribution of the particles in the granular bed. Figure 15 depicts at the right a state diagram of the segregation in the steady state, again as a function of the Froude number and the fill factor. Comparing this segregation diagram with the flow diagram of Figure 15, we note an overall strong resemblance, providing additional support for the correlation between flow regime and segregation pattern. The most pronounced differences are found for low Froude numbers in combination with low fill factors, where the high turnover rate of the bed relative to the drum causes mixing of the bed.

Figure 16 shows the mixing parameter as a function of the Froude number for a series of fill levels. At any given fill level, the degree of mixing at first improves with increasing velocity of rotation, passes through a maximum, and then decreases again. The Froude number yielding the maximum degree of mixing gradually rises from about 0.1 at 25% filling to 0.7 for a 80% filled drum, while the width of the region with near-maximum mixing strongly decreases with the fill level. The granular bed displays radial segregation for Froude numbers below the broad maximum, while Froude numbers at the opposite side of the maximum create inverted segregated beds (not visible from the plot).

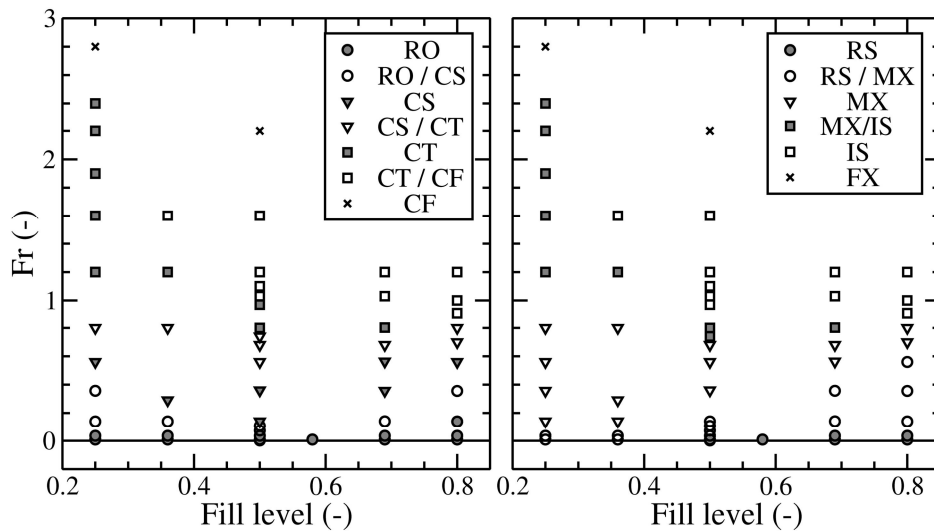


**Figure 15:** State diagrams of the flow regime (left) and the segregation state (right) plotted against the fill fraction and the Froude number. The markers are used to indicate different stationary states, see the legends to the plots.

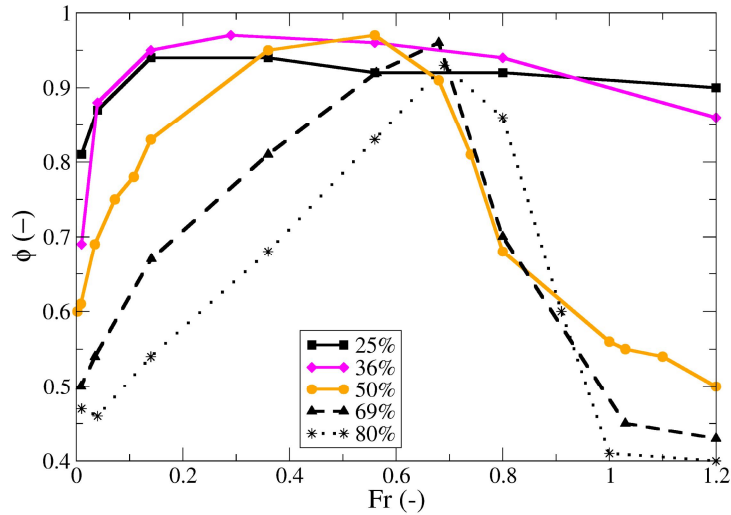


**Figure 16:** The mixing parameter of the steady state as a function of the Froude number, for various fill factors.

The highest fill level in our simulations is 92%, but these results have been excluded from the phase diagrams in Figure 15 for clarity. On the one hand, the segregation process proceeds very slowly at these high fill levels, because there is hardly any space available to shuffle the particles.

Even after 100 revolutions we are not sure whether the beds have reached their steady states. On the other hand, these runs reveal a number of new segregation forms, making the phase diagram even more complex. At Froude numbers between 0.8 and 1.1 the bed displays double segregation: an inner core of small particles and an outer ring of small particles are separated by a ring of large particles, see Figure 17A. The ring of large particles starts to contain small particles at  $Fr=1$ . Figure 17D shows how the ring and core have merged at  $Fr=1.3$  (19 rad/s) to form a large mixed region.

One may speculate that this system evolves very slowly, and hence that a continuation of the run beyond the current 100 revolutions might show a further development into an inversely segregated state. The velocity plots in Figure 17 show that the beds are again performing solid body rotations, except for the flowing layer in the top right region of the drum. The velocity difference plots

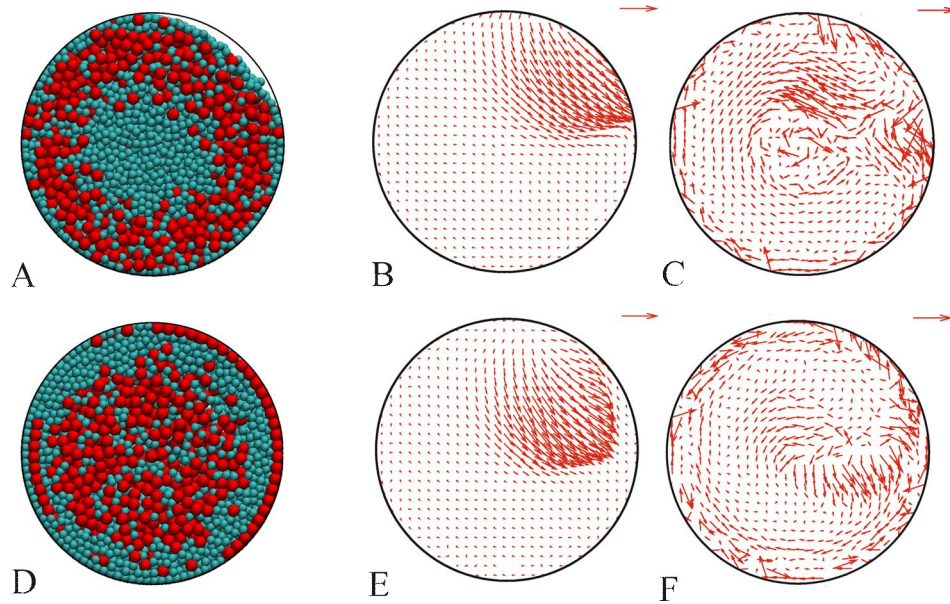


**Figure 17:** Analysis of the bed properties in rotating 92% filled drums in the cataracting regime (16 rad/s; plots **A**, **B** and **C**) and the cataracting-centrifuging regime (18 rad/s; plots **D**, **E** and **F**), showing snapshots after 100 revolutions (**A** and **D**), relative velocities (**B** and **E** with the reference arrows measuring 0.3 m/s) and velocity differences (**C** and **F** with the reference arrows indicating 0.05 m/s). See the caption of figure 6 for more details.

are surprisingly rich, with segregation taking place everywhere along the drum wall, in the centre of the drum and in the flowing region.

## CONCLUSIONS

The mixing and segregation of bidisperse granules in a rotating short cylindrical drum have been simulated using the Discrete Element Method (DEM). The influence of two easily tuneable operational parameters of the drum, namely the fill level and the velocity of revolution were investigated. By varying these two parameters, a number of distinct radial segregation patterns are observed in the bed, as well as near homogeneous mixing of the granules. The flow of the granules in the bed also strongly varies with the operational parameters of the drum. Phase diagrams of the segregation pattern and the flow regime, plotted

against the fill level and the drum velocity, are presented in Figure 15. The strong correlation between the two diagrams is indicative of their common origin. A detailed analysis of the granular motions in the various flow regimes, as described in section 3.1, suggests that the segregation is causally linked to the flow regime by a percolation mechanism: the smaller particles are more likely to fall through the voids in the flowing layer than the larger particles. This selective process, repeated over a number of drum revolutions, gives rise to the separation of small and large particles. The flow regime of the granular bed determines the location, size and density of the flowing layer, and thereby also determines the emerging segregation pattern and its rate of formation.

An interesting observation is that the simulation of a half-filled drum displays inverse segregation at a Froude number of approximately 0.8. The granules are not yet centrifuging in this simulation, since this Froude number lies well below unity. This observation is therefore not reconcilable with the previous explanation of inverse segregation as resulting from a small difference in the critical centrifuging velocities of small and large particles. Note that the minimum Froude number for inverse segregation will depend on the fill level and the various other properties of the granules and the drum, and may therefore approach unity in certain systems.

The sieving action of the percolation mechanism can only be active if both small and large particles are present in the flowing layer. A block-wise segregated starting configuration therefore requires several revolutions, during which the particles are being mixed, before the percolation mechanism effectively starts to segregate the particles. Visualization of the simulations clearly shows that block-wise segregated system mix before they segregate radially. This behaviour is also apparent from the time evolution of the degree of mixing, which in many systems rapidly rises to a local maximum after 5 to 10 revolutions before gradually decaying to the steady state value. At fill levels beyond 65% only the outer region of the bed is mixed during the initial revolutions, and an unmixed core remains. These systems segregate very slowly, and only gradually lose their unmixed core. By running long simulations it is observed that these systems eventually segregate better than half-filled drums, in contrast to previous reports. At the highest fill level studied (92%) we observe double segregation at  $0.8 < Fr < 1.1$ , but because of the extreme slow evolution of this system it can not be ruled out that this pattern is of a transient nature.

**REFERENCES**

- Allen, M. P. and Tildesley, D. J.** (1987). *Computer simulation of liquids*. Oxford, U.K., Oxford Science Publications.
- Boateng, A. A. and Barr, B. V.** (1996). Modelling of particle mixing and segregation in the transverse plane of a rotary kiln. *Chemical Engineering Science* **51**(17): 4167-4181.
- Cleary, P. W.** (1998a). Modelling confined multi-material heat and mass flows using SPH. *Applied Mathematical Modelling* **22**(12): 981-993.
- Cleary, P. W.** (1998b). Predicting charge motion, power draw, segregation and wear in ball mills using discrete element methods. *Minerals Engineering* **11**(11): 1061-1080.
- Cleary, P. W., Metcalfe, G. and Liffman, K.** (1998). How well do discrete element granular flow models capture the essentials of mixing processes? *Applied Mathematical Modelling* **22**(12): 995-1008.
- Cundall, P. A. and Strack, O. D. L.** (1997). Discrete Numerical-Model for Granular Assemblies. *Geotechnique* **29**(1): 47-65.
- Donald, M. and Roseman, B.** (1962). Mixing and demixing of solid particles. Part 1. Mechanisms in a horizontal drum mixer. *British Chemical Engineering* **7**: 749-752.
- Dury, C. M. and Ristow, G. H.** (1997). Radial segregation in a two-dimensional rotating drum. *Journal De Physique I* **7**(5): 737-745.
- Dury, C. M. and Ristow, G. H.** (1999). Competition of mixing and segregation in rotating cylinders. *Physics of Fluids* **11**(6): 1387-1394.
- Eskin, D. and Kalman, H.** (2000a). A numerical parametric study of size segregation in a rotating drum. *Chemical Engineering and Processing* **39**(6): 539-545.
- Eskin, D. and Kalman, H.** (2000b). Optimal particle acceleration in a centrifugal rotor-impact mill. *Minerals Engineering* **13**(14-15): 1653-1658.
- Hajra, S. K. and Khakhar, D. V.** (2004). Sensitivity of granular segregation of mixtures in quasi-two-dimensional fluidized layers. *Physical Review E* **69**(3).
- Henein, H., Brimacombe, J. K. and Watkinson, A. P.** (1983a). Experimental-Study of Transverse Bed Motion in Rotary Kilns. *Metallurgical Transactions B-Process Metallurgy* **14**(2): 191-205.
- Henein, H., Brimacombe, J. K. and Watkinson, A. P.** (1983b). The Modeling of Transverse Solids Motion in Rotary Kilns. *Metallurgical Transactions B-Process Metallurgy* **14**(2): 207-220.
- Hill, K. M., Caprihan, A. and Kakalios, J.** (1997). Bulk segregation in rotated granular material measured by magnetic resonance imaging. *Physical Review Letters* **78**(1).
- Hill, K. M., Gioia, G. and Amaravadi, D.** (2004). Radial segregation patterns in rotating granular mixtures: Waviness selection. *Physical Review Letters* **93**(22).
- Hoomans, B. P. B.** (2000). Granular dynamics of gas-solid two-phase flows. Enschede, The Netherlands, University of Twente. **PhD**.
- Humphrey, W., Dalke, A. and Schulten, K.** (1996). VMD: Visual molecular dynamics. *Journal of Molecular Graphics* **14**(1): 33-38.
- Jain, N., Ottino, J. M. and Lueptow, R. M.** (2005a). Combined size and density segregation and mixing in noncircular tumblers. *Physical Review E* **71**(5).
- Jain, N., Ottino, J. M. and Lueptow, R. M.** (2005b). Regimes of segregation and mixing in combined size and density granular systems: an experimental study. *Granular Matter* **7**(2-3): 69-81.

- Khakhar, D. V., Orpe, A. V., Andresen, P. and Ottino, J. M.** (2001a). Surface flow of granular materials: model and experiments in heap formation. *Journal of Fluid Mechanics* **441**: 255-264.
- Khakhar, D. V., Orpe, A. V. and Hajra, S. K.** (2003). Segregation of granular materials in rotating cylinders. *Physica a-Statistical Mechanics and Its Applications* **318**(1-2): 129-136.
- Khakhar, D. V., Orpe, A. V. and Ottino, J. M.** (2001b). Continuum model of mixing and size segregation in a rotating cylinder: concentration-flow coupling and streak formation. *Powder Technology* **116**(2-3): 232-245.
- Mellmann, J.** (2001). The transverse motion of solids in rotating cylinders - forms of motion and transition behavior. *Powder Technology* **118**(3): 251-270.
- Metcalfe, G., Shinbrot, T., McCarthy, J. J. and Ottino, J. M.** (1995). Avalanche Mixing Of Granular Solids. *Nature* **374**(6517): 39-41.
- Nakagawa, M., Altobelli, S. A., Caprihan, A., Fukushima, E. and Jeong, E. K.** (1993). Noninvasive Measurements of Granular Flows by Magnetic-Resonance-Imaging. *Experiments in Fluids* **16**(1): 54-60.
- Nityanand, N., Manley, B. and Henein, H.** (1986). An Analysis of Radial Segregation for Different Sized Spherical Solids in Rotary Cylinders. *Metallurgical Transactions B-Process Metallurgy* **17**(2): 247-257.
- Ottino, J. M. and Khakhar, D. V.** (2000). Mixing and segregation of granular materials. *Annual Review of Fluid Mechanics* **32**: 55-91.
- Rapaport, D. C.** (2002). Simulational studies of axial granular segregation in a rotating cylinder. *Physical Review E* **65**(6).
- Savage, S. B. and Lun, C. K. K.** (1988). Particle-Size Segregation in Inclined Chute Flow of Dry Cohesionless Granular Solids. *Journal of Fluid Mechanics* **189**: 311-335.
- Schäfer, J., Dippel, S. and Wolf, D. E.** (1996). Force schemes in simulations of granular materials. *Journal De Physique I* **6**(1): 5-20.
- Schutysers, M. A. I., Padding, J. T., Weber, F. J., Briels, W. J., Rinzema, A. and Boom, R.** (2001). Discrete particle simulations predicting mixing behavior of solid substrate particles in a rotating drum fermenter. *Biotechnology and Bioengineering* **75**(6): 666-675.
- Schutysers, M. A. I., Weber, F. J., Briels, W. J., Boom, R. M. and Rinzema, A.** (2002). Three-dimensional simulation of grain mixing in three different rotating drum designs for solid-state fermentation. *Biotechnology and Bioengineering* **79**(3): 284-294.
- Turner, J. L. and Nakagawa, M.** (2000). Particle mixing in a nearly filled horizontal cylinder through phase inversion. *Powder Technology* **113**(1-2): 119-123.

---

---

---

## **Chapter 3 Segregation by mass, radius and density of granular particles in a horizontal rotating drum**

## ABSTRACT

The impact of particle properties on segregation and mixing of bidisperse granular beds in a rotating horizontal drum have been studied by discrete element method (DEM) simulations. Bidispersities in radius, density and mass have pronounced influences on the mixing pattern in the stationary state, although they hardly affect the flow regime of the granules. All beds at 50% fill level mix well for a Froude number of  $\sim 0.56$ , corresponding to a flow regime intermediate to cascading and cataracting, while segregating occurs both at lower (rolling) and higher (cataracting / centrifuging) Froude numbers. These observations are explained qualitatively by assuming that the angular drum velocity dictates the flow regime, which in turn determines the effectiveness and direction of four competing (de)mixing mechanisms: random collisions, buoyancy, percolation and inertia. A further dozen particle properties have been varied, including the friction coefficients and elastic modulus, but they proved inconsequential to the degree of mixing in the steady state.

The contents of this chapter have been submitted for publication as:

**M. M. H. D. Arntz, W. K. den Otter, H. H. Beftink, W. J. Briels and R. M. Boom** (2010). Segregation by mass, radius and density of granular particles in a horizontal rotating drum.

---

---

## INTRODUCTION

Mixing of granular solids in a rotating horizontal drum is a routine processing step in a wide range of industries. Notwithstanding the numerous practical applications, the understanding of granular materials is still incomplete (Chakraborty *et al.*, 2000; Rapaport, 2007). The flow and (de)mixing behaviour of granular beds have turned out to be surprisingly complex phenomena – a change in the operational conditions or of the granular particles' properties can readily result in a sub-optimal mixing process, or even cause de-mixing of the particles, with obvious consequences for the product quality (Turner and Nakagawa, 2000; Khakhar *et al.*, 2003; Di Renzo and Di Maio, 2004). The practical importance and intriguing complexity have made granular mixing the subject of intense research in the last decades, but the translation of the more fundamental findings into reliable predictions for practical processes is still incomplete (Ottino and Khakhar, 2000; Jain *et al.*, 2005a; Rapaport, 2007).

Bidisperse granular beds of industrial relevance usually contain particles that differ in size and/or specific gravity, hence the separate and combined effects of these two granular properties on the mixing process are central in this chapter. The mixing and segregation behaviour of granules bidisperse in size has been studied extensively (Dury and Ristow, 1997; Chakraborty *et al.*, 2000; Thomas, 2000; Turner and Nakagawa, 2000; Ding *et al.*, 2002; Khakhar *et al.*, 2003; Hajra and Khakhar, 2004; Kawaguchi *et al.*, 2006), while some articles have focused on bidisperse densities (Ristow, 1994; Khakhar *et al.*, 1997). Only a few papers discuss simultaneous variations in granular size and density (Alonso *et al.*, 1991; Felix and Thomas, 2004; Jain *et al.*, 2005b, a), with a common emphasis on beds in the rolling regime. In this chapter we report on the interplay between size, mass and density during mixing and segregation processes in the rolling, cascading, cataracting and cataracting-centrifuging regimes (following the definitions of flow regimes by (Henein *et al.*, 1983; Mellmann, 2001). We will also briefly comment on the influence of other particle properties, notably the friction coefficients, compressibility and restitution coefficient, but their effects on the mixing and segregation behaviour of the bed turns out to be of minor importance. Our chosen research approach is the Discrete Element Method (DEM), i.e. numerical simulations of the translational and rotational motions of

all particles in the bed, because it offers unparalleled control over the properties of the particles.

The structure of this chapter is as follows: in the next section we describe the four segregation and mixing mechanisms at work in a rotating drum. The section Model description and characterization of mixing details the simulation model and the method employed to quantify the degree of mixing. The simulation results are described, and discussed in terms of the four segregation and mixing mechanisms, in the section Results and discussion. We end with a summary of the main conclusions.

## BACKGROUND

The mixing and segregation of bidisperse particles in granular beds is the cumulative effect of a number of mechanisms. In this chapter we will distinguish four mechanisms – random collisions, buoyancy, percolation and inertia – with the objective of attributing, whenever possible, the observed bed behaviour to a specific mechanism. Since the definitions of these mechanisms vary across the literature (Alonso *et al.*, 1991; Thompson and Grest, 1991; Khakhar *et al.*, 1997; Thomas, 2000; Jain *et al.*, 2005a), we first briefly discuss our interpretations. The *random collisions* between granules in the flowing layer promote mixing of the particles. A difference in particle specific densities (i.e. particle mass divided by particle volume) gives rise to *buoyancy*, causing less-dense particles to rise relative to denser particles in a mobile bed. While random collisions and buoyancy are the two mechanisms that would feature in a statistical mechanical description, as the sources of maximum entropy and minimum energy respectively, such a description is known to fail for granular systems (Poschel and Herrmann, 1995; Rapaport, 2007). *Percolation* is the ability of particles to pass through cavities in porous regions of a bed. As small pores are more abundant than large pores, this mechanism will separate particles by size. The final mechanism is *inertia*, the resistance of any stationary or moving object to a change in its state of motion. A collision between two unequal particles will deflect the light particle more from its initial trajectory than the heavy particle and thereby promote mixing of the particles, especially for the freely flying granules at Froude numbers close to one. Inertia also gives rise to centrifugal pseudo forces at high angular drum velocities, which alter the direction of the

buoyancy and percolation mechanisms: the denser or smaller particles, respectively, are now moving radially outward rather than vertically down. Note that the particle's mass, radius and density are not mutually independent, which in practice readily obfuscates the distinction between the segregation mechanisms. The granular mixtures investigated here have been chosen with the aim of highlighting or suppressing certain segregation mechanisms, in order to elucidate their roles. An improved appreciation of these four mechanisms, whose relative contributions vary across the various flow regimes, allows more accurate predictions of the steady state degree of mixing or segregation in practical situations.

## MODEL DESCRIPTION AND CHARACTERIZATION OF MIXING

The discrete element method (DEM) simulates the translational and rotational dynamics of spherical granules by numerically integrating their equations of motion (Cundall and Strack, 1979; Thompson and Grest, 1991; Poschel and Herrmann, 1995; Hoomans, 2000; Arntz *et al.*, 2008). The normal force exerted on particle  $i$  by particle  $j$  is described by a linear spring and dashpot model,

$$\mathbf{F}_{ij}^n = -k_{pp}^n \delta_{ij} \hat{\mathbf{n}}_{ij} - \eta_{ij}^n \mathbf{v}_{ij}^n, \quad [1]$$

with  $k_{pp}^n$  the elastic stiffness of the particles,  $\delta_{ij}$  their apparent overlap width,  $\hat{\mathbf{n}}_{ij}$  the normal unit vector from the centre of particle  $i$  to the centre of particle  $j$ ,  $\eta_{ij}^n$  the normal damping coefficient and  $\mathbf{v}_{ij}^n = (\mathbf{v}_i - \mathbf{v}_j) \cdot \hat{\mathbf{n}}_{ij} \hat{\mathbf{n}}_{ij}$  their relative velocity along this normal. The Coulomb model of tangential friction distinguishes between sticking and sliding regimes, which is unattractive from a computational point of view. In Schäfer's approximation (Schäfer *et al.*, 1996) of the sticking regime, two touching particles are sliding very slowly with a tangential force

$$\mathbf{F}_{ij}^t = -\eta_{pp}^t \mathbf{v}_{ij}^t, \quad [2]$$

where  $\eta_{pp}^t$  denotes the static friction coefficient and the tangential velocity difference at the point of contact is given by  $\mathbf{v}_{ij}^t = (\mathbf{v}_i - \mathbf{v}_j) - \mathbf{v}_{ij}^n + (r_i \boldsymbol{\omega}_i + r_j \boldsymbol{\omega}_j) \times \hat{\mathbf{n}}_{ij}$ , with  $r_i$  the radius and  $\boldsymbol{\omega}_i$  the angular velocity of particle  $i$ . The friction force in the sliding regime, which doubles as the maximum attainable friction force in the sticking regime, reads as

$$\mathbf{F}_{ij}^t = -\mu_{pp}^t |\mathbf{F}_{ij}^n| \hat{\mathbf{t}}_{ij} \quad [3]$$

with  $\mu_{pp}^t$  the dynamic friction coefficient and  $\hat{\mathbf{t}}_{ij}$  the unit vector along the tangential velocity difference. The interactions of particles with the drum walls are of the same structure as the particle-particle interactions, where the overlap widths, normal vectors and velocity differences are now calculated relative to the contact point(s) with the walls, and the mechanical parameters are replaced by  $k_{pw}^n$ ,  $\eta_{iw}^n$  and  $\mu_{pw}^t$ . The cylindrical drum wall of radius  $R$  and length  $L$  is oriented with its rotation axis along the  $y$ -axis and is closed by flat circular walls at both ends, see Figure 1.

The particles also experience a gravitational pull  $F_i^g = m_i g$  in the negative  $z$ -direction, with  $m_i$  the mass of the particle and  $g=9.8\text{m/s}^2$  the standard gravitational acceleration. We solve the particles' motions by numerically integrating Newton's second law of motion, for the preceding forces and their corresponding torques, using the Verlet 'leap-frog' scheme (Allen and Tildesley, 1987) with a fixed time step  $\Delta t$ .

The simulation parameters of our reference system are listed in Table 1, together with the ranges of parameter variations employed in this study. For comparison

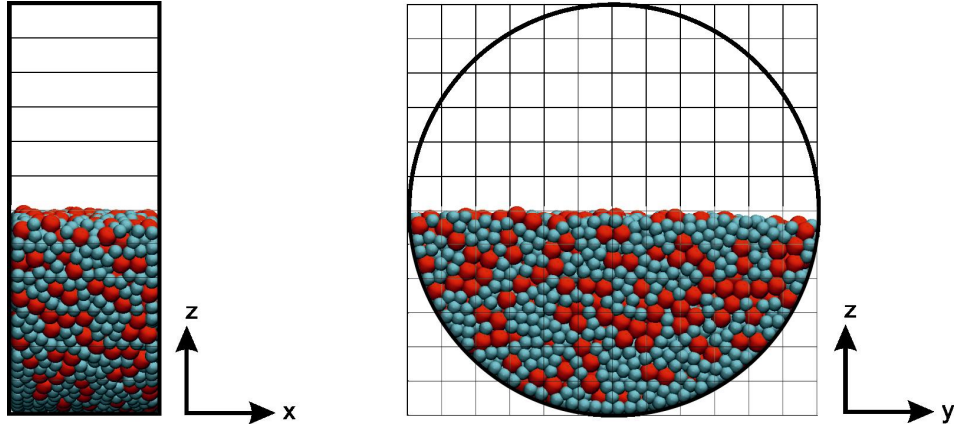


**Figure 1:** Front view (left) and side view (right) illustrating the relative dimensions of the drum and the two particle radii. The fill level is 50% in all simulations. The grid of thin lines mark the cell dimensions used in the calculation of the order parameter.

purposes, this reference system is identical to that in our prior study on the influence of the drum operational conditions on the mixing behaviour (Arntz *et al.*, 2008). As will be discussed in detail in the next section, of all varied particle properties the three most important ones turn out to be the radius, mass and density. To assess their impact, we have studied the six bidisperse systems listed in Table 2, which includes the reference system as system 1. Three of these combinations were selected to eliminate a particular segregation mechanism; equal densities in system 1, equal radii in system 2 and equal masses in system 5. The other combinations were chosen to study the cooperation or opposition of two segregation mechanisms.

The homogeneously mixed starting configurations of the simulations were created by placing particles randomly in the drum, whilst avoiding overlap, followed by a short simulation to compact the bed under the influence of gravity. After all particles had settled, their velocities were zeroed before setting the drum in motion. The number of particles in the drum was either 4,420 or 6,820, depending on the size of particle  $b$  (see Table 2), and always corresponded to a fill level of 50%.

Several methods have been developed to quantify the degree of mixing or segregation of a granular bed (Dury and Ristow, 1997; Cleary *et al.*, 1998; Dury and Ristow, 1999; Ottino and Khakhar, 2000; Porion *et al.*, 2004; Jain *et al.*, 2005a; Van Puyvelde, 2006). Here, we will use a method based on the mixing entropy in statistical mechanics,

$$S(t) = \sum_{k \in \{a,b\}} \int \rho(\mathbf{r}) x_k(\mathbf{r}) \ln x_k(\mathbf{r}) d\mathbf{r}, \quad [4]$$

with  $\rho(\mathbf{r})$  the local number density and  $x_k(\mathbf{r})$  the local fraction of  $k$ -type particles at position  $\mathbf{r}$  in the drum, and  $t$  denoting time. In practice, this integral is calculated by using a  $12 \times 1 \times 12$  grid of rectangular cells, see Figure 1. A subsequent normalization relative to the mixing entropies  $S_{\text{mix}}$  of a perfectly mixed and  $S_{\text{seg}}$  of a perfectly segregated system,

$$\phi(t) = (S(t) - S_{\text{seg}}) / (S_{\text{mix}} - S_{\text{seg}}), \quad [5]$$

**Table 1:** The simulation parameters of the granules and the drum for the reference system (system 1 in Table 2), and the ranges over which the studied particle properties were varied.

Parameter (unit)	Reference	Range
Radius $a$ particle, $r_a$ (mm)	1	-
Radius $b$ particle, $r_b$ (mm)	1.5	1.0 or 1.5
Volume fraction $a$ and $b$ particles	1	-
Number fraction $a$ and $b$ particles	$3\frac{3}{8}$	1 or $3\frac{3}{8}$
Particle specific gravity ( $\text{kg/m}^3$ )	2500	2500 - 9191
Particle-particle restitution coefficient* $e_{pp}^n$	0.831	0 - 1
Particle-wall restitution coefficient* $e_{pw}^n$	0.9	0 - 1
Particle-particle dynamic friction coefficient $\mu_{pp}^t$	0.5	0.05 - 3.5
Particle-wall dynamic friction coefficient $\mu_{pw}^t$	1.5	0.015 - 5
Particle-particle static friction coefficient $\eta_{pp}^t$ (kg/s)	1	0.001 - 2
Particle-wall static friction coefficient $\eta_{pw}^t$ (kg/s)	3	0.003 - 5
Elastic stiffness coefficients $k_{pp}^n, k_{pw}^n$ (N/m)	125	125 - 5000
Fill level	50%	-
Drum length $L$ (mm)	25	-
Drum radius $R$ (mm)	35	-
Drum angular velocity $\Omega$ (rad/s)	-	1.57 - 19
Froude number	-	$9 \cdot 10^{-3}$ - 1.3
Simulation time step (s)	$2 \cdot 10^{-6}$	-
Run length (revolutions)	30	-

\* The restitution coefficients  $e_{pp}^n$  and  $e_{pw}^n$  measure the fraction of energy conserved in head-on rotation-less particle-particle and particle-wall collisions, respectively, and are functions of the mass, the elasticity coefficient  $k_{pp}^n$  or  $k_{pw}^n$  and normal damping coefficients  $\eta_{ij}^n$  or  $\eta_{wi}^n$  of the involved particle(s) (Arntz *et al.*, 2008).

results in a conveniently scaled mixing parameter running from  $\phi = 0$  for a fully segregated system to  $\phi = 1$  for a homogeneously mixed system. Based on visual inspection of snapshots and movies, created from the regularly stored configurations by the Visual Molecular Dynamics (VMD) package (Humphrey *et al.*, 1996), we qualify a system as ‘mixed’ for  $\phi \geq 0.9$  and as ‘segregated’ for  $\phi \leq 0.65$ . A more detailed explanation of this mixing parameter is given in ref (Arntz *et al.*, 2008). The simulations typically lasted for 30 revolutions to ensure

that a steady state had been reached, while several simulations, especially those deep in the centrifuging regime, required longer runs. For initially homogeneously mixed beds the mixing parameter steadily decays from the start value  $\phi = 1$  to its final value, while initially block-wise segregated beds often pass through a mixed intermediate before demixing again to their final state (McCarthy and Ottino, 1998; Arntz *et al.*, 2008).

## RESULTS AND DISCUSSION

DEM simulations were performed over a wide range of angular drum velocities  $\Omega$  for all six particle mixtures of Table 2. The flow profiles of the granular beds were found to be insensitive to the employed granular properties, and fully determined by the Froude number,  $Fr = \Omega^2 R/g$ , i.e. the dimensionless ratio of centrifugal and gravitational forces. Following the classification scheme of flow profiles by (Mellmann, 2001), the granular bed is in the rolling regime for  $10^{-4} < Fr < 0.035$ , cascading for  $0.12 < Fr < 0.46$ , cataracting for  $0.77 < Fr < 1.0$ , cataracting-centrifuging for  $1.0 < Fr < 2.23$  and centrifuging for  $Fr > 2.23$ , with smooth transitions between these regimes. The rotating drum empowers the four segregation mechanisms, as described in the introduction, to collectively create a mixed or segregated steady state by working in unison or in discord. The final configuration and its degree of mixing, therefore, reflect the relative effectiveness of the four segregation mechanisms within the limitations posed by the flow profile and the particle properties.

The mixing curves in Figure 2 are remarkably similar for all simulated systems, with segregation predominant at low drum velocities, as illustrated in Figure 3. The degree of mixing  $\phi$  rises with increasing angular velocity, then passes through a well-mixed range centred around  $Fr = 0.56$ , and finally decreases with a further increase in the drum velocity. Segregation prevails at both tails of the plot. Movies and snapshots of these simulations reveal the formation of cylindrical cores within the bed, running the entire distance between the two vertical walls bounding the drum. Interestingly, the radially segregated patterns at low  $Fr$  are consistently inverted at high  $Fr$ . Visualization of the simulations also confirms the high degree of mixing at intermediate drum angular velocities.

**Table 2:** Radii, masses and densities of the  $a$  and  $b$ -type particles for the six simulated bidisperse granular beds. System 1 is the reference system described in Table 1.

System	$r_a$ (mm)	$r_b$ (mm)	$\rho_a$ (kg/m <sup>3</sup> )	$\rho_b$ (kg/m <sup>3</sup> )	$m_a$ (mg)	$m_b$ (mg)
1	1.0	1.5	2500	2500	10.5	35.3
2	1.0	1.0	7500	2500	31.4	10.5
3	1.0	1.5	2500	7500	10.5	106.
4	1.0	1.5	7500	2500	31.4	35.3
5	1.0	1.5	7500	2220	31.4	31.4
6	1.0	1.5	9191	2220	38.5	31.4

These results will be discussed below in detail, to analyse which segregation mechanism dominates under specific conditions, where for clarity we have separated the low ( $<0.56$ ) and high ( $>0.56$ ) Froude regimes. Note that the simulations of (Arntz *et al.*, 2008), which included the current reference system, indicate that the peak of optimal mixing shifts with increasing (decreasing) fill levels to higher (lower) Froude numbers.

#### LOW ROTATIONAL VELOCITIES

For low  $Fr$  values, below the mixing maximum, the bed is in the rolling or cascading regime, see Figure 4 and Figure 5, and consists of a densely packed passive bulk that slowly rotates with the drum and a flowing layer on top (Nakagawa *et al.*, 1993; Mellmann, 2001). The reduced number density, or increased porosity, of this mobile layer is due to the frequent collisions between the relatively fast moving particles under a high local velocity gradient, see Figure 4 and Figure 5, and thereby creates a productive environment for the segregation and mixing mechanisms. The velocity difference plots, see Figure 4c and Figure 5c, indicate where segregation and mixing occur, and thereby permit an interpretation in terms of the four mechanisms. For instance, they reveal that in the rolling regime segregation occurs throughout the flowing layer, while in the cataracting regime the segregation is concentrated in the bottom-right region of the flowing layer and to a lesser extend in the top-left region. Such a shift of locus is not without consequences, even if the same segregation mechanism

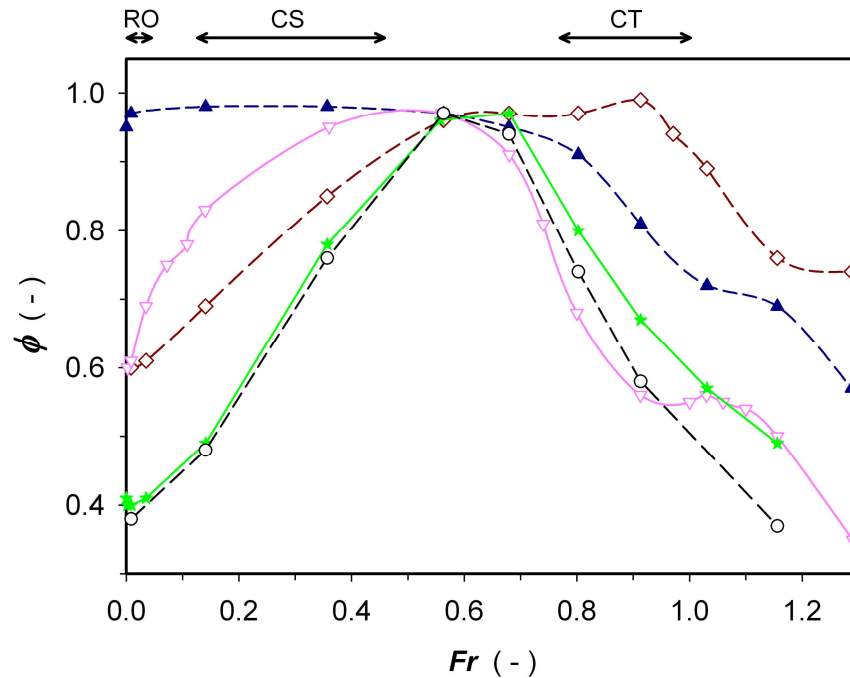


**Figure 2:** The mixing parameters  $\phi$  of steady-state half-filled drums as function of the Froude number  $Fr$  for five bidisperse granular mixtures differing in mass, radius and/or density of the particles. Systems 1 (open triangles down), 2 (open diamond) and 5 (open circles) represent mixtures with identical densities, radii and masses, respectively. System 3 is drawn as solid triangles up and System 4 as solid stars. System 6 is left out since the graph comparable to the graph of System 5. Further details on the particle properties are provided in Table 2. The arrows on top of this figure mark the ranges of the rolling (RO), cascading (CS) and cataracting (CT) flow regimes.

remains dominant, for the overall segregation behaviour of the bed (Arntz *et al.*, 2008).

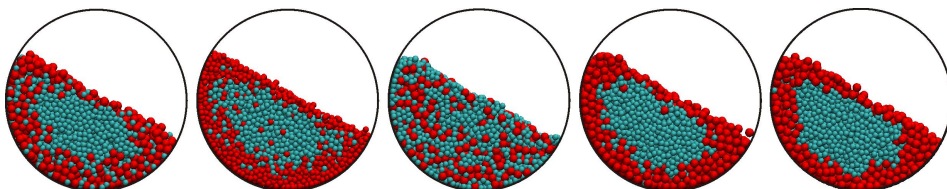


**Figure 3:** Steady states at low Froude numbers ( $\Omega=1.57$  rad/s for the first five bidisperse beds listed in table 2. The  $a$ -type particles are depicted in light green, the  $b$ -type particles in dark red.

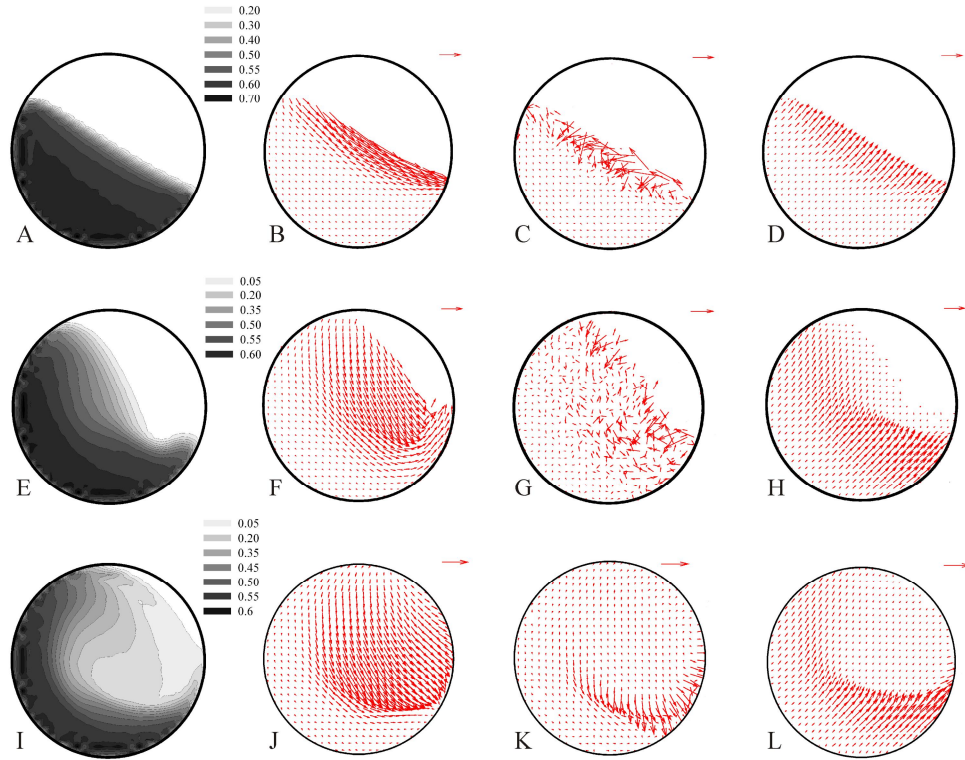


**Figure 4:** Analysis of the granular bed of system 2. The horizontal rows represent, from top to bottom, beds in the rolling ( $\Omega = 1.57$  rad/s,  $Fr = 0.01$ ), cascading ( $\Omega = 12.6$  rad/s,  $Fr = 0.56$ ) and cataracting regime ( $\Omega = 16.0$  rad/s,  $Fr = 0.91$ ). The vertical columns show, from left to right, the locally occupied volume fraction, the relative particle velocity with respect to the uniform rotation of the drum ( $\mathbf{v}_i - \boldsymbol{\Omega} \times \mathbf{r}_i$ , with the reference arrows in the top right corners representing 0.2, 0.9 and 1.1 m/s, respectively, from top to bottom), the velocity difference between the two particle types ( $\mathbf{v}_a - \mathbf{v}_b$ , with reference arrows of 0.013, 0.05 and 0.14 m/s) and the width of the local velocity distribution [the horizontal (vertical) components of the plotted vectors denote the standard deviations along the horizontal (vertical) direction; the reference arrows measure 1/75, 1/30 and 1/20 m/s, respectively].

The particles in system 1 differ in size, but are of equal density and consequently impervious to the buoyancy mechanism. Our discussion of this system will be brief, because segregation in the absence of buoyancy has been discussed in a number of studies (Nityanand *et al.*, 1986; Savage and Lun, 1988; Cantelaube

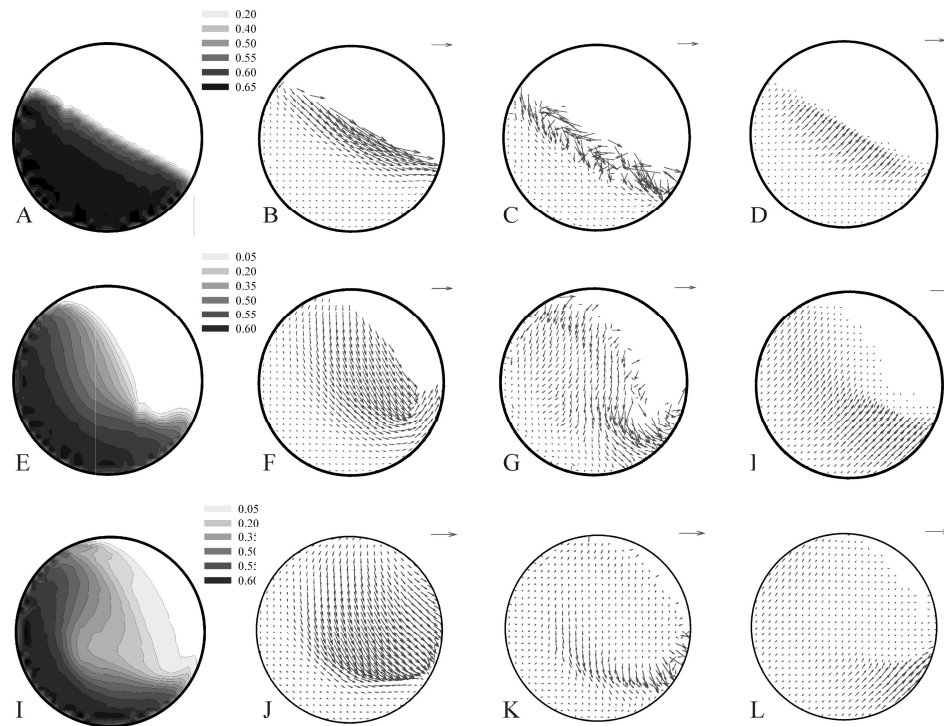


**Figure 5:** Analysis of the granular bed of system 4. The conditions and set-ups of the graphs are identical to those in Fig. 3. Note the strong similarities with Fig. 3, despite the marked differences in the properties of the  $b$ -type particle. The disparities are largely limited to the velocity differences and velocity standard deviations at the higher Froude numbers.

and Bideau, 1995; Dury and Ristow, 1997) and because a detailed analysis of this particular system has appeared elsewhere (Arntz *et al.*, 2008). For comparison purposes, we note that the moderate segregation ( $\phi \geq 0.6$ ) results from the downward percolative motions of the small particles in the flowing layer (Arntz *et al.*, 2008), culminating in a radial core of the smaller  $a$ -type granules, see Figure 3. With increasing angular velocity, *i.e.* towards the cascading regime, the flowing layer becomes more porous, hence less selective to percolation of small particles, and mixing by random collisions becomes prominent. This mixing process is further supported by an increase of the particles' velocities with  $Fr$ , which also enhances the inertia mechanism.

The particles in system 2 have different densities, but equal radii to eliminate the percolation mechanism. Again, the reduced number density and relatively high velocities of particles in the flowing layer, see Figure 4, promote reshuffles of particles. At low Froude numbers segregation occurs along the entire length of the flowing layer, but most prominently where the layer is at its thickest. The gradual formation of a radial core of the denser  $a$ -type particles, see Figure 3, is attributed to the buoyancy mechanism, *i.e.* the denser particles are sinking down in the flowing layer till they settle on a more closely packed region. Although the  $a$  and  $b$ -type particles are comparable in mass to the  $b$  and  $a$ -type particles of system 1, respectively, the heavier particles accumulate in the core in system 2 but in the periphery in system 1, which suggests that at these low Froude numbers the segregation process is more sensitive to radius and density than to mass. With increasing Froude number the random collision and inertia mechanism become more important, thus reducing and near  $Fr = 0.56$  even destroying the segregation process in system 2.

In system 3 the radii and densities are chosen such that their associated segregation effects are acting in opposite directions: the percolation mechanism drives the small and low-density  $a$ -type particles to the radial core, while the buoyancy mechanism strives for a core of the large and high-density  $b$ -type particles. Figure 2 and Figure 3 show that this system remains well-mixed for angular drum velocities in the rolling and cascading regimes (Alonso *et al.*, 1991; Jain *et al.*, 2005b, a). The absence of segregation, despite the order of magnitude difference in the particles' masses, supports the suggestion that mass is of little importance at these low Froude numbers.

If, in contrast, the  $a$ -type particle is both smaller and denser than the  $b$ -type particle, as in systems 4, 5 and 6, then buoyancy and percolation co-operate in driving the  $a$ -type particles to the radial core, see Figure 3. The mixing parameter, see Figure 2, indicates that the resulting segregation is indeed more intense than in systems 1 and 2, where only either one of these two mechanisms is active. Here again, the segregation becomes less intense and eventually vanishes with the Froude number rising to 0.56. A comparison of systems 4 and 6 shows that an increase in the density ratio, from 3 to 4, does not significantly enhance segregation, suggesting that the buoyancy mechanism has already reached its optimal performance at the former ratio.

### HIGH ROTATIONAL VELOCITIES

At high angular velocities of the drum, i.e. for Froude numbers exceeding 0.56, the bed is in the cataracting or cataracting-centrifuging regime. Figure 6 shows that there are two regions with high particle mobility's in the cataracting regime. Particles rolling down the surface of the bed are susceptible to segregation by percolation and buoyancy. The particles following ballistic trajectories through the sparsely populated volume above the bed collide only infrequently and hence hardly contribute to (de)mixing.

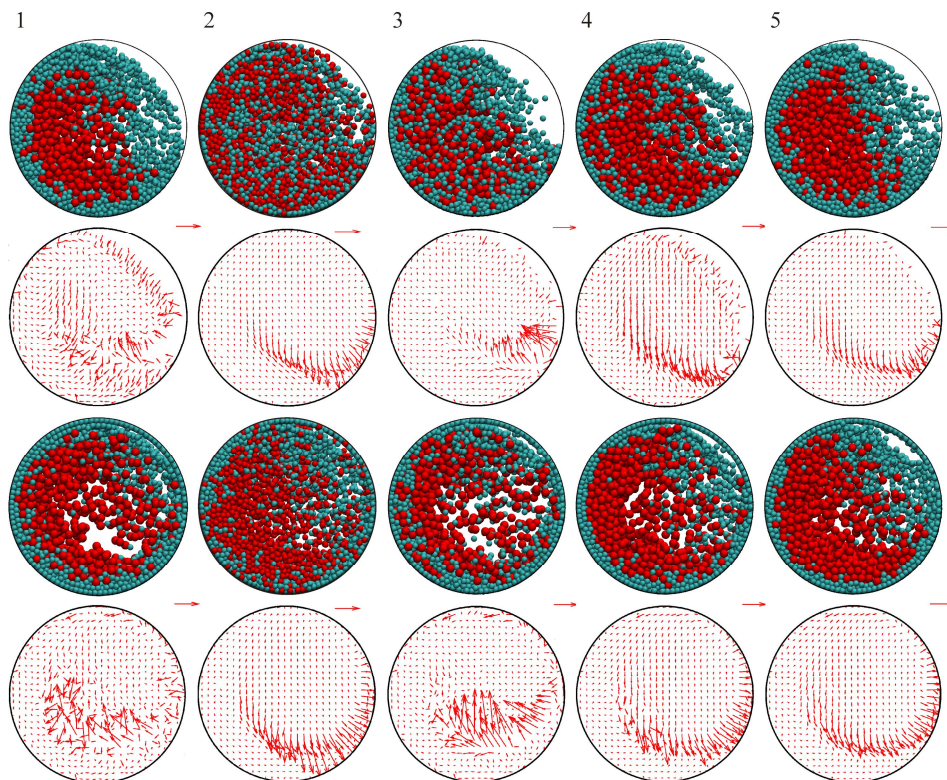


**Figure 6:** Snapshots and velocity-difference plots for systems 1 through 6 (left to right) at drum angular velocities of 16 rad/s ( $Fr=0.91$ ) (top two rows) and 18 rad/s ( $Fr=1.16$ ) (bottom two rows). The  $a$ -type particles are depicted in light green, the  $b$ -type particles in dark red. The reference arrows in the second row correspond with 0.04, 0.14, 0.1, 0.1 and 0.14 m/s, and those in the fourth row with 0.08, 0.17, 0.07, 0.2 and 0.22 m/s.

Both particle flows are reunited at the lower end of the flowing layer. In the cataracting-centrifuging regime, for Froude numbers above 1.0, one or more layers of centrifuging particles cover the entire drum well. These layers may show buoyancy and percolation effects, but at higher drum velocities become too closely packed to permit relative particle motions. Airborne particles impinging on the inner layer make a small contribution to the (de)mixing process.

The reference system, with particles bidisperse in size, shows a moderate to intense segregation at high Froude numbers. This segregation results from percolation in the flowing layer. As discussed by (Arntz *et al.*, 2008), the shift of the main percolation region from the centre of the flowing layer to the tail of the layer has inverted the net effect of the percolation mechanism, which now gives rise to a radial core of large particles (“inverse radial segregation”) in stead of a core of small particles (regular radial segregation).

The equal radius particles of system 2 are well mix in the cataracting regime, suggesting that a mass or density difference alone is insufficient to induce segregation in this Froude regime. However, the velocity difference plots in

Figure 6 show large inward pointing arrows in the lower right side, indicative of inward motion of the lighter particles relative to the denser and heavier particles. A more detailed analysis and visual inspection of movies reveal that the airborne particles impinge on the bed surface in this region and bounce back before being taken up by the bed. The inertia mechanism, i.e. lighter particles rebound more strongly than heavier particles, then gives rise to large relative velocity differences, see Figure 6, and large standard deviations, see Figure 4, in this region. The random nature of the collisions, with light and heavy particles bouncing back in various directions, promotes mixing and effectively suppresses possible segregation mechanisms. Nevertheless, a gradual decrease of the order parameter is observed for Froude numbers exceeding 0.9, where the buoyancy effect induced by the centrifugal pseudo force drive the denser particles to the drum wall.

The density ratio of the particles in system 3 was specifically chosen to balance the percolation and buoyancy mechanisms in the rolling and cascading regimes. Figure 2 shows that this balance does not extend to the cataracting regime, where

percolation has now gained the upper hand and drives the smaller particles to the wall.

The density of the larger  $b$ -type particle in system 5 was tuned to obtain two particle types with equal mass and thus to eliminate the inertia mechanism. The standard deviations in the velocities are indeed considerably reduced, as can be seen by comparing Figure 5L with Figure 4L. The percolation and buoyancy mechanisms are seen to collaborate for the lower Froude numbers, although here the collaboration effect in driving the denser and smaller  $a$ -type particle to the periphery is less clear, see Figure 2. Systems 4 and 6 behave similar to system 5.

#### OTHER PARTICLE PROPERTIES

Besides the radius, mass and density, we have also systematically varied all other particle parameters appearing in the force equations (1) through (3) over the ranges indicated in Table 1, and assessed their respective influences on the segregation process. These simulations were mainly carried out by altering, one by one, the particle properties of the reference system, with most simulations confined to the rolling regime to keep the required computer time manageable and brief excursions to other systems and higher drum angular velocities to confirm the general validity of our findings. While changes in the radius (system 2) or density (systems 3 and 4) relative to the reference system notably affect the degree of mixing, the explored variations of the dynamic inter-particle friction coefficients  $\mu_{aa}^t$ ,  $\mu_{bb}^t$  and  $\mu_{ab}^t$ , the particle-wall friction coefficients  $\mu_{pw}^t$ , the particle-particle and particle-wall static friction coefficients  $\eta_{pp}^t$  and  $\eta_{pw}^t$ , the particle-particle stiffness elastic  $k_{pp}^n$  and the normal damping coefficients  $\eta_{pp}^n$  and  $\eta_{pw}^n$  (which are related to the tabulated restitution coefficients  $e_{pp}^n$  and  $e_{pw}^n$ ) hardly effect the mixing behaviour. Only at certain extreme values are differences detectable, like an immobile bed for low particle-wall friction forces and an increased degree of mixing for fully elastic ( $e_{pp}^n = 1$ ) particle-particle collisions.

Of particular interest is the roughness of the particles, which is represented in the current simulations by the dynamic tangential friction coefficient  $\mu_{pp}^t$  and the friction coefficient  $\eta_{pp}^t$ , because some simulation models are build on the assumption that differences in roughness give rise to segregation (Chakraborty *et al.*, 2000; Puri and Hayakawa, 2001; Newey *et al.*, 2004). We find no evidence for this assumption, in line with the experimental observations by (Pohlman *et*

*al.*, 2006). Only low friction coefficients, *i.e.* for  $\mu_{pp}^t$  below about 0.25, yield noticeable deviations from the reference system. In mixtures of rough and very smooth particles, a thin layer of predominantly smooth particles forms at the vertical drum walls while the middle of the drum remains similar to that in the reference simulation. Furthermore, mixtures of smooth particles appear to segregate less well, with more small particles at the periphery and more large particles in the core, than otherwise equal mixtures of rough particles.

## CONCLUSIONS

The mixing and segregation behaviour of a bidisperse granular bed in a horizontal rotating drum will, at least in principle, depend on all mechanical properties of the granular particles involved. We have performed an extensive set of DEM simulations to assess the impact of dozen properties and find that three parameters dominate, namely the ratios of the radii, densities and masses of the two particle types in the drum. These three parameters are related to percolation, buoyancy and inertia, respectively, which in a rotating drum compete with the ubiquitous random collisions to establish a steady state. A remarkable pivotal point is reached at a Froude number of 0.56, where all simulated systems attain a well-mixed steady state, while segregation and inverse segregation are generally observed at low and high Froude numbers, respectively. The picture that emerges in this study, building on the earlier ideas by (Arntz *et al.*, 2008) and (Nityanand *et al.*, 1986), is that the relative efficiencies of these four segregation and mixing mechanisms, and hence the degree of segregation in the stationary state, are largely determined by the prevailing flow regime. The latter is controlled mainly by the Froude number and the fill level of the drum, and appears insensitive to the mechanical properties of the particles. Other particle properties, like their elasticity and the friction coefficients for normal and tangential motion turn out to be of little consequence for the segregation process.

## REFERENCES

- Allen, M. and Tildesley, D. (1987). Computer simulation of liquids. Oxford, U.K., Oxford Science Publications.
- Alonso, M., Satoh, M. and Miyanami, K. (1991). Optimum Combination of Size Ratio, Density Ratio and Concentration to Minimize Free-Surface Segregation. *Powder Technology* **68**(2): 145-152.

- Arntz, M. M. H. D., den Otter, W. K., Beftink, H. H., Bussmann, P. J. T., Briels, W. J. and Boom, R. M.** (2008). Granular mixing and segregation in a horizontal rotating drum: a simulation study on the impact of rotational speed and fill level. *AIChE Journal* **54**(12): 3133-3146.
- Cantelaube, F. and Bideau, D.** (1995). Radial Segregation in a 2d Drum - an Experimental-Analysis. *Europhysics Letters* **30**(3): 133-138.
- Chakraborty, S., Nott, P. R. and Prakash, J. R.** (2000). Analysis of radial segregation of granular mixtures in a rotating drum. *European Physical Journal E* **1**(4): 265-273.
- Cleary, P. W., Metcalfe, G. and Liffman, K.** (1998). How well do discrete element granular flow models capture the essentials of mixing processes? *Applied Mathematical Modelling* **22**(12): 995-1008.
- Cundall, P. A. and Strack, O. D. L.** (1979). Discrete Numerical-Model for Granular Assemblies. *Geotechnique* **29**(1): 47-65.
- Di Renzo, A. and Di Maio, F. P.** (2004). Comparison of contact-force models for the simulation of collisions in DEM-based granular flow codes. *Chemical Engineering Science* **59**(3): 525-541.
- Ding, Y. L., Forster, R., Seville, J. P. K. and Parker, D. J.** (2002). Segregation of granular flow in the transverse plane of a rolling mode rotating drum. *International Journal of Multiphase Flow* **28**(4): 635-663.
- Dury, C. M. and Ristow, G. H.** (1997). Radial segregation in a two-dimensional rotating drum. *Journal De Physique I* **7**(5): 737-745.
- Dury, C. M. and Ristow, G. H.** (1999). Competition of mixing and segregation in rotating cylinders. *Physics of Fluids* **11**(6): 1387-1394.
- Felix, G. and Thomas, N.** (2004). Evidence of two effects in the size segregation process in dry granular media. *Physical Review E* **70**(5).
- Hajra, S. K. and Khakhar, D. V.** (2004). Sensitivity of granular segregation of mixtures in quasi-two-dimensional fluidized layers. *Physical Review E* **69**(3).
- Henein, H., Brimacombe, J. K. and Watkinson, A. P.** (1983). Experimental-Study of Transverse Bed Motion in Rotary Kilns. *Metallurgical Transactions B-Process Metallurgy* **14**(2): 191-205.
- Hoomans, B. P. B.** (2000). Granular dynamics of gas-solid two-phase flows. Enschede, The Netherlands, University of Twente. **PhD**.
- Humphrey, W., Dalke, A. and Schulten, K.** (1996). VMD: Visual molecular dynamics. *Journal of Molecular Graphics* **14**(1): 33-38.
- Jain, N., Ottino, J. M. and Lueptow, R. M.** (2005a). Combined size and density segregation and mixing in noncircular tumblers. *Physical Review E* **71**(5).
- Jain, N., Ottino, J. M. and Lueptow, R. M.** (2005b). Regimes of segregation and mixing in combined size and density granular systems: an experimental study. *Granular Matter* **7**(2-3): 69-81.
- Kawaguchi, T., Tsutsumi, K. and Tsuji, Y.** (2006). MRI measurement of granular motion in a rotating drum. *Particle & Particle Systems Characterization* **23**(3-4): 266-271.
- Khakhar, D. V., McCarthy, J. J. and Ottino, J. M.** (1997). Radial segregation of granular mixtures in rotating cylinders. *Physics of Fluids* **9**(12): 3600-3614.
- Khakhar, D. V., Orpe, A. V. and Hajra, S. K.** (2003). Segregation of granular materials in rotating cylinders. *Physica a-Statistical Mechanics and Its Applications* **318**(1-2): 129-136.

- McCarthy, J. J. and Ottino, J. M.** (1998). Particle dynamics simulation: a hybrid technique applied to granular mixing. *Powder Technology* **97**(2): 91-99.
- Mellmann, J.** (2001). The transverse motion of solids in rotating cylinders - forms of motion and transition behavior. *Powder Technology* **118**(3): 251-270.
- Nakagawa, M., Altobelli, S. A., Caprihan, A., Fukushima, E. and Jeong, E. K.** (1993). Noninvasive Measurements of Granular Flows by Magnetic-Resonance-Imaging. *Experiments in Fluids* **16**(1): 54-60.
- Newey, M., Ozik, J., Van der Meer, S. M., Ott, E. and Losert, W.** (2004). Band-in-band segregation of multidisperse granular mixtures. *Europhysics Letters* **66**(2): 205-211.
- Nityanand, N., Manley, B. and Henein, H.** (1986). An Analysis of Radial Segregation for Different Sized Spherical Solids in Rotary Cylinders. *Metallurgical Transactions B-Process Metallurgy* **17**(2): 247-257.
- Ottino, J. M. and Khakhar, D. V.** (2000). Mixing and segregation of granular materials. *Annual Review of Fluid Mechanics* **32**: 55-91.
- Pohlman, N. A., Ottino, J. M. and Lueptow, R. M.** (2006). End-wall effects in granular tumblers: From quasi-two-dimensional flow to three-dimensional flow. *Physical Review E* **74**(3).
- Porion, P., Sommier, N., Faugere, A. M. and Evesque, P.** (2004). Dynamics of size segregation and mixing of granular materials in a 3D-blender by NMR imaging investigation. *Powder Technology* **141**(1-2): 55-68.
- Poschel, T. and Herrmann, H. J.** (1995). Size Segregation and Convection. *Europhysics Letters* **29**(2): 123-128.
- Puri, S. and Hayakawa, H.** (2001). Segregation of granular mixtures in a rotating drum. *Physica A* **290**(1-2): 218-242.
- Rapaport, D. C.** (2007). Radial and axial segregation of granular matter in a rotating cylinder: A simulation study. *Physical Review E* **75**(3).
- Ristow, G. H.** (1994). Granular dynamics: a review about recent molecular dynamics simulations of granular materials. *Annual Reviews of Computational Physics*. D. Stauffer, World Scientific. **I**: 275-308
- Savage, S. B. and Lun, C. K. K.** (1988). Particle-Size Segregation in Inclined Chute Flow of Dry Cohesionless Granular Solids. *Journal of Fluid Mechanics* **189**: 311-335.
- Schafer, J., Dippel, S. and Wolf, D. E.** (1996). Force schemes in simulations of granular materials. *Journal De Physique I* **6**(1): 5-20.
- Thomas, N.** (2000). Reverse and intermediate segregation of large beads in dry granular media. *Physical Review E* **62**(1).
- Thompson, P. A. and Grest, G. S.** (1991). Granular Flow - Friction and the Dilatancy Transition. *Physical Review Letters* **67**(13).
- Turner, J. L. and Nakagawa, M.** (2000). Particle mixing in a nearly filled horizontal cylinder through phase inversion. *Powder Technology* **113**(1-2): 119-123.
- Van Puyvelde, D. R.** (2006). Simulating the mixing and segregation of solids in the transverse section of a rotating kiln. *Powder Technology* **164**(1): 1-12.

---

**Chapter 4 Repeated segregation and energy dissipation in an axially segregated granular bed**

## ABSTRACT

Discrete element simulations were used to study the segregation behaviour in a bed of bidisperse granules in a rotating drum. In the final state the large particles ended up in the upper part of the bed near the vertical walls. In order to arrive at this state, the system went through two cycles of structural changes, on top of which fast oscillations were observed between an axially segregated and a somewhat more mixed state. These oscillations were sustained by different angles of repose near the vertical walls and in the middle of the bed. Concomitantly with the structural changes the system's energy dissipation went through two cycles after which it settled into a state of minimal dissipation.

The contents of this chapter have been accepted for publication as:

**M. M. H. D. Arntz, W. K. den Otter, H. H. Beftink, R. M. Boom and W. J. Briels**  
(2010), Repeated segregation and energy dissipation in an axially segregated granular bed.  
*Europhysics Letters*

---

---

## INTRODUCTION

Understanding flow of granular matter is of great practical importance, since it occurs in many industrial processes at one stage or another. Flow of granular particles that are heterodisperse in size often results in segregation of the various components. For example, an initially homogeneously mixed bidisperse bed of particles in a horizontal rotating drum in many cases segregates after only a few rotations, with the smaller particles generally accumulating in a submerged core spanning the entire length of the drum (Das Gupta *et al.*, 1991; Nakagawa *et al.*, 1997). The boundary of this core performs erratic undulations with increasing amplitudes (Nakagawa *et al.*, 1997; Newey *et al.*, 2004; Taberlet *et al.*, 2004) until it reaches the outer surface and becomes visible as a sequence of bands of smaller particles separated by bands of larger particles (Nakagawa, 1994; Hill *et al.*, 1997; Nakagawa *et al.*, 1997; Fiedor and Ottino, 2003; Newey *et al.*, 2004; Taberlet *et al.*, 2004). On further rotation, the submerged connections between these bands break apart and the bed becomes axially segregated (Rapaport, 2002; Alexander *et al.*, 2004; Taberlet *et al.*, 2006). On very long time-scales the bands generally diffuse and merge until ultimately only three bands (Nakagawa, 1994), and sometimes only two bands (Chicharro *et al.*, 1997), remain. The above description is a generic summary of many experimental findings, which sometimes may differ in their details. It has been confirmed by molecular dynamics simulations of dissipative grains with surface frictions by Taberlet *et al.* (Taberlet *et al.*, 2004). Detailed experimental investigations have been performed by Kahn *et al.* (Kahn *et al.*, 2004).

Experiments on bidisperse rotating beds (Hill and Kakalios, 1995; Fiedor and Ottino, 2003; Alexander *et al.*, 2004) indicate that end-wall effects can initiate band formation or determine the structure of the bands near the end-walls. In this chapter, we report results of discrete element model (DEM) simulations of a drum with an aspect ratio of  $L/D = 0.73$ , with  $L$  being the length of the drum and  $D$  its diameter. This drum is small enough to be dominated by the presence of the end-walls, yet long enough to be called three dimensional. The rather small system size allows runs that are long enough to perform a detailed study of transient oscillations after the onset of rotation. In order to analyse the results of our simulations we introduce three different types of order parameter, each of which gives information about the presence or absence of a different kind of

structure. Together these order parameters allow a detailed monitoring of the evolution of the bed, and the end-wall effects in particular. Moreover we will calculate various contributions to the dissipation of energy and find that on the long run the system strives for a state with minimal energy dissipation. This observation will be discussed at the appropriate point later in this chapter.

## MODEL DESCRIPTION AND CHARACTERIZATION OF MIXING

In the discrete element model the particle positions, velocities and angular velocities are updated by means of a numerical integration of the classical equations of motion, given the contact forces exerted among neighbouring particles (Cundall and Strack, 1979). Forces between particles  $i$  and  $j$  are zero in case the corresponding width of the apparent overlap region  $\delta_{ij}$  is zero. Otherwise the normal force exerted on particle  $i$  by particle  $j$  is calculated as

$$\mathbf{F}_{ij}^n = -k_n \delta_{ij} \hat{\mathbf{n}}_{ij} - \eta_n \mathbf{v}_{ij}^n \quad [1]$$

Here  $\hat{\mathbf{n}}_{ij}$  the normal unit vector from the centre of particle  $i$  to the centre of particle  $j$ ; and  $\mathbf{v}_{ij}^n = (\mathbf{v}_i - \mathbf{v}_j) \cdot \hat{\mathbf{n}}_{ij} \hat{\mathbf{n}}_{ij}$  their relative velocity along this normal. Moreover,  $k_n$  is the elastic stiffness coefficient, and  $\eta_n$  the normal damping coefficient. The latter is uniquely related to the so called restitution coefficient  $e_v$ , which can easily be measured experimentally. The tangential force is calculated according to Schäfer's approximation of the Coulomb model (Schäfer *et al.*, 1996), and is equal to

$$\mathbf{F}_{ij}^t = -\eta_t \left( \mathbf{v}_{ij}^t + (R_i \boldsymbol{\omega}_i + R_j \boldsymbol{\omega}_j) \times \hat{\mathbf{n}}_{ij} \right) \quad [2]$$

or

$$\mathbf{F}_{ij}^t = -\mu |\mathbf{F}_{ij}^n| \hat{\mathbf{t}}_{ij} \quad [3]$$

the actual force being the one with the smallest absolute value. Here  $\mathbf{v}_{ij}^t = \mathbf{v}_{ij} - \mathbf{v}_{ij}^n$  and  $\hat{\mathbf{t}}_{ij} = \mathbf{v}_{ij}^t / |\mathbf{v}_{ij}^t|$ ;  $R_i$  is the radius of particle  $i$  and  $\boldsymbol{\omega}_i$  its angular velocity. Finally,  $\eta_t$  is the viscous friction coefficient and  $\mu$  the Coulomb friction coefficient. length  $L = 220$ mm and its diameter  $D = 300$ mm. The particles have radii  $R_1 = 2$  mm and  $R_2 = 4$  mm respectively. When densely close packed, the particles occupy one fourth of the total volume of the drum, with

eight times as many small particles as there are large particles. The drum is rotated with angular speed  $\omega = \pi/2$  rad/s. The simulation parameters are: time step  $\Delta t = 5 * 10^{-6}$  s, density of the particles  $\rho = 2500$  kg/m<sup>3</sup>, normal spring constant  $k_n = 125$  N/m, normal friction coefficients are all calculated using a restitution coefficient of 0.1, tangential friction coefficient  $\eta_t = 1.0$  kg/s, and Coulomb friction coefficient  $\mu = 0.5$ . We have carefully checked that the time step is small enough to guarantee conservation of energy during frictionless collisions.

We characterize the type and degree of segregation by a number of order parameters all deriving from the entropy of mixing (Arntz *et al.*, 2008)

$$S = \sum_{k \in \{i, j\}} \int \rho(\mathbf{r}) x_k(\mathbf{r}) \ln x_k(\mathbf{r}) d\mathbf{r}, \text{ normalized according to}$$

$$\phi = \frac{S - S_{\text{seg}}}{S_{\text{mix}} - S_{\text{seg}}}. \quad [4]$$

Here  $\rho(\mathbf{r})$  is the particle density at  $\mathbf{r}$  and  $x_k(\mathbf{r})$  is the local number fraction of particles of type  $k$ .  $S_{\text{seg}}$  is the entropy of the fully segregated system and  $S_{\text{mix}}$  that of the fully mixed system. Different order parameters are obtained by numerically calculating the integral using different grids. In all cases the grid was chosen such that each filled cell contained about 75 particles. In particular,  $\phi_o$  corresponds to a grid of cubic cells,  $\phi_r$  to a grid of bars along the drum axis, and  $\phi_a$  to a grid of discs perpendicular to the drum axis. The subscripts indicate the type of information that is given by the particular entropy. So,  $\phi_o$  gives information about the overall mixing of the various components,  $\phi_r$  is small in case of segregation along the radius of the drum and  $\phi_a$  is small in case of segregation along the axis.

## RESULTS AND DISCUSSION

In the next few paragraphs we describe the structural changes that take place after the onset of rotation. In Figure 1 we have plotted the time development of all three order parameters during a simulation of 80 revolutions. The most striking features of this plot are the two minima of  $\phi_o$  after 11 and 38 revolutions respectively. In Figure 2 we have plotted top, bottom and side views of the drums at these points during the simulation.

The most striking features of this plot are the two minima of  $\phi_o$  after 11 and 38 revolutions respectively. In Figure 2 we have plotted top, bottom and side views

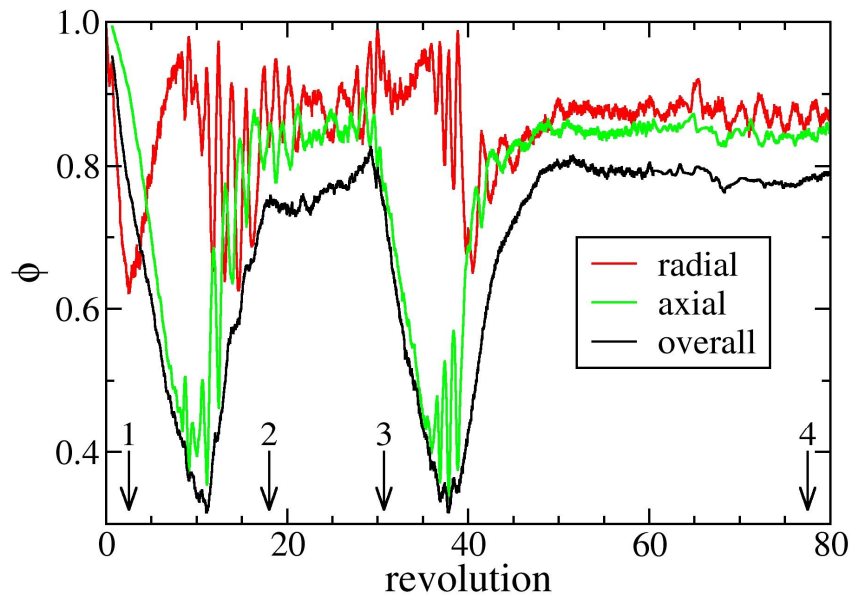


**Figure 1:** Three types of entropy are plotted as a function of the number of revolutions after onset of rotation of the drum.  $\phi_r$  is low when radial segregation is pronounced,  $\phi_a$  when axial segregation is pronounced, while  $\phi_o$  quantifies the overall mixing state. All entropies take values between 0 and 1. Snapshots of the system at the two deep minima are shown in Figure 2, snapshots at the four instances marked by arrows are shown in Figure 3.

of the drums at these points during the simulation.

In both cases the drums are axially segregated with the smaller particles in the middle section and the larger particles near the end walls. No small particles are visible in the side views, while only very few large particles are seen in the middle sections of the top and bottom views. Interestingly there is a small asymmetry between the top and bottom views, in the sense that the middle section is slightly narrower in the top view than in the bottom view. The strong axial segregation in these two states is also signalled by minima in the corresponding axial order parameters. We next discuss some of the details of Figure 1. Four points, all having approximately the same  $\phi_o$ , have been marked on the horizontal axis, corresponding to the four snapshots in Figure 3.

At the time of the first snapshot, after 2.5 revolutions, radial segregation is more or less complete, corroborated by the radial entropy  $\phi_r$  having a clear minimum at this instant. The top and bottom surfaces are well covered by large particles, while the small particles constitute the inner core of the drum as is clear from the

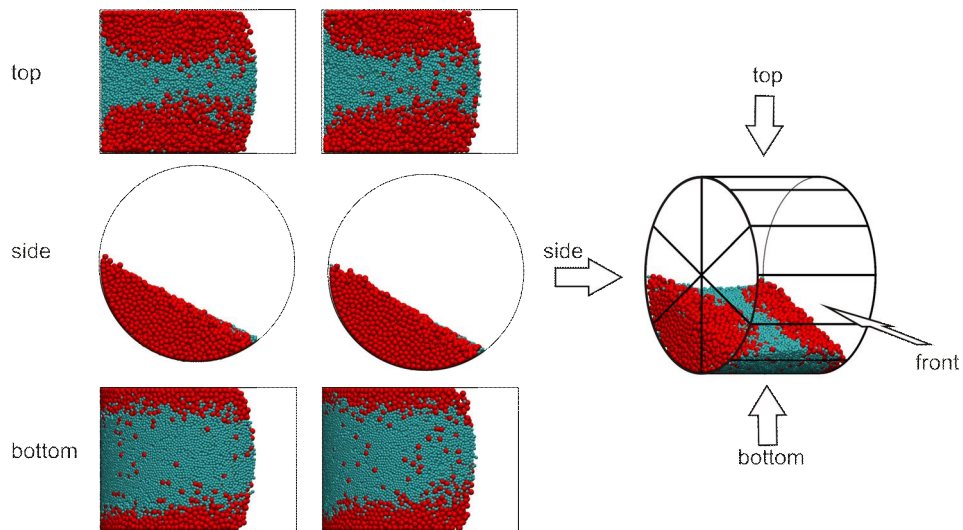


**Figure 2:** Top, side and bottom views of the drum after 11 revolutions (left) and 38 revolutions (middle), corresponding to the two minima of the overall and axial order parameters in Figure 1. A three-dimensional view of the drum is presented on the right, with arrows indicating the various directions of view. The radius of the large particle (red) is twice that of the small particle (blue).

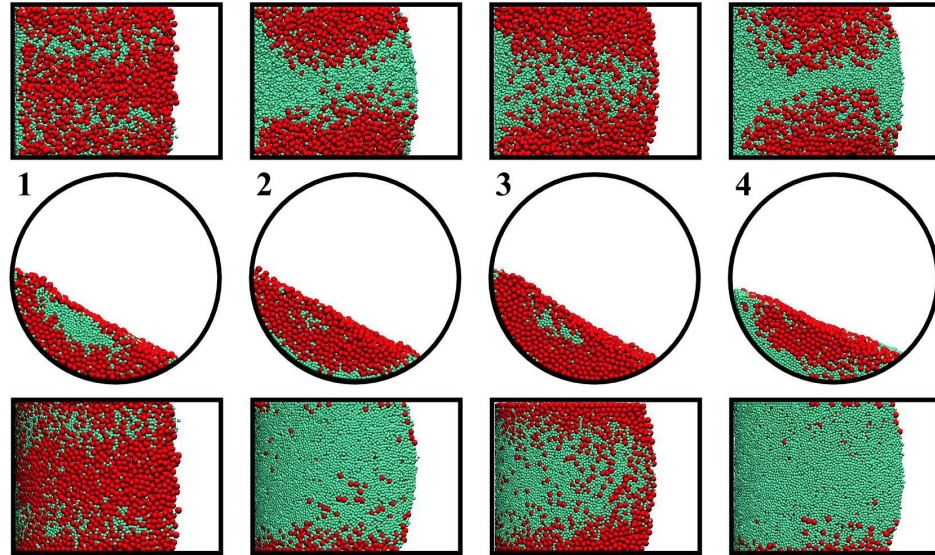


**Figure 3:** Four snapshots taken at increasing times corresponding with the arrows in Figure 1, showing top views (top), side views (centre) and bottom views (bottom). The first snapshot is taken after 2.5 revolutions, when radial segregation is very pronounced. The second snapshot is taken after 18 revolutions. Most large particles have been removed from the bottom surface and put near the vertical walls; this state very much resembles the final stationary state. Between the second and the final state the system makes one more cycle through a sequence of states with low overall order parameter, which starts after about 30 revolutions when the structure is like in the third snapshot.

side view. From this time on axial segregation sets in as indicated by a further

decrease of  $\phi_a$ , while radial segregation is temporarily blurred again, indicated by a rise of  $\phi_r$ . After 11 rotations both  $\phi_o$  and  $\phi_a$  reach temporary minima,

corresponding to pronounced axial segregation as discussed above. On continuation of the run, both  $\phi_o$  and  $\phi_a$  rise quickly until they reach a quasi plateau where this rise becomes very slow. The second and third snapshots are

taken at the beginning and end of this plateau. In the second snapshot (see Figure 3) the state of axial segregation (see Figure 2) has been destroyed to some extent and most of the large particles have been expelled from the bottom wall. At the end of the quasi plateau the system has developed into a state which is partly radially segregated and partly axially segregated, shown in the third snapshot.

This state is apparently rather unstable, since from here on the whole process more or less repeats itself. The system goes again through a state of axial segregation and next climbs again to some plateau with roughly constant order parameters. This time, hardly any developments occur on the plateau as is clear from the resemblance of the second and fourth snapshot in Figure 3, the latter being taken at the very end of the run. We have continued the run for another twenty revolutions and found no new developments. Moreover, we have performed two additional runs of 60 revolutions and found similar behaviour. We now concentrate on one more aspect of Figure 1. During the fast increases of  $\phi_o$  and  $\phi_a$ , oscillations with a period of about 1.5 revolutions are observed both in  $\phi_a$  and in  $\phi_r$ , but with opposite phases.

These oscillations are absent in  $\phi_o$ , indicating that the oscillations exchange axial for radial segregation without changing the overall segregation. A series of snapshots is shown in Figure 4, capturing the evolution of one single fast oscillation. When  $\phi_a$  is maximal, the band of small particles in the middle of the drum is wide at the bottom and narrow at the free surface. In the minima of  $\phi_a$  this difference has disappeared. These oscillations are different from the ones reported in the literature (Choo *et al.*, 1997; Choo *et al.*, 1998; Taberlet *et al.*, 2006), where the widths of the small-particle bands at the surface vary by transport of particles through a radial core, while our system lacks such a core. The mechanism that sustains the observed fast oscillations can easily be understood. The reason is that the large particles, once they are driven to the periphery of the drum, have an angle of repose which is about four to six degrees

larger than that of the small particles in the central part of the drum. As a result, on their way down at the surface of the bed, the large particles have a tendency to move inward, flooding the central part of the surface. For the same reason of having a somewhat larger angle of repose than the small particles, the tendency to move inward is reversed once the large particles have covered half their way down. The trajectories of the large particles at the surface of the bed are therefore very much as drawn in Figure 3 of Pohlman *et al.* (Pohlman *et al.*, 2006). The fast oscillations mentioned above occur because the large particles at the surface tend to move in large chunks being either at the upper surface or at the lower surface of the bed. When these chunks gradually disperse the oscillations disappear. It is worth mentioning that the dependence of the angle of repose on the position along the axis of the drum is not so much caused by the fact that it is

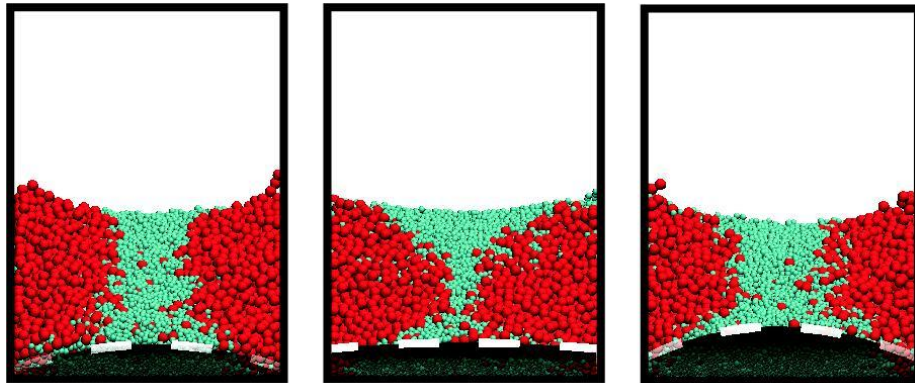


**Figure 4:** Three consecutive front views at different phases of a fast oscillation. In the outer two  $\phi_a$  is small, while in the inner one  $\phi_a$  is large. In all snapshots the large particles are mostly near the vertical walls. In the left one the angle of repose is larger near the vertical wall than in the middle of the drum, making the large particles roll inwards until halfway the upper surface and then outward again; this continues until in the middle snapshot the angle of repose has been equalised along the drum. Continuing rotation then builds up a new difference of angles of repose until this is maximal in the right snapshot. The dashed line highlights the front contact line of the bed and the cylindrical drum wall, separating the particles in contact with the wall (dark) from the particles not in contact with the wall (light). This line, like the rear contact line, bends and straightens during a fast oscillation.

the large particles which are at the periphery of the drum while the small particles are in the centre, but rather is an effect caused by the end walls themselves. Indeed, in additional simulations of monodisperse systems we found that both the small particles as well as the large particles had a somewhat larger angle of repose near the end-walls than in the centre of the drum. The oscillations discussed above are therefore the single result of the presence of the end-walls.

This conclusion was further corroborated by simulations of the bi-disperse system with periodic boundary conditions, in which case no oscillations occurred. Until now we have described the structural changes that occur in the drum after the onset of rotation. The next obvious thing to do is to ask for a rule that governs the evolution just described. This question naturally consists of two parts, first, is there a final, stationary or periodic (or chaotic) state, and second, what principle governs the evolution from the initial to the final state? The latter of these questions is far beyond the scope of this paper. As to the former, we will

only state a few observations done on our system. As is well known, stationary solutions of the Navier-Stokes equations neglecting the non-linear terms obey the principle of minimal dissipation (Strutt, 1873; Kim and Karilla, 1991; Batchelor, 2002). A similar principle has been put forward by Glansdorff and Prigogine (Glansdorff and Prigogine, 1971) to describe the occurrence of dissipative structures in non-equilibrium systems. We therefore have calculated the energy dissipation in our system after the onset of rotation, and will present our findings in the remaining part of this chapter. For an extensive discussion of possible laws governing non-equilibrium structures we refer to a review paper by Martyushev and Seleznev (Martyushev and Seleznev, 2006) and some of the older literature (Strutt, 1873; Onsager, 1931; Kohler, 1948; Ziegler, 1977). Additional discussion may be found in the book of Öttinger (Öttinger, 2005). In Figure 5 we show the time evolution of the total dissipation in the system and its various contributions.

Obviously, on small time scales the dissipation fluctuates to some extent due to small displacements of the particles around some macroscopic state. As a result, in all references below to the various components of the total dissipation, averages over small time windows are implied. Moreover it is perhaps worth mentioning that the dissipation that we discuss here is basically the dissipation of energy in the form of heat in the particles, and is not related to the changing structural entropy that we have used to define order parameters. First of all we notice that the total dissipation is about 25 percent smaller in the final stationary state than in the initial fully mixed state. From the various contributions to the dissipation on the long term we infer that it is mainly the lowering of the dissipation in the small particles that is responsible for the overall decrease of dissipation. The dissipation due to collisions of the large particles among each other is almost the same in the final stationary state as in the initial mixed state. Dissipation due to small-small collisions decreases slightly with time, while the dissipation due to small-large collisions decreases most. This is in accordance with the observed segregation phenomena and lends credit to the principle of minimal dissipation as a selection criterion for the final stationary state. In more detail, we notice that during the second decade of revolutions the system temporarily settles in a state with just slightly more dissipation than in the final stationary state.

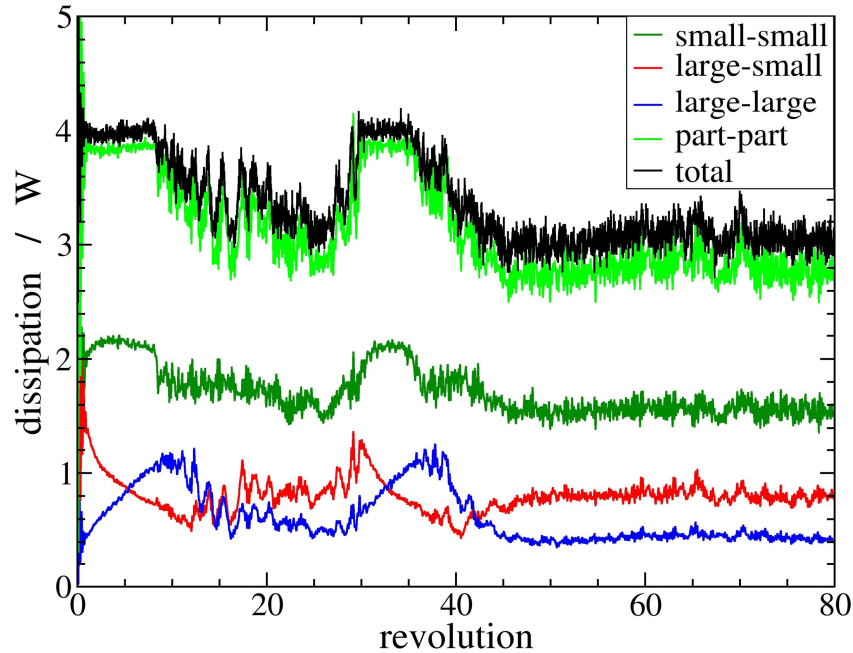


**Figure 5:** Energy dissipation in units of Watt as a function of the number of drum revolutions. During the early stage the total dissipation hardly changes, despite considerable changes in the individual contributions which reflect structural changes in the bed. Between revolutions 8 and 30 the total dissipation gradually relaxes to a quasi-stationary minimum. Near revolution number 30 the dissipation rises again just to go through the whole process again and to end in a final stationary state with minimal energy dissipation.

Moreover, there is a close resemblance between the evolution of the various contributions to the dissipation during this transition period and that during the initial period. Compare for example the evolution of the various contributions to the total dissipation between 2.5 and 12.5 revolutions with that between 30 and 40 revolutions. Surprisingly, during these periods, while the contributions of the small-large and large-large collisions to the total dissipation change substantially, their sum remains virtually constant. We finally investigate where at the periphery of the system the power that is dissipated in the interior has been delivered. In Figure 6 we plot the various contributions to the delivered power at the various walls, as well as their final sum.

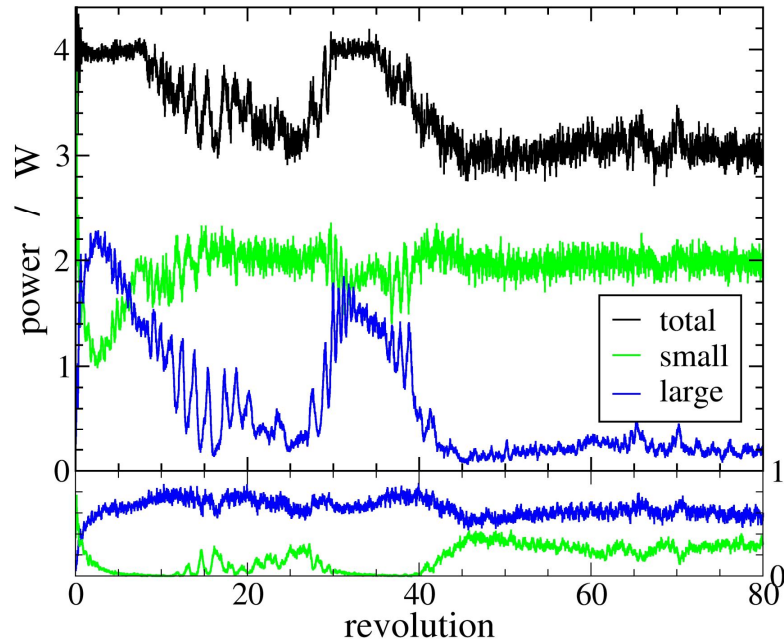


**Figure 6:** Various contributions to the delivered power in units of Watt as a function of the number of drum revolutions, with the upper and lower panel showing the power delivered at the cylindrical wall and the flat end walls, respectively. Again the state of minimal consumed power is arrived at via two cycles of similar evolution. It is seen that the dissipation is minimised by lowering the power transfer to the large particles. This is done by removing the large particles from contacts with the cylindrical walls.

We notice that most of the power is delivered at the cylindrical wall, and that the small amount of power delivered at the end-walls is more or less constant, independent of the actual type of particles present near these walls. Only during the later part of axial segregation and on the plateau in Figure 1 does the total consumed power decrease, mainly as a result of a decrease of the transfer of energy to the ever fewer large particles near the cylindrical wall. It is rather amazing that a temporary rise of the total dissipation to its initial level is finally followed by a decrease to a level slightly below its minimum up to that time. A similar behaviour has been found in shear banding systems of visco-elastic liquids (Van den Noort *et al.*, 2007; Van den Noort and Briels, 2008) where the evolution of the total dissipation was non-monotonous in order to finally reach a level which was lower than any of its minima attained before.

## CONCLUSIONS

In summary, we have been able to quantify the details of structural evolutions in a bed of granular particles after starting to rotate the bed by using different measures of the entropy of the bed. Moreover we have found that the overall development is towards a state of minimal dissipation.

## REFERENCES

- Alexander, A., Muzzio, F. J. and Shinbrot, T. (2004). Effects of scale and inertia on granular banding segregation. *Granular Matter* **5**(4): 171-175.
- Arntz, M. M. H. D., den Otter, W. K., Beftink, H. H., Bussmann, P. J. T., Briels, W. J. and Boom, R. M. (2008). Granular mixing and segregation in a horizontal rotating drum: a simulation study on the impact of rotational speed and fill level. *AIChE Journal* **54**(12): 3133-3146.
- Batchelor, G. K. (2002). *An Introduction to Fluid Dynamics*. Cambridge, UK, Cambridge University Press.
- Chicharro, R., Peralta-Fabi, R. and Velasco, R. (1997). Segregation in dry granular systems. *Powders and Grains 97*. P. Behringer and J. Jenkens. Rotterdam, Balkema: 479-482.
- Choo, K., Baker, M. W., Molteno, T. C. A. and Morris, S. W. (1998). Dynamics of granular segregation patterns in a long drum mixer. *Physical Review E* **58**(5).
- Choo, K., Molteno, T. C. A. and Morris, S. W. (1997). Traveling granular segregation patterns in a long drum mixer. *Physical Review Letters* **79**(16).
- Cundall, P. A. and Strack, O. D. L. (1979). Discrete Numerical-Model for Granular Assemblies. *Geotechnique* **29**(1): 47-65.
- Das Gupta, S., Khakhar, D. V. and Bhatia, S. K. (1991). Axial Transport of Granular Solids in Horizontal Rotating Cylinders .1. Theory. *Powder Technology* **67**(2): 145-151.
- Fiedor, S. J. and Ottino, J. M. (2003). Dynamics of axial segregation and coarsening of dry granular materials and slurries in circular and square tubes. *Physical Review Letters* **91**(24).
- Glansdorff, P. and Prigogine, I. (1971). *Thermodynamic theory of structure, stability and fluctuations*. London, UK, John Wiley & Sons Ltd.
- Hill, K. M., Caprihan, A. and Kakalios, J. (1997). Bulk segregation in rotated granular material measured by magnetic resonance imaging. *Physical Review Letters* **78**(1).
- Hill, K. M. and Kakalios, J. (1995). Reversible Axial Segregation of Rotating Granular Media. *Physical Review E* **52**(4).
- Kahn, Z. S., Tokaruk, W. A. and Morris, S. W. (2004). Oscillatory granular segregation in a long drum mixer. *Europhysics Letters* **66**: 212.
- Kim, S. and Karilla, S. J. (1991). *Microhydrodynamics. Principles and selected applications*. Stoneham, MA, USA, Butterworth-Heinemann.
- Kohler, M. (1948). Oscillatory granular segregation in a long drum mixer. *Zeitschrift für Physik* **124**: 772-789.

- Martyushev, L. M. and Seleznev, V. D.** (2006). Maximum entropy production principles in physics, chemistry and biology. *Physics Reports* **426**: 1-45.
- Nakagawa, M.** (1994). Axial Segregation of Granular Flows in a Horizontal Rotating Cylinder. *Chemical Engineering Science* **49**(15): 2540-2544.
- Nakagawa, M., Altobelli, S. A., Caprihan, A. and Fukushima, E.** (1997). NMRI study: axial migration of radially segregated core of granular mixtures in a horizontal rotating cylinder. *Chemical Engineering Science* **52**(23): 4423-4428.
- Newey, M., Ozik, J., Van der Meer, S. M., Ott, E. and Losert, W.** (2004). Band-in-band segregation of multidisperse granular mixtures. *Europhysics Letters* **66**(2): 205-211.
- Onsager, L.** (1931). Reciprocal relations in irreversible processes. *Physical Review* **37**: 405-426.
- Öttinger, H. C.** (2005). Beyond equilibrium Thermodynamics. Hoboken, NJ, USA, Wiley Interscience.
- Pohlman, N. A., Ottino, J. M. and Lueptow, R. M.** (2006). End-wall effects in granular tumblers: From quasi-two-dimensional flow to three-dimensional flow. *Physical Review E* **74**(3).
- Rapaport, D. C.** (2002). Simulational studies of axial granular segregation in a rotating cylinder. *Physical Review E* **65**(6).
- Schäfer, J., Dippel, S. and Wolf, D. E.** (1996). Force schemes in simulations of granular materials. *Journal De Physique I* **6**(1): 5-20.
- Strutt, J. W.** (1873). Proceedings of the London Mathematical Society.
- Taberlet, N., Losert, W. and Richard, P.** (2004). Understanding the dynamics of segregation bands of simulated granular material in a rotating drum. *Europhysics Letters* **68**(4): 522-528.
- Taberlet, N., Newey, M., Richard, P. and Losert, W.** (2006). On axial segregation in a tumbler: an experimental and numerical study. *Journal of Statistical Mechanics-Theory and Experiment*(7).
- Van den Noort, A. and Briels, W. J.** (2008). Brownian dynamics simulations of concentration coupled shear banding. *Journal of Non-Newtonian Fluid Mechanics* **152**(1-3): 148-155.
- Van den Noort, A., Den Otter, W. K. and Briels, W. J.** (2007). Coarse graining of slow variables in dynamic simulations of soft matter. *Europhysics Letters* **80**(2).
- Ziegler, H.** (1977). An introduction to thermomechanics. Amsterdam, The Netherlands, North Holland Publishing Co.

---

---

**Chapter 5 End walls induce axial  
segregation in a horizontal  
rotating drum**

## ABSTRACT

The influence of end walls on segregation of bidisperse granular beds in a short rotating horizontal drum is studied by discrete element method (DEM). Whereas non-closed periodically continued drums segregate radially, all simulations of drums with end walls resulted in axial segregation with two bands at low friction between the particles and the end-wall and three bands at high friction. Various simulations show irregular transitions between two approximately equally stable states, with rapid oscillations preceding the conversions. The formation of two axial bands lowers the energy dissipation by the bed, whereas neither radial segregation nor axial segregation into three bands reduced the power absorption at constant angular velocity. Roughening up the end-walls also increased the rate of axial segregation.

The contents of this chapter have been submitted for publication as:

**M. M. H. D. Arntz, W. K. den Otter, H. H. Beftink, R. M. Boom and W. J. Briels** (2010), End walls induce axial segregation in a horizontal rotating drum.

---

---

## INTRODUCTION

A striking property of agitated heterogeneous granular materials is their tendency to segregate, which has large practical relevance since many industrial products are mixed powders or granules (Turner and Nakagawa, 2000; Khakhar *et al.*, 2003; Di Renzo and Di Maio, 2004). Here we focus on segregation in a short and partially filled horizontal rotating drum, as one of the simplest geometries for studying segregation phenomena. In the rolling regime, the granular bed will mostly rotate with the drum and flow is primarily restricted to a small layer at the top of the bed (Nakagawa *et al.*, 1993; Mellmann, 2001). One may expect the granules to flow down the slope of the bed, perpendicular to the axis of rotation, but experiments on monodisperse beds by Pohlman, Maneval and collaborators (Maneval *et al.*, 2005; Pohlman *et al.*, 2006a) revealed a significant axial flow near the end-walls of the tumbler. Axial flow near the end-walls is also observed in discrete element method (DEM) simulations of monodisperse beds in short drums (Pohlman *et al.*, 2006a; Pohlman *et al.*, 2006b; Chen *et al.*, 2008). But axial flow is not observed in the absence of end-walls, i.e. for periodically continued and hence axially symmetric drums, suggesting the axial flow to be induced by the symmetry-breaking end walls. Several authors have suggested that the end-walls play a role in the induction of axial segregation (Hill and Kakalios, 1994; Caps *et al.*, 2003; Fiedor and Ottino, 2003). In DEM simulations, bidisperse beds readily segregate axially in short drums, whereas beds in long drums and in periodically continued drums typically show very slow axial segregation (Ottino and Khakhar, 2000). A similar trend is found in experiments (Hill and Kakalios, 1995; Ottino and Khakhar, 2000). We have recently observed oscillatory behaviour of segregating and segregated beds in a short drum, which was attributed to the end-walls (Arntz *et al.*, 2008). Collectively, these findings indicate that the end-walls are likely to affect the transition from radial to axial segregation.

In this chapter we study the influence of end-walls on the segregation process, through discrete element simulations of a bidisperse bed in a short drum, by varying the properties of the end-walls from rough via smooth and energy-conserving to non-existent. A short drum both increases the relative importance of the end-walls and permits studying the long-time stability of the observed segregations. The results indicate that the end-walls are indeed a driving force

behind axial segregation: they dictate to a large extent the segregation pattern of the steady state, as well as giving rise to fast (one to two revolution) and slow (dozens of revolutions) oscillations that take the bed to and from its steady state. Our approach is described in the Methods section, the results are presented and discussed in the section Results and Discussion, and the chapter ends with a summary of the main conclusions in the section Conclusions.

## METHODS

In the discrete element model, the granules are modeled as discrete elements, moving in a space bounded by walls featuring specific interactions with the particles. The particle positions, velocities and angular velocities are updated by numerical integration of the classical equations of motion, given the contact forces exerted among neighbouring particles (Cundall and Strack, 1979). The normal force exerted on particle  $i$  by particle  $j$  is calculated as

$$\mathbf{F}_{ij}^n = \begin{cases} -k_n \delta_{ij} \hat{\mathbf{n}}_{ij} - \eta_n \mathbf{v}_{ij}^n & \text{for } \delta_{ij} > 0 \\ 0 & \text{for } \delta_{ij} \leq 0 \end{cases} \quad [1]$$

Here  $\hat{\mathbf{n}}_{ij}$  the normal unit vector from the centre of particle  $i$  to the centre of particle  $j$  and  $\mathbf{v}_{ij}^n = (\mathbf{v}_i - \mathbf{v}_j) \cdot \hat{\mathbf{n}}_{ij} \hat{\mathbf{n}}_{ij}$  their relative velocity along this normal. Further,  $k_n$  is the elastic stiffness coefficient and  $\delta_{ij}$  denotes the width of the apparent overlap region of the colliding particles  $i$  and  $j$ , i.e.  $\delta_{ij} = (R_i + R_j) - |\mathbf{r}_i - \mathbf{r}_j|$  with  $R_i$  and  $R_j$  the radii, and  $\mathbf{r}_i$  and  $\mathbf{r}_j$  the position vectors of particles  $i$  and  $j$ , respectively. The normal damping coefficient  $\eta_n$  is directly related to the restitution coefficient  $e_v$ , which is easily accessible experimentally.

The tangential force is calculated according to Schäfer's approximation of the Coulomb model (Cleary, 1998) as the smallest absolute value of

$$\mathbf{F}_{ij}^t = -\eta_t \left( \mathbf{v}_{ij}^t + (R_i \boldsymbol{\omega}_i + R_j \boldsymbol{\omega}_j) \times \hat{\mathbf{n}}_{ij} \right) \quad [2]$$

and

$$\mathbf{F}_{ij}^t = -\mu |\mathbf{F}_{ij}^n| \hat{\mathbf{t}}_{ij}. \quad [3]$$

Here  $\mathbf{v}_{ij}^t = \mathbf{v}_{ij} - \mathbf{v}_{ij}^n$  is the tangential velocity difference, with direction  $\hat{\mathbf{t}}_{ij} = \mathbf{v}_{ij}^t / |\mathbf{v}_{ij}^t|$ , and  $\boldsymbol{\omega}_i$  denotes the angular velocity of particle  $i$ . Finally,  $\eta_t$  is the viscous friction coefficient and  $\mu$  the Coulomb friction coefficient. Interactions between particles and the drum are similar to particle-particle interactions, with distances and velocity differences calculated relative to the contact points with the walls.

The cylindrical drum of diameter  $D = 300$  mm and length  $L = 220$  mm is oriented with its axis along the horizontal  $y$ -axis and is closed by two identical flat circular walls at either end. The origin of the coordinate system coincides with the centre of the drum, with a gravitational force pulling in the negative  $z$ -direction and the drum rotating at an angular velocity of  $\omega = \pi/2$  rad/s around the  $y$ -axis. The bed of small and large particles, with radii  $R_1 = 2$  mm and  $R_2 = 4$  mm, respectively, occupies one fourth of the drum volume when densely packed. With eight times as many small particles as there are large particles, both particle types occupy identical volumes. Both particle types have the same specific gravity  $\rho = 2500$  kg/m<sup>3</sup>, tangential friction coefficient  $\eta_t = 1.0$  kg/s and normal spring constant  $k_n = 125$  N/m, with normal friction coefficients based on a restitution coefficient of 0.1. The Coulomb friction coefficient  $\mu$  equals 0.5 for particle-particle interactions and 1.5 for collisions with the cylindrical drum wall - the four applied friction coefficients for collisions with the flat end-walls are listed in Table 1. The table also contains two additional systems, system 5 with fully elastic end-wall collisions and system 6 without end-walls, to further explore the effects of the end-walls.

For the current combinations of parameters, the integration of the equations of motion by the Verlet leap-frog algorithm (Allen and Tildesley, 1987) requires a

**Table 1:** Coulombic friction coefficients  $\mu$  and restitution coefficients  $e_v$  for collisions between particles and the flat end-walls terminating the drum. There are no end-walls in drum 6, which is continued by periodic boundary conditions (P.B.C) instead.

Drum	$\mu$ (-)	$e_v$ (-)
1	1.5	0.1
2	0.375	0.1
3	0.15	0.1
4	0	0.1
5	0	1.0
6	P.B.C.	P.B.C.

time step of  $\Delta t = 5 \cdot 10^{-6}$  s to guarantee conservation of energy during frictionless ( $\mu^t = \eta^t = 0$ ) collisions.

The type and degree of segregation are characterized by order parameters  $\phi$  derived from the entropy of mixing (Arntz *et al.*, 2008),

$$S = \sum_{k \in \{i, j\}} \int \rho(\mathbf{r}) x_k(\mathbf{r}) \ln x_k(\mathbf{r}) d\mathbf{r}, \quad [4]$$

Where  $\rho(\mathbf{r})$  is the particle density at position  $\mathbf{r}$  and  $x_k(\mathbf{r})$  is the local number fraction of particles of type  $k$ . This entropy is subsequently normalised by

$$\phi = \frac{S - S_{\text{seg}}}{S_{\text{mix}} - S_{\text{seg}}}, \quad [5]$$

with  $S_{\text{seg}}$  and  $S_{\text{mix}}$  the entropies of fully segregated and fully mixed systems, respectively. Three specific order parameters are defined by numerically calculating the integral using three distinct grids: a 3D grid of cubic cells measures the overall order parameter  $\phi_o$ , a 2D grid of bars of length  $L$  aligned along the drum axis quantifies the radial order  $\phi_r$ , while the axial order  $\phi_a$  is evaluated from a 1D stack of discs with radius  $R$ . In each case, the cell size was chosen such that filled cells contained about 75 particles. The reader is referred to (Arntz *et al.*, 2008; Atkins and Paula, 2010) for more details.

## RESULTS AND DISCUSSION

The six end-walls listed in Table 1 were combined with four initial states: a homogeneously mixed state, an axially segregated state with two bands (one band of large particles and one band of small particles) and two axially segregated states with three bands (a layer of small particles sandwiched between two layers of large particles and the inverse stacking). Five to ten simulations were run for every combination, by using random numbers to generate independent initial ‘microscopic’ configurations corresponding to the same ‘macroscopic’ partitioning of the bed (Arntz *et al.*, 2008). These simulations typically lasted for about 30 revolutions, at which point the systems had reached a steady state or were clearly heading for a particular steady state. The ‘steady

state' is here operationally defined as a situation where the three order parameters remain essentially constant over a period of ten drum revolutions – in a steady state the microscopic configuration keeps changing perpetually while the bed retains the same macroscopic configuration. One run of every set was continued for over 100 revolutions to assess the stability of the steady state over longer times. In this section we first discuss the steady states, followed by an analysis of the kinetics of the segregation processes leading to this steady state, and finally a discussion of the probable mechanisms that underlie both the segregation process and the resulting steady state.

### STEADY STATES

The dependence of the granular bed's preferred state on the end-wall conditions is probably best explored by simulating an initially homogeneously mixed bed. The simulations at high end-wall frictions then develop three banded large-small-large structures (LSL), as indicated in Table 2 for drums 1 and 2. The two interfaces between the layers are, however, not flat but smoothly curved, as illustrated in snapshot 4 of Figure 1, with the central band of small particle band extending underneath the layer of large particles to cover the entire cylindrical drum wall (marked in the table by  $L_wSL_w$ ).

**Table 2:** Dependence of the steady state configuration on drum type and initial configuration. The abbreviation LS stands for a drum segregated in a layer of small particles and a layer of large particles, SLS denotes two layers of small particles surrounding a layer of large particles, and LSL a layer of small particles sandwiched between two layers of large particles. The notation  $L_w$  for drums 1 and 2 indicates that the axial layer of large particles is shielded from the cylindrical drum walls by a coat of small particles,  $L_r$  for drum 3 signifies a layer of large particles with a small radial core of small particles, and  $L_s$  for drums 4 and 5 denotes that this layer of large particles contains relatively many small particles. Drum 6 segregates radially (R) when initiated in a mixed state, while the periodic boundary conditions of this drum restrict axial stacks to an even number of layers.

Drum	mixed	SLS	LS	LSL
1	$L_wSL_w$	$L_wSL_w$	$L_wS$	$L_wSL_w$
2	$L_wSL_w$	$L_wS_wL$	$L_wS$	$L_wSL_w$
3	$L_rSL_r$	LS	LS	$L_rSL_r$
4	LS	LS	LS	$L_sSL_s$
5	LS	LS	LS	$L_sSL_s$
6	R	-	LS	-

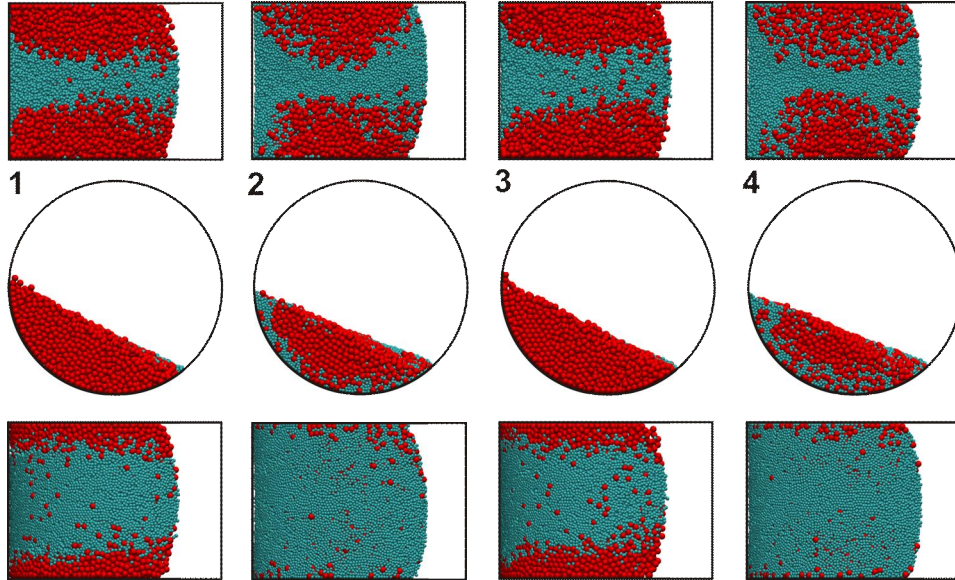


**Figure 1:** Four snapshots from drum 1 taken at increasing times corresponding with the dots in Figure 2, showing top views (top), side views (centre) and bottom views (bottom). The first snapshot is taken after 10 revolutions, when axial segregation (LSL) is very pronounced. The second snapshot is taken after 25 revolutions. Most large particles have been removed from the bottom surface and put near the vertical walls. Between the second and the final state, snapshot 4, the system makes one more cycle through a sequence of states with low overall order parameter, which starts after about 30 revolutions when the structure is like in the third snapshot.

A superficially three-banded LSL structure is also obtained at the small tangential end-wall friction of drum 3, but this time the two flanking layers of large particles contain a small radial core of small particles ( $L_rSL_r$ , see Figure 2). Two well-separated axial bands of large and small particles (LS, see Figure 2), are formed at the vanishing tangential end-wall frictions of drums 4 and 5. Axial segregation is not observed for granular beds in the periodically continued drum 6, which merely segregate radially, in line with the extremely slow axial segregation in previous experimental and simulation studies of long and quasi-infinite drums (Choo *et al.*, 1997; Aranson and Tsimring, 1999; Taberlet *et al.*, 2006).

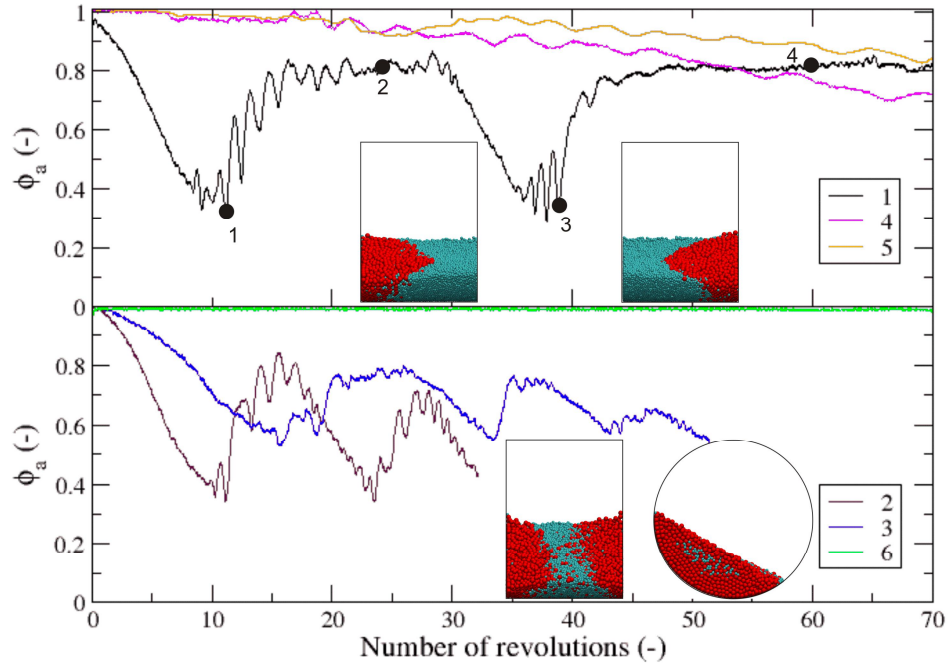


**Figure 2:** The axial order parameter  $\phi_a$  plotted against the number of revolutions for initially mixed beds in drums with various end-wall properties (listed in Table 1). Note that this parameter does not distinguish between two or three bands. Snapshots after 110 revolution of drum 4 and 5 are depicted in the top panel and snapshots after 50 revolutions of drum 3 are added in the bottom panel. Snapshots of drum 1 after 10, 25, 40 and 60 revolutions are given in Figure 1.

Simulations started with granular beds in LSL and LS patterns, i.e. the two observed axially segregates steady states, indicate that both macroscopic configurations qualify as steady states for all five drums with explicit end-walls.

Again, the steady states are not ideally segregated: the two-banded system at non-zero end-wall friction develops a curved interface with the layer of small particles extending between the cylindrical drum wall and the bulk phase of large particles ( $L_wS$ ); the three-banded system at small tangential end-wall friction acquires a small radial core of small particles within the layers of large particles ( $L_rSL_r$ ), whereas at vanishing tangential friction with the end-walls a relatively large number of small particles becomes dispersed in the two bands of large particles after 90 revolutions ( $L_sSL_s$ ). Of practical importance is the notion that the initial configuration of the bed can survive for a long time, which suggests

that the ‘activation’ barriers separating the steady states are fairly high and makes it difficult to identify with certainty the preferred steady state of the bed. We will return to this question in the section Segregation mechanisms. In this context it is interesting to note that granular beds with an initial small-large-small (SLS) layering, which never appeared as a steady state in any of the previous simulations, follow the same trend as the initially homogeneously mixed systems - a three-banded LSL pattern for drums with end-wall friction and a two-banded LS segregation at vanishing friction – thereby suggesting again that these are the favoured steady states. The only difference is at the low friction of drum 3, where the mixed drums yield a three-layered LSL segregation while the unstable SLS configuration evolves into a two-layered LS pattern.

### **SEGREGATION RATES**

The end-walls also affect the dynamics of the segregation process. We will once more consider the four different starting configurations to analyse the evolution to their respective steady states.

The initially mixed beds always pass through the two stages of initial rapid radial segregation followed by slow axial segregation into two or three bands. The evolution of radial segregation, as quantified by the radial order parameter  $\phi_r$ , is plotted in Figure 3 for various settings of the end-walls. A high degree of ordering is reached after about three revolutions, regardless of the end-wall frictions. Since the order parameter for the drum with periodic boundary initially follows the same profile, it may be concluded that the end-walls are of little influence to the radial segregation process. Beyond three to five revolutions, however, the importance of end-walls becomes apparent: all beds in drums with explicit walls lose their radial ordering within a couple of revolutions, whereas the bed in the periodically continued drum remains in a radially segregated state for at least 120 revolutions, at which point the simulation was terminated. The mere presence of end-walls suffices to induce axial segregation.

End-walls with vanishing tangential friction, even end-walls with a restitution coefficient of unity, induce the gradual development of axial segregation in the course of about 70 revolutions, as shown by the axial order parameters of drums 4 and 5 in Figure 2. Note however, that steady state is reached after  $\gg$  70 revolutions. Coulombic friction with the end-walls considerably accelerates the axial segregation process, shortening the induction period to approximately 15

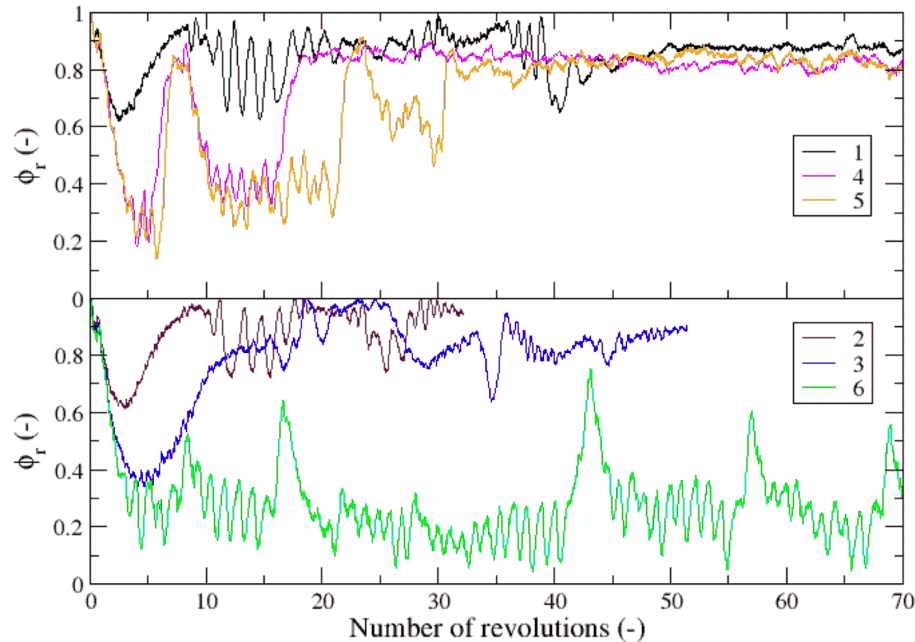


**Figure 3:** The radial order parameter  $\phi_r$  plotted against the number of revolutions for initially mixed granular beds, showing the impact of the end-wall (see Table 1 for details) on the segregation process. All systems develop radial segregation within the first few revolutions, which subsequently disappears equally rapidly in all drums with explicit end-walls. Radial segregation is long-lived under periodic boundary conditions only, i.e. in drum 6.

revolutions in drum 3. Increasing the higher friction coefficient to  $\mu = 3/8$  reduces the segregation process to about 10 revolutions in drum 2, while a further roughening of the end-walls hardly decreases the equilibration period. Curiously, extending these simulations well beyond the equilibration period shows that the  $L_wSL_w$  steady state of the bed does not survive indefinitely, but is repeatedly interrupted by short-lived excursions to an LSL pattern with an improved segregation - the small particles retract from underneath the band of large particles and the two interfaces become flatter.

An example of these short lapses can be seen in Figure 2 for drum 1 after about 35 revolutions; a further discussion of the origins of this behaviour is deferred to the next section.

The evolution of the axial order parameter for the initially unstable SLS bed is depicted in Figure 4. In the simulations with rough end-walls, drums 1 and 2, the bed becomes randomly mixed in the first couple of revolutions, to be followed by the two stages of radial segregation and axial segregation as discussed above for the initially homogeneous bed.

The  $L_wSL_w$  steady state is again alternated with brief stints of LSL. A markedly different path is traversed by the beds in drums with smooth end-walls, drums 3

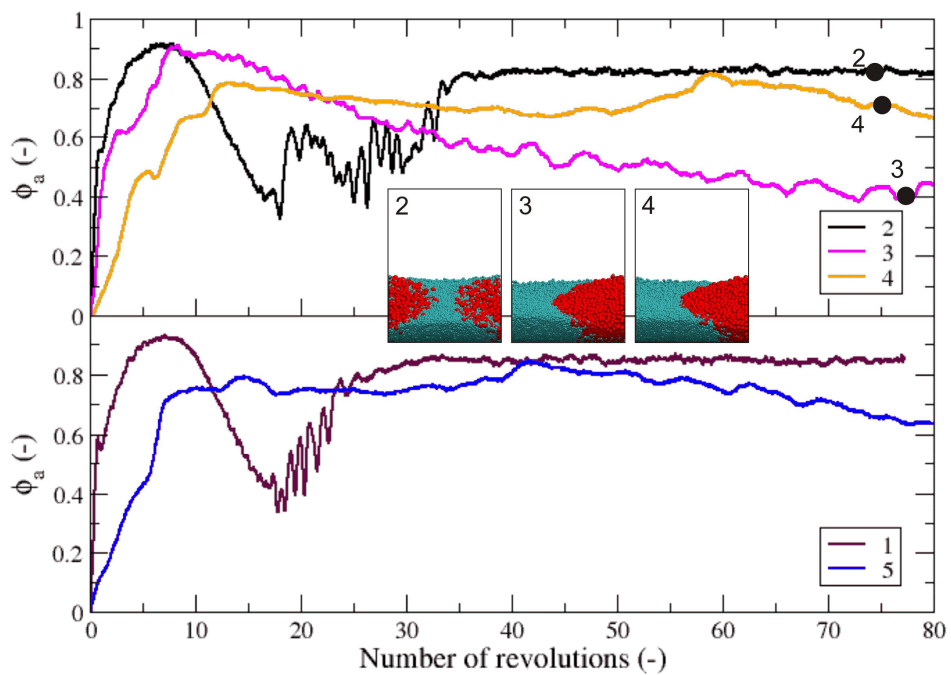


**Figure 4:** The axial order parameter  $\phi_a$  plotted against the number of revolutions for beds initiated with an unstable three-banded SLS layering, using three types of end-walls. Snapshots illustrate the state of the beds after 90 revolutions, with the small particles coloured blue and the large particles in red. Snapshots of drums 1 and 5 have been omitted for clarity, as they are similar to drums 2 and 4, respectively.

Note: the configuration of 3 and 4 look similar whereas the order parameters vary greatly. This is due to a larger core of small particles present in the large-particles band of drum 4 in comparison to drum 3 (see e.g. side view snapshot in Figure 7 on page 104), and similar for the large-particles core in the small-particles band. In time these cores will vanish as indicated by the slow decrease of the order parameter.

through 5, where either one of the two flanking bands of small particles gradually grows at the expense of the opposite band.

This exchange of particles, results in the rapid transient rise of the axial order parameter in Figure 4. While this segregation process into two bands is considerably slower than the formation of the three-banded LSL at higher frictions, it nevertheless proceeds quicker than the formation of two bands from an initially homogeneous bed in the same drum.

### **SEGREGATION MECHANISMS**

The two preceding sections have highlighted the existence of several distinct segregation processes, depending on both the tangential friction at the end-walls of the drum and the segregation state of the bed, and the peculiar instabilities of the three-banded structure in a short drum. In this section we discuss these processes in terms of the dynamics of the granules, in order to better understand these observations.

Drums with rough end-walls see a rapid transition of unstable initial bed configurations into a radially segregated state, by the percolation mechanism described in detail in (Arntz *et al.*, 2008), which is followed within about 10 revolutions by axial segregation into three relatively pure bands (LSL), see also Figure 1 snapshot 1.

The tangential friction at the end-walls tends to drag the neighbouring particles along, causing them to be transported further along the rotation direction of the drum than the particles in the middle of the drum. Hence, the average slope of the bed is about  $5^\circ$  steeper near the end-walls than in the middle, and the two contact lines of the system, i.e. the lines traced out by the edges of the bed touching the cylindrical drum wall, are smoothly curved in the rotation direction near the end-walls, as illustrated in Figure 5 for a three-banded state. The resulting non-planar flow layer on top of the bed, which already develops when the system is still radially segregated, probably explains the rapid axial segregation observed in short drums. A particle arriving at the centre ( $y \approx 0$ ) of the rear contact line, after being carried along by the bulk rotation at the bottom of the bed, will glide down the flowing layer to the front contact line, with the symmetry of the bed implying that the particle remains near the centre of the bed.

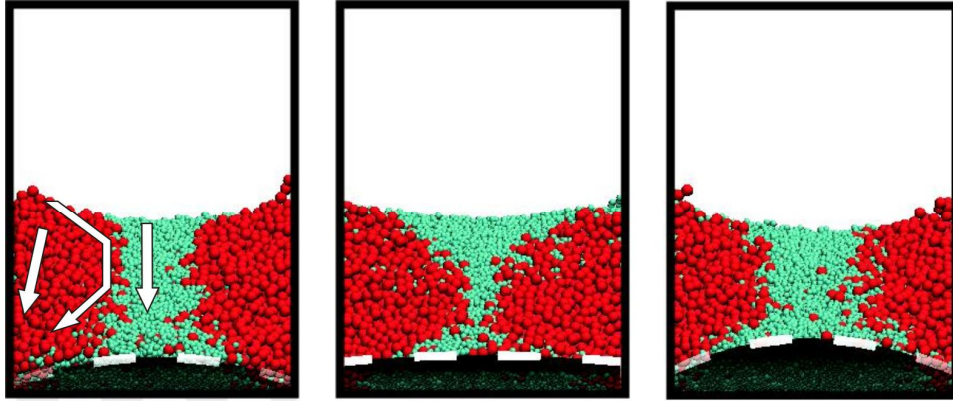


**Figure 5:** Snapshots corresponding to the oscillation in  $\varphi_a$  and  $\varphi_r$  at revolution 11.2, 11.9 and 12.5 respectively. The dashed line highlights the front contact line of the bed and the cylindrical drum wall, separating the particles in contact with the wall (dark) from the particles not in contact with the wall (light). This line, like the rear contact line, bends and straightens during a fast oscillation. The arrows in the left most figure indicate the flow profile of three random particles entering the flowing layer at three different locations.

But a particle arriving at the rear contact line close to an end-wall experiences a locally concave flowing layer, which drives the particle away from the walls and toward the centre of the drum as it slides down-hill. The bottom section of the bed is convex, thus driving the particle back to the end-wall – usually the end-wall where the particle originated from, but in the current short drum the particles occasionally cross over to the opposing end-wall. Snapshots illustrating these curved trajectories, which have recently been observed by several groups for monodisperse systems (Maneval *et al.*, 2005; Pohlman *et al.*, 2006b; Chen *et al.*, 2008), are illustrated in Figure 5 for a three-banded configuration. These curved trajectories in combination with percolation promotes axial segregation;

small particles percolate through the flowing layer and end up deeper inside the bed, while the large particles accumulate on top of the flowing layer and are transported back to the end walls. The resulting rapid formation of axial bands in short drums contrasts with the very slow axial segregation in long drums, which is believed to evolve from radial segregation by the growth of local fluctuations in the diameter of the radial core (Newey *et al.*, 2004; Taberlet *et al.*, 2006). The wall-mechanism described here might stimulate the latter process, by initiating

---

axial segregation at the two extreme ends of the drum. The axial motion of the granules also affects the number of particles in contact with the end-walls, as well as the type of these particles, and thereby modifies the effective total tangential friction between the end-walls and the bed.

A reduction in the friction may cause the bed to lose its hold on the drum: the bed will then slide down in its entirety, reducing its angle of repose, until the bed regains its grip and once more starts to rotate with the drum. Several repetitions of this sequence of events in drum 1 are seen in Figure 6 bottom panel, between 10 and 25 revolutions, as rapid oscillations in the angle of repose. Movies of the dynamics of the bed, generated by the Visual Molecular Dynamics (VMD) program, confirm this behaviour. Over the course of several oscillations the average angle of repose gradually decreases from about  $32^\circ$  (next to an end-wall) to approximately  $25^\circ$ . Simultaneously, the axial and the radial order parameter also pass through a rapid series of oscillations before arriving at their new plateau values, see drum 1 in Figure 3 and Figure 2, snapshots belonging to such an oscillation are given in Figure 5. These transitions have been confirmed by movies of the simulations to correspond to a well-segregated LSL state developing into a more complex  $L_wSL_w$  configuration. Surprisingly, long simulations reveal that the  $L_wSL_w$  state may occasionally convert back into the more ordered LSL state, as happens in the short excursion after 35 and 120 revolutions in Figure 6 top panel, thereby restarting the above described sequence of events. The *raison d'être* of the irregular reversals to LSL, which may well be triggered by accidental variations in the microscopic configuration of the bed, is under investigation.

The LSL state typically survives for considerably shorter periods of time than the  $L_wSL_w$  configuration, suggesting that the latter is the preferred configuration in drums with rough end-walls (as listed in Table 2).

The power required to rotate the drum at a constant angular velocity, which in practical situations will be provided by an engine, is readily calculated from the simulations. For an initially mixed bed in a drum with rough end-walls, the demanded power is essentially constant during the first 8 revolutions, as depicted in Figure 6 centre panel; note that this graph does not include the power consumed at  $t = 0$  to overcome the inertia of the drum.

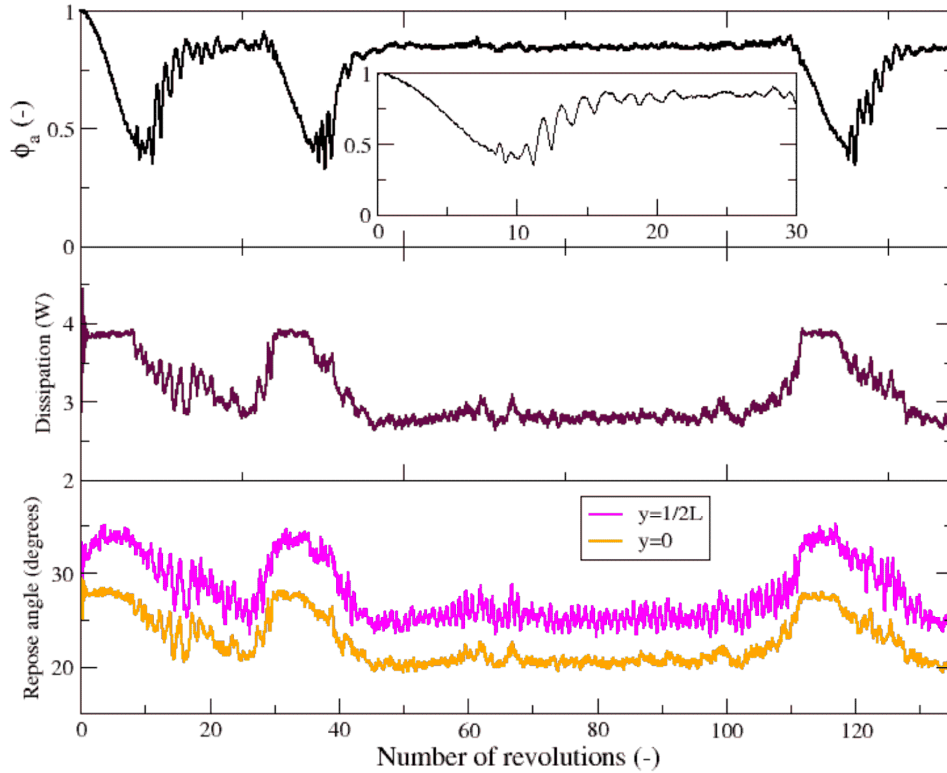


**Figure 6:** The axial order parameter, angle of repose and the power dissipation as functions of the number of revolutions, for an initially homogeneous bed in a drum with rough end-walls (drum 1). As the angles of repose at the two end-walls,  $y = \pm 1/2L$ , are very similar and overlap, only one of these curves is shown. The angle of repose in the centre of the drum,  $y = 0$ , follows this curve closely, with an average difference of 5 to 6 degrees. The power supply to the drum fluctuates in phase with the angle of repose and out phase with the order parameter, varying between a low value of 2.7 W when the bed is  $L_wSL_w$  segregated and a high value of 3.9 W when the bed is in the more ordered LSL configuration. Slow and fast oscillations of the axial order parameter for an initially mixed bed in a drum with rough end-walls (drum 1). The steady  $L_wSL_w$  state is interrupted twice, around 35 and around 120 revolutions, by a brief excursion to the LSL state with a concomitant increase in the power consumption.

Apparently, the successive transitions of the bed from mixed to radially segregated to three-banded LSL do not substantially change the power consumption (Rapaport, 2007). The power supply, and hence the closely related rate of energy dissipation by the bed, decrease, however, when the LSL layering

evolves into an  $L_wSL_w$  pattern, as happens twice in Figure 6. The energy consumption rises again with the occasional lapses from  $L_wSL_w$  into LSL, which occurs in Figure 6 after 35 and 120 revolutions. A list of energy dissipation, sorted by drum type and segregation, is provided in Table 3.

Interestingly, the steady states (the rightmost two columns of the table) typically require less power than the transient states encountered on the path to equilibrium. This suggests that minimum dissipation is an important mechanism in establishing the preferred segregation state of the granular bed. But as discussed in section Steady states, this mechanism is not alone in determining the steady state of the bed.

In drums with smooth end-walls the angles of repose near these walls fluctuate considerably, as shown in Figure 7, with no correlation between the two angles nor with the angle in the centre of the drum. The spontaneous build-up of a steep angle near either of the walls again causes the particles to flow down that slope along curved trajectories, which are illustrated in Figure 8 for an SLS configuration in drum 5.

As for the drum with rough end-walls, the axial motion promotes the formation of axial bands by transporting the particles towards locations where percolation segregates the particles by size. The development of the angle of repose in Figure 7 shows how the SLS bed repeatedly develops a large angle of repose, alternating between the end-walls, before finally settling in an LS configuration with a

**Table 3:** The rate of energy delivery by the engine driving the drum, expressed in Watts. The energy dissipation rates for any chosen type of end-walls are remarkably insensitive to the state of the bed for the four ideal states: homogeneously mixed, radially segregated and three-banded with flat interfaces (second column). A reduction of the dissipation is observed for less-well segregated three-banded beds and for beds with two bands – the rates listed in the last two columns correspond with the steady states reported for these drums in Table 1.

Drum	Mixed / R / LSL / SLS	$L_wSL_w /$ $L_rSL_r / L_sSL_s$	LS / $L_wS$
1	3.9	2.8	2.7
2	3.7	2.5	2.5
3	3.6	2.5	2.0
4	3.6	2.1	1.8
5	3.6	2.1	1.8
6	3.6	-	1.8

systematically higher angle of repose at the side of the large particles.

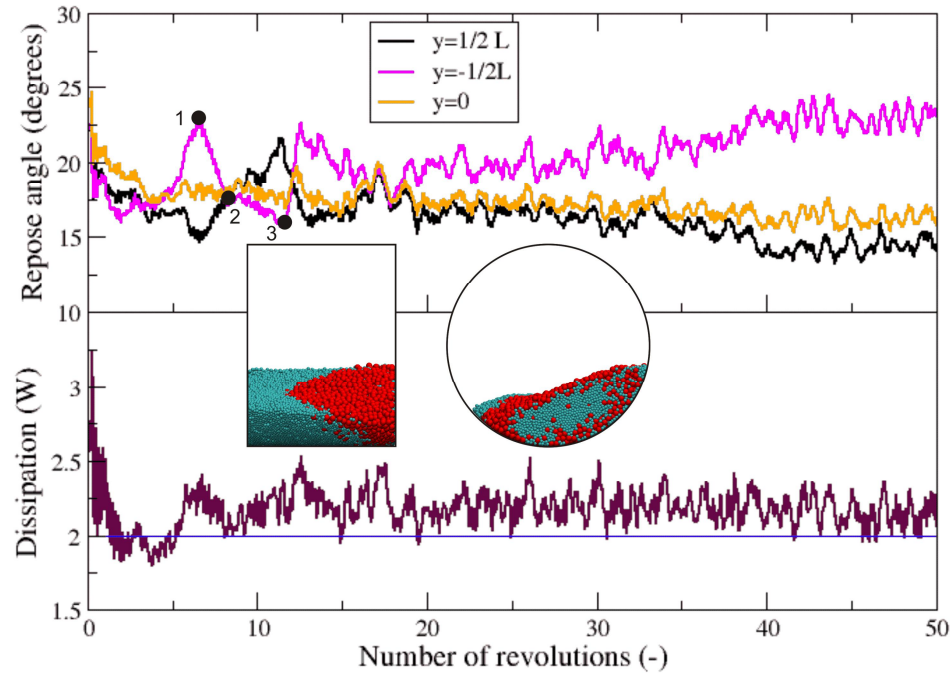


**Figure 7:** In the upper panel the angles of repose of the granular bed, in the middle ( $y = 0$ ) and at the two energy-conserving end-walls ( $y = \pm 1/2 L$ ), is plotted against of the number of revolutions. The bed starts in an SLS state, and after several aborted attempts (dots) eventually develops an LS configuration. Snapshots of the configuration obtained after 50 revolutions are inserted. In the bottom panel the power dissipation is plotted. A line  $y=2$  is added to visualize the slow decrease of power dissipation in time during the purification of the two bands.

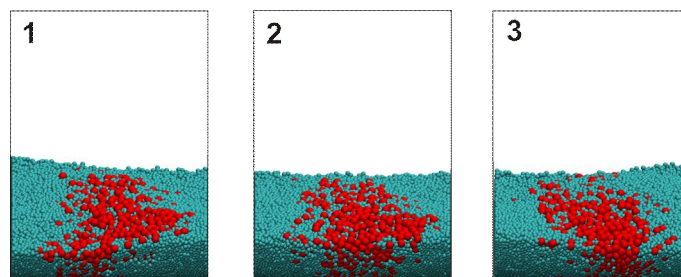


**Figure 8:** Snapshots of an SLS bed in drum 5 during the third oscillation in the angle of repose in Figure 7, as seen from the front of the drum. Belonging to dots in Figure 7.

Figure 9 shows that the axial distribution of the large particles grows wider with every attempt, while simultaneously moving consistently to the positive end of the drum. Interestingly, this suggests that the preferred side has already been established at the start of the simulation.

The set of simulations started with macroscopically identical SLS configurations shows no preferred end-wall for the final single band of small particles, as expected. It is clear, however, that the band of large particles in an asymmetric macroscopic SLS state has the propensity to increase the asymmetry by drifting to that side of the drum that contains most large particles and fewest small particles. A similar correlation is observed between the distribution of large particles in the initial mixed configuration and the final segregation of the drum.

An initially mixed bed in a drum with smooth end-walls at first rapidly forms a radial core, see drums 4 and 5 in Figure 3, followed by a similar sequence of attempts to segregate axially through the build-up and decay of alternating steep slopes at the end-walls. The axial distribution of the large particles, see Figure 10, shows that the bed again has a propensity to steadily increase the asymmetry of the distribution, resulting in the accumulation of large particles at one end of

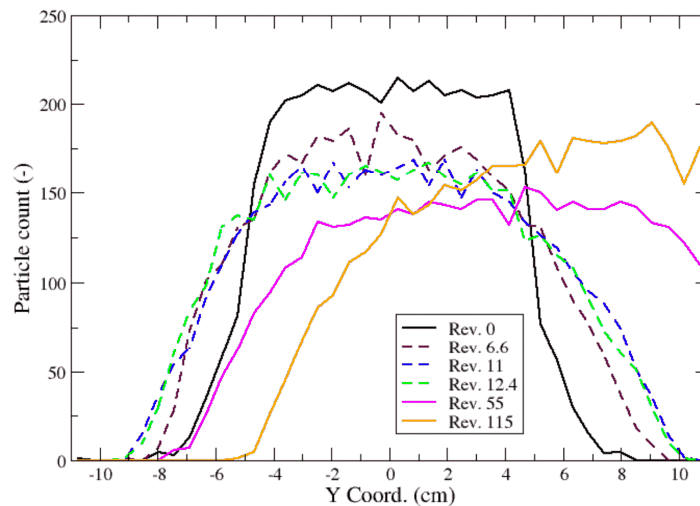


**Figure 9:** Concentration profiles of the large particles, at various numbers of revolutions during the evolution of an SLS state into an LS state in a drum with energy-conserving end-walls. See Figure 11 for matching snapshots of the granular bed.

the drum. A weak tendency to segregation into a three-banded LSL state is discernable in the distributions after 7 and 31 revolutions, but it does not set through. The energy dissipation rate of the bed slowly decreases as axial segregation proceeds, and levels off when the stationary two-banded state is reached.

In the simulations with periodic boundary conditions, rather than explicit end-walls, the radially and the axially segregated state are both long-lived. Studies on long and on periodically continued drums have shown that a radial core will eventually, after very many revolutions, give way to axial banding (Newey *et al.*, 2004; Taberlet *et al.*, 2004). The influence of the end-walls is thus mainly on the dynamics of the system, not on the final steady state. For the first couple of revolutions, the segregation of a homogeneous bed is seen in Figure 3 and Figure

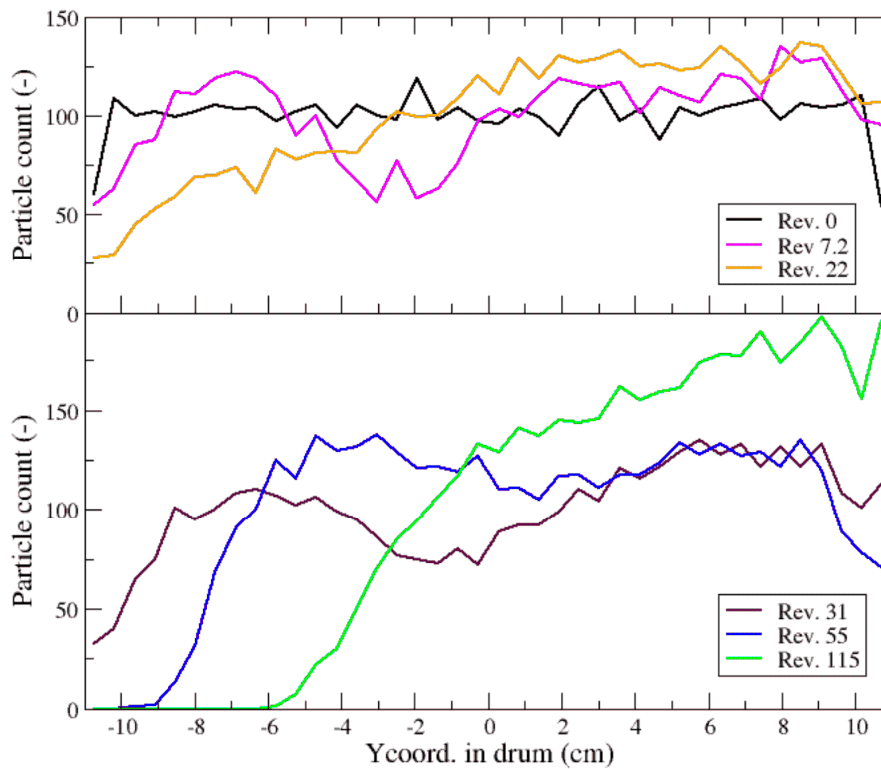


**Figure 10:** Concentration profiles of large particles in drum 5, while the initial mixed bed gradually turns into a two-banded configuration.

2 to be very similar for systems with and without end-walls. The beds in drums with smooth walls start to develop axial segregation in two or three stepwise increments of the radial order parameter, see Figure 3. After 20 (drum 4) to 35 (drum 5) revolutions axial segregation sets in, see Figure 2, and the increments in the radial order parameter stop. The bed in a short periodically continued drum shows similar increments in the radial order parameter, see Figure 2, but here these increments do not stop within the 120 revolutions of the simulation. These increments occur when large particles accumulate at the top of the flowing layer.

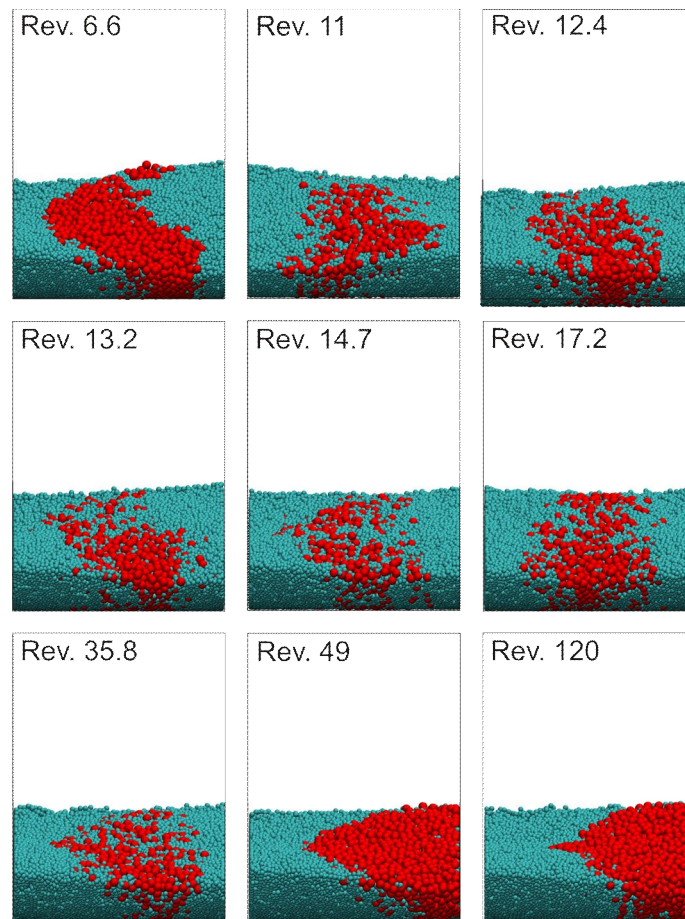


**Figure 11:** Snapshots of an SLS state developing into an LS state in drum 5. The matching density profiles of the large particles are shown in Figure 9.

When the flowing layer takes them up, they rapidly becomes remixed, see Figure 12, before being regenerated again from scratch. In the smaller oscillations of that plot less large particles accumulate near the top of the flowing layer. For this

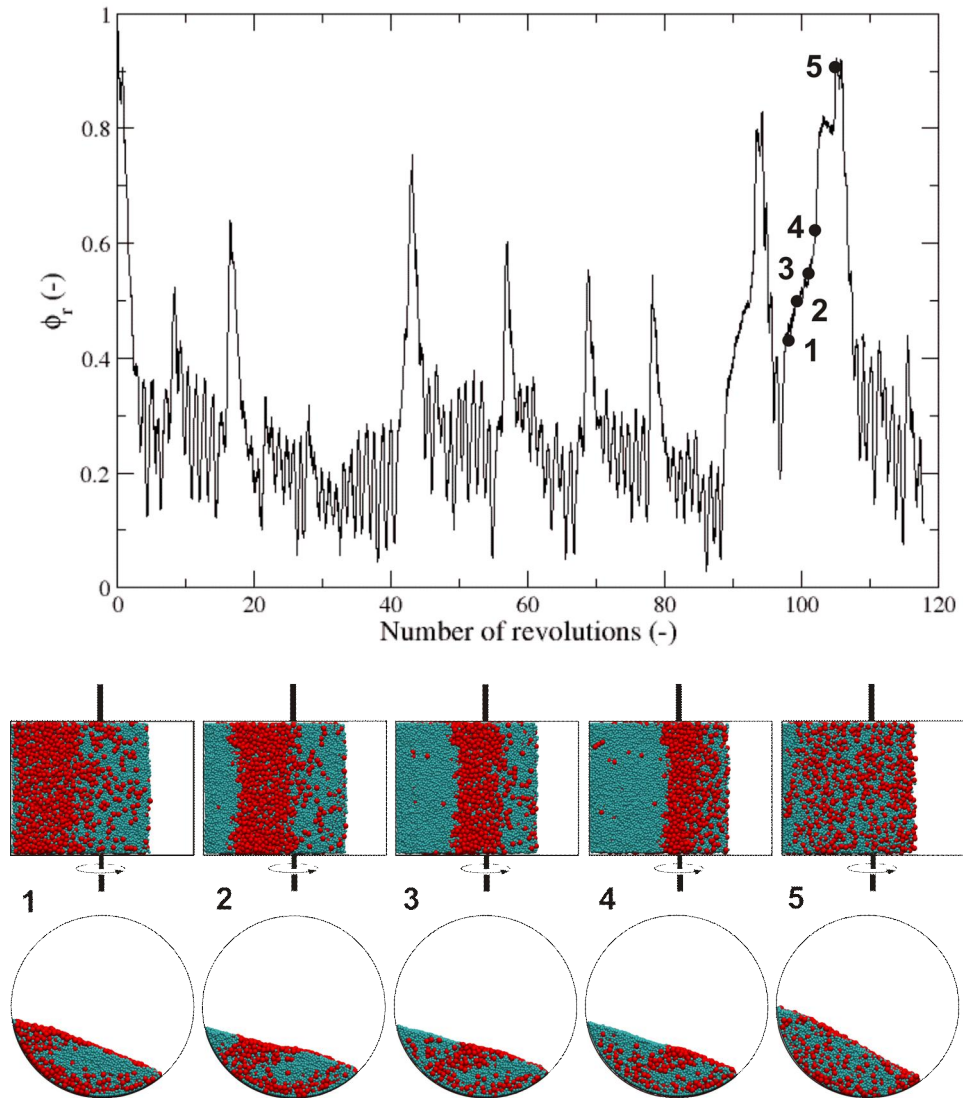


**Figure 12:** Graph of  $\phi_r$  for drum 6 and snapshots (top and side view) showing the configuration changes in an increment in the order parameter of a radially segregated bed in a drum with periodic boundary conditions.

---

reason the remixing gives her a less pronounced mixed state.

## CONCLUSIONS

The influence of the end-walls on the segregation of bidisperse granular beds in rotating short horizontal drums was assessed in an extensive set of DEM simulations, by varying both the end-wall properties and the initial configuration of the bed. For mixed beds, the mere presence of end-walls suffices to induce axial segregation, whereas periodically continued drums without end-walls are trapped in the radially segregated stage preceding axial segregation. This indicates that confinement affects the segregation process, by promoting axial banding in a radially segregated bed. Furthermore, the tangential friction between bed and end-walls also modifies the banding: beds in drums with rough end-walls segregate into three axial bands, with large particles accumulating in the two outer layers (LSL), while smooth walls give rise to two axial bands (LS). In both cases, the bands of large particles are partly carried by small particles acting as ‘ball-bearings’ between large particles and the cylindrical drum wall. The simulations indicate that the tangential friction at the end-walls induces an axial back-and-forth flow of particles rolling down the flowing layer near the end-walls. This flow carries large and small particles towards active percolation regions, where a fraction of the smaller particles settle, before returning – now enriched in the larger particles - to the end-walls.

The two aforementioned steady states are not necessarily recovered in simulations with differently ordered starting configuration, suggesting that there are activation barriers between well-segregated states. Hence, a bed in a metastable configuration may go through several ‘attempts’ before successfully making the transition to a more stable state, as seen for instance in Figure 7 for the transition from LSL to LS in drum 5. The inability of the bed in a periodic drum to make the transition from a radial to the more stable (see below) axial segregation, despite a series of attempts, may indicate that the end-walls lower the barrier for this transition and/or enhance the attempt frequency.

Calculations of the power consumptions by stationary rotating drums indicate that the long-lived states dissipate less energy per unit of time than the short-lived unstable states (see Table 3). The current simulations suggests that

minimization of the energy dissipation rate may play a role, besides the conventional percolation mechanism, in determining the stability of segregated states. As discussed above, the presence of activation barriers between steady states may prevent the system from reaching the optimum state within a specified time frame. For the bed in the periodically continued drum, for instance, we expect it to relax eventually from radial to axial ordering – since the latter has both a considerably lower dissipation rate and much smaller oscillations of its order parameters - even though this transition was not observed within the 120 revolutions of our simulation.

A peculiar feature emerging in drums with rough end-walls is the instability of the ‘steady state’. An initially homogenous mixed bed adopts a slightly disordered three-banded state, which is interrupted at unpredictable intervals by short excursions to a three-banded state with a deeper segregation, see Figure 6. We speculate that the erratic dynamics of the granules (i.e. the microscopic state of the bed) occasionally results in a configuration that destabilizes the prevailing macroscopic state of the bed, thereby inducing the transition. These accidental transitions furthermore imply that the activation barrier separating the two three-banded states will be fairly low. Interestingly, the short excursions are accompanied by a temporary increase in the energy dissipation rate of the bed, which in view of the above speculations may be a contributing factor to the short survival times of the more-ordered state.

## REFERENCES

- Allen, M. P. and Tildesley, D. J.** (1987). *Computer simulation of liquids*. Oxford, U.K., Oxford Science Publications.
- Aranson, I. S. and Tsimring, L. S.** (1999). Dynamics of axial separation in long rotating drums. *Physical Review Letters* **82**(23).
- Arntz, M. M. H. D., den Otter, W. K., Beeftink, H. H., Bussmann, P. J. T., Briels, W. J. and Boom, R. M.** (2008). Granular mixing and segregation in a horizontal rotating drum: a simulation study on the impact of rotational speed and fill level. *AIChE Journal* **54**(12): 3133-3146.
- Atkins, P. and Paula, J. D.** (2010). *Physical Chemistry*. Oxford, Oxford University Press.
- Caps, H., Michel, R., Lecocq, N. and Vandewalle, N.** (2003). Long lasting instabilities in granular mixtures. *Physica A: Statistical Mechanics and its Applications* **326**(3-4): 313-321.

- Chen, P. F., Ottino, J. M. and Lueptow, R. M.** (2008). Subsurface granular flow in rotating tumblers: A detailed computational study. *Physical Review E* **78**(2).
- Choo, K., Molteno, T. C. A. and Morris, S. W.** (1997). Traveling granular segregation patterns in a long drum mixer. *Physical Review Letters* **79**(16).
- Cleary, P. W.** (1998). Predicting charge motion, power draw, segregation and wear in ball mills using discrete element methods. *Minerals Engineering* **11**(11): 1061-1080.
- Cundall, P. A. and Strack, O. D. L.** (1979). Discrete Numerical-Model for Granular Assemblies. *Geotechnique* **29**(1): 47-65.
- Di Renzo, A. and Di Maio, F. P.** (2004). Comparison of contact-force models for the simulation of collisions in DEM-based granular flow codes. *Chemical Engineering Science* **59**(3): 525-541.
- Fiedor, S. J. and Ottino, J. M.** (2003). Dynamics of axial segregation and coarsening of dry granular materials and slurries in circular and square tubes. *Physical Review Letters* **91**(24).
- Hill, K. M. and Kakalios, J.** (1994). Reversible Axial Segregation of Binary-Mixtures of Granular-Materials. *Physical Review E* **49**(5).
- Hill, K. M. and Kakalios, J.** (1995). Reversible Axial Segregation of Rotating Granular Media. *Physical Review E* **52**(4).
- Khakhar, D. V., Orpe, A. V. and Hajra, S. K.** (2003). Segregation of granular materials in rotating cylinders. *Physica a-Statistical Mechanics and Its Applications* **318**(1-2): 129-136.
- Maneval, J. E., Hill, K. M., Smith, B. E., Caprihan, A. and Fukushima, E.** (2005). Effects of end wall friction in rotating cylinder granular flow experiments. *Granular Matter* **7**(4): 199-202.
- Mellmann, J.** (2001). The transverse motion of solids in rotating cylinders - forms of motion and transition behavior. *Powder Technology* **118**(3): 251-270.
- Nakagawa, M., Altobelli, S. A., Caprihan, A., Fukushima, E. and Jeong, E. K.** (1993). Noninvasive Measurements of Granular Flows by Magnetic-Resonance-Imaging. *Experiments in Fluids* **16**(1): 54-60.
- Newey, M., Ozik, J., Van der Meer, S. M., Ott, E. and Losert, W.** (2004). Band-in-band segregation of multidisperse granular mixtures. *Europhysics Letters* **66**(2): 205-211.
- Ottino, J. M. and Khakhar, D. V.** (2000). Mixing and segregation of granular materials. *Annual Review of Fluid Mechanics* **32**: 55-91.
- Pohlman, N. A., Meier, S. W., Lueptow, R. M. and Ottino, J. M.** (2006a). Surface velocity in three-dimensional granular tumblers. *Journal of Fluid Mechanics* **560**: 355-368.
- Pohlman, N. A., Ottino, J. M. and Lueptow, R. M.** (2006b). End-wall effects in granular tumblers: From quasi-two-dimensional flow to three-dimensional flow. *Physical Review E* **74**(3).
- Rapaport, D. C.** (2007). Radial and axial segregation of granular matter in a rotating cylinder: A simulation study. *Physical Review E* **75**(3).
- Taberlet, N., Losert, W. and Richard, P.** (2004). Understanding the dynamics of segregation bands of simulated granular material in a rotating drum. *Europhysics Letters* **68**(4): 522-528.

- Taberlet, N., Newey, M., Richard, P. and Losert, W.** (2006). On axial segregation in a tumbler: an experimental and numerical study. *Journal of Statistical Mechanics-Theory and Experiment*(7).
- Turner, J. L. and Nakagawa, M.** (2000). Particle mixing in a nearly filled horizontal cylinder through phase inversion. *Powder Technology* **113**(1-2): 119-123.

---

## **Chapter 6 Discussion**



---

## INTRODUCTION

Mixing of solids is one of the most common operations in the industry. Examples are the mixing of cement, production of pharmaceutical products, and the production of a range of food products. One such example is the preparation of mixtures of spices. These spices have to be mixed homogeneously, while the individual grains are inhomogeneous, and the mixture may even be composed of different types of spices. While mixing of granules which are homogeneous in size, shape and density and other properties is easy, when granules of different size or density are brought together, they tend to de-mix, and special care has to be taken in the design of the mixing process to avoid this segregation. In addition, the mixed spices have to be sterilized. This is usually done with steam. The spices have to be homogeneously heated by the steam, and cooled again, which implies that fast and homogeneous mixing is crucial.

A new process has been proposed to have a better sterilization of spices by mixing the spices with zeolite granules. Zeolite granules in direct contact with product granules (spices or herbs) adsorb water from the product; in turn, the zeolite releases adsorption heat, which heats up the product, which may lead to sterilization of the spices. If the heating is not sufficient for sterilization, steam may be injected, which will also be adsorbed by the zeolite, leading to further heating. As the moisture and heat transfer is dependent on close contact between the zeolite and the spices, fast mixing is essential. This ensures that each individual product grain will be heated long enough to guarantee sterilization, yet short enough to avoid degradation by e.g. Maillard reactions. However, spices are mechanically fragile. During sterilization of black pepper, for instance, it is important to avoid damage to the skin of the pepper grains. Excessive exposure to shear should therefore be avoided, however, mixing is coupled to application of shear. To prevent such damage, low-shear mixers such as the Nauta mixer or the helical-blade mixer may be used. The horizontal rotating drum is another common type of low-shear mixer that is commonly used in the food industry, for example in the production of seasonings, pet food formulations, nuts and seeds, vitamins and minerals premixes, coated snacks or sweets, and in other industries (mixing of asphalt, cement, pharmaceuticals) (Sherrit *et al.*, 2003; Kuo *et al.*, 2005).

Many mixers that result in fast mixing expose the product to intense shear forces; other may be milder but result in slower mixing. Mixers that produce large mechanical and thermal stress are e.g. granulators, the Cyclomix<sup>®</sup> or extruders; the Nauta or conical-blade mixers are milder. The relation between exposure to shear and mixing efficiency is however not clearly understood. The major problem in this is that inhomogeneous powders and granulates have the intrinsic tendency to segregate (i.e., to counter-act the mixing). Even though most mixers have been empirically optimised to ensure good mixing, this can be at least partially undone by subsequent handling of the material. Better understanding of segregation of inhomogeneous granular materials under flow will therefore lead to better product consistency, and may lead to simpler process design, for example by making specific mixing steps unnecessary by ensuring that in other parts of the process segregation does not take place.

*Segregation* or separation of granular systems is usually done with filters or screens, and in some cases with air classification. Understanding of the segregation of granular systems under flow, could lead to the use of this phenomenon as a positive effect. However, this is only possible when the dynamics of segregation are well understood.

Both from the perspective of having more efficient handling of mixed granular products, and from the perspective of using segregation as separation mechanism, better understanding is required. The aim of this thesis was therefore to obtain this understanding. We chose the use of the simplest geometry that is still practically relevant: the horizontal, rotating drum.

Experimental studies on granular media are often hampered with complexity: very many parameters may influence the outcome of an experiment, and thus one is never sure which parameter determines the specific outcome. In computer simulations, one can limit the system's complexity, and very accurately control the individual parameters. The method of discrete particle modelling was chosen, as this is a numerical method that captures the complete dynamics of granular systems, allowing for different configurations, while its parameters can easily be translated to practically relevant particle properties and process parameters.

---

## CONCLUSIONS FROM PREVIOUS CHAPTERS

In **chapter 2** the dependence of mixing and segregation on the fill level and the rotational velocity of the drum are investigated.

An order parameter was introduced, based on the concept of entropy, which was found to serve very well for characterization of the degree of mixing.

In a half filled drum the particle bed segregated radially at low Froude numbers ( $Fr < 0.25$ ), while the radial segregation inverted at high Froude numbers ( $Fr > 0.7$ ). At a critical Froude number ( $Fr = 0.56$ ), all systems were well mixed. The same pattern was evident for other fill levels, although the critical Froude number was slightly shifted.

We found that segregation as well as inverted segregation was caused by percolation, in which smaller particles percolate in between the moving larger particles. The critical  $Fr$  number is indicative of a cascading-cataracting regime, in which random collisions dominate, leading to a mixed state.

The results were summarized in two state diagrams in Figure 1. The state diagram representing the flow regime is qualitatively similar to experimental results reported in literature for somewhat different systems (Mellmann, 2001). We thus believe that the global structure of the state diagram is rather insensitive to the specific characteristics of the granular material (size, size distribution, surface properties).

In practice granular mixtures generally are not bidisperse, but polydisperse. We therefore simulated a drum with three types of particles differing in size as displayed in Figure 2. The results were qualitatively similar to those for a bidisperse system, with the intermediate particles residing in regions in between the other two.

In **chapter 3** the concept of the state diagrams as developed in chapter 2 was translated to other particle systems, with variation in particle softness, density and roughness.

The state diagrams developed in chapter 2 were found to be applicable here as well. In line with chapter 2, with the critical  $Fr$  number at 0.56 again, we found

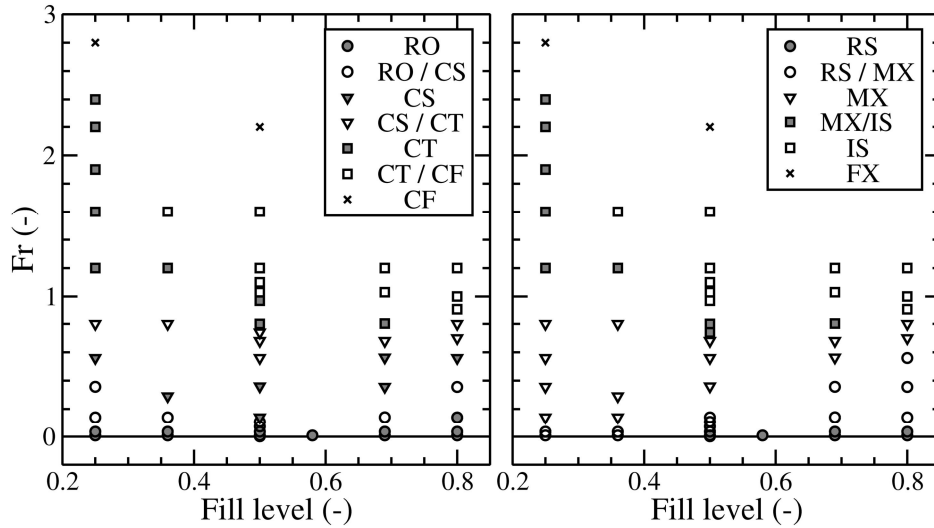


**Figure 1:** State diagrams of the flow regime (left) and the segregation state (right) plotted against the fill fraction and the Froude number. The markers are used to indicate different stationary states, see the legends to the plots.

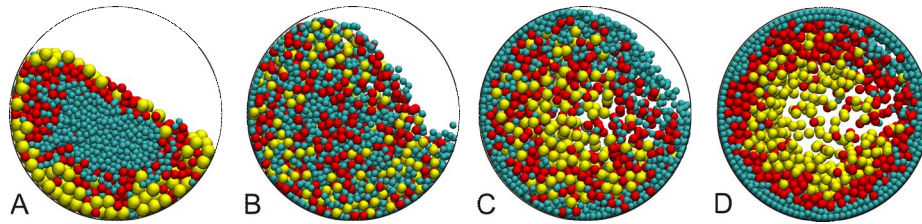


**Figure 2:** Snapshots of a granular bed with three particle types in different flow regimes, illustrating the segregational phenomena **A.** radial segregation **B.** mixing **C.&D.** inverted segregation.

that for low and high Froude numbers ( $Fr < 0.56$  and  $Fr > 0.8$ ), particles that differ in size and/or density will segregate radially. Without a difference in density or size, no segregation will take place, regardless of variations in roughness and/or softness. As size and density work in opposite direction, it is possible to balance the two exactly, such that no segregation takes place at all.

In **chapter 4**, axial segregation was studied. There is some evidence that the presence of the end wall (vertical ends of the drum) induce this type of segregation, and therefore we focused on this, by using a drum that is relatively

short ( $L/D = 0.7$ ). It was found that particles have a pronounced 3-D motion in the rotating bed. Next to the rotating motion, the particles also travel from the vertical walls towards the centre and back. Small particles percolate through the flowing layer and end up deeper inside the bed, and the larger particles therefore accumulate on top of the flowing layer and are transported back to the vertical walls. The result is the formation of axial bands with large particle bands adjacent to the end walls. In a relatively short drum the curved flow profiles give rise to strong oscillations in composition; from axially separated into three bands to a layer of small particles below the large particles bands. These oscillations can continue for many drum rotations; then subside into an axially segregated configuration, which was found to have the minimum energy dissipation; however after some time the oscillations can start again. This whole sequence can occur many times in a row.

It is not without reason to assume that the presence of the end walls is important in this effect. For example, (Chen *et al.*, 2008) saw that the curved flow profile in a monodisperse system was not present without friction with the end walls. In **chapter 5** the influence of the friction of the particles with the end-walls in a bidisperse system was therefore investigated. As long as end wall were present, axial segregation took place; a drum with periodic boundary conditions (simulating an infinitely long drum) remained radially segregated over the span of time simulated. The mere presence of end walls was found to initiate axial segregation, which is in agreement with literature (Hill and Kakalios, 1994, 1995; Caps *et al.*, 2003).

A striking observation was the dependence of the final configuration on end-wall roughness. With smooth end walls, two axial bands were formed; with rough end walls, three bands were found (large-small-large). This could explain why some authors find three bands as the final configuration bands (Nakagawa, 1994) and other two (Chicharro *et al.*, 1997).

## CONSEQUENCES FOR PROCESS DESIGN

In chapters 2 and 3 it was found that there is a critical Froude number at which the two types of radial segregation cancel, and mixing is obtained, independent on the properties. Operating a rotating mixer at this speed would allow for a

broad range of designs, and would yield mixing almost independent of the type of granular load. It should be borne in mind, however that the critical number was somewhat (but not strongly) dependent on the fill level. A different fill level would therefore require a slight adaptation of the rotation speed. A higher fill level means less bed revolutions per drum revolution but also above 50% of fill a smaller flowing layer. To compensate for these small differences, high fill levels need a somewhat higher rotation velocity to increase the size of the flowing layer and simultaneously increase the mixing due to random collisions.

More importantly, when other unit operations than mixers would operate in the same regime, segregation would be avoided there. For example, a storage vessel could be rotated at the critical  $Fr$  number, or a transportation tube could be rotated to give the same  $Fr$  number.

Other methods could be applied as well, though they would imply a slightly more complex design. One may for example vary the rotational velocity of the drum every e.g. 5 revolutions in order to change the flow regime from rolling to cataracting and back. This would reverse the segregation process with every change. Frequent adjustment of the flow regime will keep the small particles migrating through the bed, resulting in a mixed bed.

An adaptation of this would be to alternate the flow. In chapter 2 we observed that for angular drum velocities in the cataracting regime and beyond, it takes some time before the particles in the dense bottom of the bed have adjusted to the instantaneously introduced angular velocity of the drum. A peak in the order parameter characterizes this transient regime. Consequently, it is possible to improve the degree of mixing by prolonging this slip regime by alternating the rotational velocity between positive and negative velocities after e.g. every 2 revolutions.

In practice most of the time short baffles are added to the drum wall to disturb the flow profile and introducing more chaos into the system. (Shi *et al.*, 2007) showed with DEM that the effect of these baffles is small. However, placing a central baffle truncates the flowing layer, leading to good mixing. The translation to commercial scale is ongoing.

It is interesting that the concept of the critical  $Fr$  number would enable us to first have good mixing between dissimilar particles by operating at the critical  $Fr$  number, and then segregate the particles again by simply changing the rotational rate. This would be of great value for systems in which temporary physical contact between dissimilar particles is required. One such system will be discussed below.

The oscillations that were shown in the segregation (chapters 4 and 5) may have an application in improving macro mixing. A drum mixer is usually not a very efficient mixer. Even when the system operates in a regime that gives mixing, it takes several revolutions before the system is completely mixed. Long-range migration is considered slow in these systems. However, by designing the system such that the oscillations will set in, we will see a continuous long-range migration of both the larger and the smaller particles. Even though we have not investigated macro mixing in these systems. We may expect that the oscillations will speed this up.

#### **A CASE STUDY: ZEOLITE CONTACT STERILIZATION OF SPICES AND HERB**

Spices in general are sterilized by heating with steam. The spices are brought into a mixer, which is closed and evacuated. Steam is then introduced, which partially condenses on the spices, and heats them up. By releasing the pressure, the condensed steam evaporates again, and the spices cool down.

This process suffers from mass transfer limitation, as the steam first tends to condense on the outer parts of the bed, and thus the bed has to be mixed. Since the spices are mechanically quite sensitive, the shear has to be minimized. This is aggravated by the fact that the spices become moist during the sterilization process, due to the condensed steam. Application of a drum that rotates at the critical  $Fr$  number may well be an option here.

An innovation that is relevant to this process, is sterilization by direct contact with zeolite granules. These zeolite granules are of a hydrophilic (Al-rich) type, which has a very high heat of adsorption for water. A bed of spices that is mixed with these zeolite, could be contacted with steam. The steam now does not condense on the spices but is adsorbed into the zeolite granules. These granules

heat up strongly, and heat is transferred by contact to the adjacent spices. As soon as the sterilisation temperature is reached, steam injection stops. The process is stopped by opening the system, as was the case with the conventional process. The advantage of this process is that the spices remain dry, which minimized mechanical damage, while the amount of heating can be easily controlled by the amount of steam. The zeolite can be later regenerated by heating above 250 °C, at which temperature the water is released again as steam.

This process depends on thorough mixing of the zeolite and the spices. Since these particles are quite different in density and generally also in size and surface properties, segregation may be expected. By operating in the right regime (e.g., at the critical  $Fr$  number), mixing will result. Designing the system such that the oscillations found in chapters 4 and 5 will occur, will help in establishing fast mixing over long distances.

Whereas the existing process is strictly a batch process, one may envisage that the findings in this thesis may enable the process to be operated in continuous mode. The size of the zeolite grains can be chosen such that the size and density ratio of the zeolite and pepper grains balance each other; mixing results (see chapter 2). During the process, the zeolite granules absorb water and their density increases. This change in density can disturb the balance between percolation and buoyancy, leading to segregation of the saturated zeolite grains from the mixture into the outermost layer, which can then be removed. Application of such a system in a rotating cylinder, in which the spices would slowly be transported, would then result in a continuous sterilization process.

If mixing due to the exact balance between density and size is found too critical in practice, it is possible to first operate at the critical  $Fr$  number, to ensure mixing (allowing for the oscillations could speed up macro mixing) and then reduce the rotation rate, which will lead to segregation of the zeolite into bands. These can then be easily removed.

Thus, by making use of the right regimes, it is found that a rotating drum is in fact a very flexible system: exactly the fact that it can revert from mixer to segregator gives it potential for processing complex granular mixtures.

---

## OUTLOOK

The radial segregation phenomena, as discussed in chapters 2 and 3 can be relatively well understood. The 3-D (radial and axial) segregation dynamics have shown us previously unknown behaviour such as the recurring oscillations and the two possible final configurations one minimizing the energy dissipation the other not.

End walls were shown to have strong influence. The reason for this is not yet clear and would merit further research. Formation of two bands leads to minimization of the energy dissipation. This could imply that the system strives to have just one boundary layer between the two types of particles instead of two. The l-s-l configuration was found to be at least meta-stable, while the S-l-S configuration was not. The preference of large particles to segregate at the end walls is not understood.

It is therefore clear that the mechanisms behind these phenomena should be further pursued.

## METHOD OF INVESTIGATION

The method that we have chosen is very suited for mechanistic simulations on smaller scale; however the fact that every granule has to be modelled apart implies that it is not feasible to go to larger systems, as the number of particles in a system is dependent on the third power of the dimension.

A second disadvantage of DEM is that although the relation to the properties of the individual particles is clear, this also imposes that the relation to macroscopic properties, such as rheological behaviour, is much less clear. Well-established statistical mechanical and fluid dynamics descriptions for fluids are not applicable to granular systems. Continuous models can be made but rely on sufficient insight in the bulk behaviour to extract constitutive relations by averaging over the individual particles.

We should however ultimately aim for the transition towards ‘continuous modelling’, because it will allow the simulation of larger systems with calculation times in the order of minutes rather than weeks or sometimes even

months, as is usual for DEM. Future DEM studies should be aimed for providing the basis for this.

## CONCLUSION

The discrete element modelling approach used in this thesis was found to be suitable for studying granular dynamics in heterogeneous systems. We could well reproduce experimental findings, but by the accurate control over all properties, in a simulation it was possible to obtain much better insight than is possible with experiments alone.

The underlying mechanisms of particle segregation were partly identified. The inverted radial segregation was explained, as was the formation of large axially segregated bands near the end walls. The motivation for the formation of two axial segregated bands and the formation of a small particle layer beneath the large particle layers could be the minimization of the energy dissipation, but the results on this are not consistent. Although these steps are made, we are not yet able to explain all the phenomena described in literature or found in this thesis.

Even though we could formulate some guidelines on the design of mixers and segregators, for quantitative design methods, we will have to make the step to continuous models. However, on the basis of the guidelines we could envisage an improved sterilization process, and even sketch how this could be made continuous.

It is clear that granular dynamics is a field that still holds many secrets, and will continue to enthrall scientists and engineers over the world. This thesis has contributed several aspects to the understanding, but more has to be done before this field can be considered mature.

## REFERENCES

- Caps, H., Michel, R., Lecocq, N. and Vandewalle, N.** (2003). Long lasting instabilities in granular mixtures. *Physica A: Statistical Mechanics and its Applications* **326**(3-4): 313-321.
- Chen, P. F., Ottino, J. M. and Lueptow, R. M.** (2008). Subsurface granular flow in rotating tumblers: A detailed computational study. *Physical Review E* **78**(2).

- 
- Chicharro, R., Peralta-Fabi, R. and Velasco, R.** (1997). Segregation in dry granular systems. *Powders and Grains 97*. P. Behringer and J. Jenkens. Rotterdam, Balkema: 479-482.
- Hill, K. M. and Kakalios, J.** (1994). Reversible Axial Segregation of Binary-Mixtures of Granular-Materials. *Physical Review E* **49**(5).
- Hill, K. M. and Kakalios, J.** (1995). Reversible Axial Segregation of Rotating Granular Media. *Physical Review E* **52**(4).
- Kuo, H. P., Hsu, R. C. and Hsiao, Y. C.** (2005). Investigation of axial segregation in a rotating drum. *Powder Technology* **153**(3): 196-203.
- Mellmann, J.** (2001). The transverse motion of solids in rotating cylinders - forms of motion and transition behavior. *Powder Technology* **118**(3): 251-270.
- Nakagawa, M.** (1994). Axial Segregation of Granular Flows in a Horizontal Rotating Cylinder. *Chemical Engineering Science* **49**(15): 2540-2544.
- Sherrit, R. G., Chaouki, J., Mehrotra, A. K. and Behie, L. A.** (2003). Axial dispersion in the three-dimensional mixing of particles in a rotating drum reactor. *Chemical Engineering Science* **58**: 401-415.
- Shi, D., Abatan, A. A., Vargas, W. L. and McCarthy, J. J.** (2007). Eliminating segregation in free-surface flows of particles. *Physical Review Letters* **99**(14).

---

## Summary

Mixing of granular solids is a processing step in a wide range of industries. In the food industry for example, it is important in drying and sterilization of spices and herbs, in freeze-drying, in the production of instant soups, and in the coating of snacks and candies. The fundamental phenomena in granule mixing are still poorly understood, making it difficult to *a priori* predict the effectiveness of mixing processes.

While mixing of granules is easy when the particles are homogeneous in size, shape and density and other properties, in practice they are not. With such a mixture, homogenizing is far more complex, since the heterogeneous particles tend to segregate, and special care has to be taken in the design of the mixing process to avoid this. The practical importance and intriguing complexity of the dynamics of granular systems have made them the subject of intense research in the last decades, but the general insight in the behaviour of these systems is still far from complete.

In view of the practical need for better understanding and control of solids mixing, the work in this thesis has two closely coupled objectives. The first objective is to obtain a better understanding of segregation mechanisms. This insight should enable the enhancement of mixing and at the same time suppress segregation, or vice versa, namely the deliberate and controlled segregation of a mixture. The second objective is to provide guidelines for mixing operations that can be derived from insights extracted from the data on mixing behaviour at different rotational velocities and fill levels. From this perspective, we here report an extensive numerical study of mixing and segregation in a bed of bidisperse granules in a rotating horizontal drum, which is the simplest relevant geometry in industrial practice.

Two types of segregation can occur: fast radial segregation during which smaller or denser particles accumulate along the axis of rotation; and slow axial segregation with fully segregated bands of small and large particles perpendicular to the rotating axis, with in general particle bands of large particles adjacent to the end walls. This thesis reports on both radial and axial segregation phenomena in a horizontally rotating drum.

While visual observation of the particle bed was used as a qualitative observation technique to determine the degree of mixing/segregation, in parallel a more quantitative method was developed as well, which was based on calculating the entropy over the systems. By subdividing the system with a lattice, calculating the entropy of mixing in each cell of the lattice, and summarizing them over the system, a measure for the degree of overall segregation was obtained. By using different grids (a 3D mesh, a 2D set of slices perpendicular to the axis, or 2D bars parallel to the axis), different types of segregation could be distinguished.

The radial segregation dynamics were investigated in semi-2D (very short) drums, which inhibits axial segregation. Diagrams were prepared that visualise the mixing behaviour as function of the Froude number (rotational speed) for systems with different bidisperse systems. It was found that while almost all systems showed radial segregation at low  $Fr$  (rolling regime), and most showed inverted radial segregation at high  $Fr$  (cataracting or centrifuging regime), at  $Fr \approx 0.56$  all systems became radially mixed. This could be understood by assuming a percolation mechanism. In the moving layer on top of the load, smaller particles percolate in between the moving larger particles, down to the centre of the load, as long as the motion is not too fast. The same phenomenon is inverted at high speeds. In between, the flowing layer is expanded in such a way that many large voids are present, which makes the percolation mechanism less selective on the particle size. The little segregation that occurs is negligible, since the two phenomena described above work in different directions. Surprisingly this transitional  $Fr$  number is the same for all investigated systems.

Since axial segregation is always preceded by radial segregation, it is logical to also study axial segregation. This was done by studying longer drums, which allows axial segregation to develop along the axis. Axial segregation was found for most systems; its occurrence is mostly dictated by differences in size.

It was found that for drums that have intermediate length, surprising dynamic behaviour results. The axial segregation developed with low and high frequency oscillations. While the low frequency oscillations could be understood as the development and migration of segregated areas in the system, the higher frequency oscillations, with a period of 10 to 20 revolutions, were not identified before. This oscillatory behaviour is probably coupled to the use of intermediately sized drums, as this behaviour has not been seen with very long drums. We ascribe the oscillations to the influence of the (vertical) end walls, which expose the adjacent particles to different forces than those particles inside the drum load. These differences induce an axial flow in the system. The particles adjacent to the vertical walls tend to be lifted higher than the particles far away from the vertical walls. This creates a concave profile of the load surface throughout the drum, inducing the particles (in the rolling regime) to follow a path away from the vertical walls towards the centre of the drum. Once past the centre, the particles flow back to the vertical walls in response to the locally convex bed profile.

Even in this particular flow profile the percolation mechanism is of importance: smaller particles percolate through the flowing layer and end up deeper inside the bed, while the larger particles accumulate on top of the flowing layer and are conveyed back to the vertical walls. Due to the percolation of the small particles the final end configuration must clearly be a banding configuration of large-small-large particle bands. Prolonged rotation of the bed increases the concave form of the flowing layer. This induces fast oscillations and a sudden mixing of a part of the large particle band with the small particle band, giving fast mixing and leading to a configuration, in which a small-particle band is formed below the large-particles bands. Subsequently segregation into three bands (large-small-large) slowly occurs again, after which the asymmetry in the angle of repose further increases. The configuration, in which larger particles accumulate on top of the bed adjacent to the end walls, coincides with a minimum in energy dissipation, which is not present when the systems segregates radially or axially into three pure bands.

The effect found implies that the end walls are important in the dynamics of axial segregation. This effect is studied further by varying the end wall properties. The above mentioned fast and slow oscillations vanish in systems that have smoother end walls, while also the rate of segregation decreases; nevertheless the same

axially segregated three band (large-small-large) state of mixing resulted finally. Reducing the friction further to completely smooth end walls however changed the final configuration into a two-banded system. Systems with no end wall at all, simulated through periodic end walls, only gave radial segregation over the (considerable) simulated time span. We expect here that as long as there is still a driving force for axial segregation, the absence of the induction of axial flow by the end walls make the transition very slow or impossible. The formation of two axial bands lowers the energy dissipation by the bed, whereas neither radial segregation nor axial segregation into three bands reduced the power absorption at constant angular velocity.

While the oscillatory behaviour is relevant in its own right, their study also allows shedding some light on the fundamental mechanisms underlying the segregation mechanisms, and especially the transition from radial to axial segregation. The fact that this is dependent on not only the properties of the granular materials, but also on the geometry and design of the drum, implies that these findings have relevance to the design and operation of processes.

Some general guidelines were formulated and illustrated with the example of the design of a sterilisation process for spices and herbs. In the currently used steam sterilisation process, mixing and homogeneity is essential. Homogeneity is even more important in a new process, in which zeolite granules are mixed with the spices: The zeolite granules adsorb the steam and heat up because of the heat of adsorption, avoiding humidification of the spices. The subsequent heating of the spices relies on contact heating between spices and zeolite. To avoid local hot spots and the resulting deterioration of the spices, good mixing between the two is very important. The results of this thesis may be used to both ensure proper sterilization by good mixing as well as deliberately induced segregation to separate spices and zeolite as soon as the sterilisation process is completed.

## Samenvatting

Het mengen van granulaire vaste stoffen wordt als bewerkingsstap in vele industrieën toegepast. In de levensmiddelenindustrie is mengen bijvoorbeeld van belang bij het drogen en steriliseren van specerijen en kruiden, bij vriesdrogen, bij de productie van kant-en-klare soepen, en bij de coating van snacks en snoepgoed. De fundamentele verschijnselen, die een rol spelen in het mengen van granulaire vaste stoffen, worden echter nog slecht begrepen, waardoor het moeilijk is om *a priori* de doeltreffendheid van mengprocessen te voorspellen.

Het mengen van granulaten is eenvoudig wanneer de deeltjes homogeen zijn in grootte, vorm en dichtheid en andere eigenschappen. In de praktijk is een granulaat nooit volledig homogeen. Mengen is dan veel ingewikkelder, omdat het heterogene mengsel van deeltjes kan gaan segregeren. Om dit te voorkomen dient hier in het ontwerp van het mengproces extra aandacht aan besteed te worden. De grote praktische relevantie en de intrigerende complexiteit van de dynamica van de granulaire systemen heeft ervoor gezorgd dat segregatie de afgelopen decennia onderwerp is geweest van intensief onderzoek. Desondanks is het algemene inzicht in het gedrag van deze systemen nog verre van volledig.

Bezien vanuit de praktische behoefte aan een beter inzicht in en daarmee beheersing van granulaire menging heeft het werk in dit proefschrift twee nauw verweven doelstellingen. De eerste doelstelling is het verkrijgen van een beter inzicht in de fundamentele mechanismen van segregatie. Dit inzicht moet het mogelijk maken om menging te versterken en segregatie te onderdrukken, of vice versa, namelijk het gecontroleerd laten segregeren. De tweede doelstelling is om richtlijnen aan te reiken voor mengstappen op basis van data van menggedrag bij verschillende rotatiesnelheden en vulgraden. Vanuit dit perspectief verslaan wij hier een uitgebreide numerieke studie van menging en segregatie in een bed

van bidisperse granulaten in een horizontaal roterende trommel, de eenvoudigste geometrie met industriële relevantie.

Twee typen van segregatie kunnen optreden: snelle radiale segregatie, waarbij kleinere of massievere deeltjes zich ophopen langs de rotatie-as, en langzame axiale segregatie met volledig gescheiden banden van kleine en grote deeltjes, loodrecht op de roterende as, met in het algemeen deeltjesbanden van grote deeltjes bij de drum-uiteinden. Dit proefschrift behandelt zowel radiale als axiale segregatiefenomenen in een horizontaal roterende trommel.

Terwijl visualisaties van de granulaire bedden werden gebruikt als kwalitatieve methode om de menggraad te bepalen, is een meer kwantitatieve methode ontwikkeld op basis van de entropie van de verschillende systemen. Een maat voor het segregatieniveau van het systeem werd verkregen door het systeem in een rooster onder te verdelen, en door vervolgens per roostercel de mengentropie te berekenen, en dit te middelen voor het hele systeem. Door verschillende roosters (een 3D rooster, een set van 2D plakken loodrecht op de trommelas, of 2D staven evenwijdig aan de as) te gebruiken, konden verschillende vormen van segregatie onderscheiden worden.

De dynamica van radiale segregatie werd onderzocht in zeer korte quasi-2D trommels zonder noemenswaardige axiale segregatie. Zo werden er voor verschillende bidisperse systemen grafieken gegenereerd, die het menggedrag als functie van het Froude-getal  $Fr$  (dimensieloos toerental) visualiseren. Hieruit bleek dat, hoewel bijna alle systemen radiaal segregeren bij lage  $Fr$  (rolregime), en de meeste systemen geïnverteerde radiale segregatie vertonen bij hoge  $Fr$  (waterval- of centrifuge-regime), bij  $Fr \approx 0,56$  alle systemen radiaal mengen en dus niet segregeren. Dit is te begrijpen, wanneer een percolatiemechanisme aangenomen wordt: In de snel bewegende toplaag van het deeltjesbed in de trommel vallen kleinere deeltjes tussen de bewegende grotere deeltjes door, richting het centrum van het bed, zolang de trommelbeweging niet te snel is. Dit verschijnsel wordt geïnverteerd bij hoge draaisnelheden. Bij tussenliggende draaisnelheden neemt het onderscheidend vermogen van de stromende laag af vanwege de toenemende porositeit. De eventuele scheiding, die nog plaatsvindt, wordt teniet gedaan doordat bovengenoemde twee verschijnselen elkaar opheffen. Verrassend is dat het Froude-getal voor dit overgangsregime hetzelfde is voor alle onderzochte systemen.

Axiale segregatie wordt steeds voorafgegaan door radiale segregatie. Het is daarom logisch om ook axiale segregatie te onderzoeken. Daartoe zijn langere 3D-trommels bestudeerd waarin axiale segregatie zich kon ontwikkelen. Axiale segregatie werd in de meeste systemen gevonden. Het optreden van deze axiale segregatie blijkt vooral bepaald te worden door verschillen in deeltjesgrootte.

Middellange trommels vertoonden zeer verrassend dynamisch gedrag. De axiale segregatie ontwikkelde zich met oscillaties met lage en hogere frequenties. Hoewel de oscillaties met hogere frequenties kunnen worden opgevat als de ontwikkeling en migratie van gesegregeerde gebiedjes in het systeem, zijn de oscillaties met lage frequenties met een periode van 10 tot 20 omwentelingen niet eerder opgemerkt. Dit oscillerende gedrag hangt waarschijnlijk samen met het gebruik van middellange trommels, want het werd niet waargenomen bij zeer lange trommels. Wij schrijven de oscillaties toe aan de invloed van de trommeluiteinden, die de aangrenzende deeltjes blootstellen aan andere krachten dan de deeltjes midden in de trommel. Dit verschil induceert een axiale stroming in het systeem. De deeltjes grenzend aan de verticale wanden worden, door hun contact met deze bewegende wanden, hoger opgeheven dan de deeltjes ver van de verticale wanden. Dit creëert in axiale richting een hol profiel van het bovenoppervlak van de drumlading, waardoor de deeltjes (in het rolregime) van de verticale trommelwanden af bewegen richting het centrum van de trommel. Aangekomen in het centrum, zullen de deeltjes in hun verdere weg naar beneden terugvloeien richting de verticale wanden, aangezien het bedprofiel in het lagere deel van de stromende laag bol is.

Ook bij dit stromingsprofiel speelt het percolatiemechanisme een rol: kleinere deeltjes percoleren door de stromende laag van deeltjes en eindigen uiteindelijk dieper in het bed, terwijl de grotere deeltjes zich ophopen aan de bovenzijde van de stromende laag deeltjes, en vervolgens weer naar de verticale wanden gevoerd worden. Hierdoor zal de uiteindelijke configuratie onmiskenbaar een groot-klein-groot axiaal segregatiepatroon moeten hebben. Na verdere rotatie neemt echter de holling en daarmee de axiale snelheid van het stromende bed toe, leidend tot snelle oscillaties en een plotselinge menging van delen van de grote-deeltjesbanden met de kleine-deeltjesband. Dit resulteert in een stationaire configuratie, waarin een band van kleine deeltjes wordt gevormd onder banden met grote deeltjes. Vervolgens bouwt zich weer traag een driebands segregatie (groot-klein-groot) op, waarna de asymmetrie van de rusthoek verder toeneemt.

De configuratie waarbij grote deeltjes zich eindstandig ophopen aan de bovenkant van het bed gaat gepaard met een minimum aan energiedissipatie. Dit is niet het geval voor de systemen die radiaal of axiaal segregeren in drie zuivere banden.

Het gevonden effect betekent dat verticale eindwanden belangrijk zijn voor de dynamica van axiale segregatie. Dit effect is verder onderzocht door het variëren van de eigenschappen van de eindwand. De bovengenoemde snelle en trage oscillaties verdwijnen in systemen die gladdere eindwanden hebben, terwijl ook de snelheid van segregatie is afgenomen. Uiteindelijk leidden echter ook deze gladdere wanden tot eenzelfde type axiale segregatie in drie banden (groot-klein-groot). Verdere verlaging van de wrijving tot volmaakt gladde eindwanden veranderde het uiteindelijke segregatiepatroon tot een dubbelbands systeem. Systemen zonder eindwanden vertoonden alleen radiale segregatie in de onderzochte tijdspanne. We denken dat het ontbreken van axiale stroming de overgang van radiale segregatie naar axiale segregatie erg traag of zelfs onmogelijk maakt, ondanks het feit dat er nog steeds sprake is van een drijvende kracht voor axiale segregatie. De vorming van twee axiale banden verlaagt de energiedissipatie in het bed, terwijl noch radiale noch axiale segregatie in drie banden de vermogensopname reduceert bij constante hoeksnelheid.

Oscillatiegedrag op zich is al zeer relevant, maar bestudering hiervan stelt ons voorts in staat om enig licht te werpen op de fundamentele mechanismen die ten grondslag liggen aan segregatie, in het bijzonder de overgang van radiale naar axiale segregatie. Het feit dat dit niet alleen afhankelijk is van de eigenschappen van de granulaten, maar ook van de geometrie en het ontwerp van de trommel, impliceert dat deze bevindingen van nut kunnen zijn voor het ontwerp en bedrijven van industriële processen.

Enkele algemene richtlijnen zijn geformuleerd en geïllustreerd aan de hand van het praktijkvoorbeeld van het ontwerp van een sterilisatieproces voor kruiden en specerijen. Mengen is cruciaal in de huidige stoomsterilisatie; dit geldt des te meer voor een nieuw proces waarin zeolietkorrels worden gemengd met de kruiden. Deze zeolietkorrels adsorberen de stoom en dientengevolge warmen zij de kruiden op middels de vrijkomende adsorptiewarmte. Dit voorkomt de (ongewenste) bevochtiging van de kruiden, en bestaat bij de gratie van contactverwarming van specerijen en zeolieten. Een goede menging van de twee

materialen is echter een vereiste om lokale oververhitting van kruiden te voorkomen. De resultaten van dit proefschrift kunnen gebruikt worden om zich van een dergelijke werking te vergewissen, maar ook om segregatie tussen de twee typen granulaten op te wekken zodra de sterilisatie heeft plaatsgevonden.

---

## List of publications

**M. M. H. D. Arntz, W. K. den Otter, H. H. Beeftink, W. J. Briels and R. M. Boom.** Segregation by mass, radius and density of granular particles in a horizontal rotating drum. *Submitted for publication.*

**M. M. H. D. Arntz, W. K. den Otter, H. H. Beeftink, R. M. Boom and W. J. Briels.** End walls induce axial segregation in a horizontal rotating drum. *Submitted for publication.*

**M. M. H. D. Arntz, W. K. den Otter, H. H. Beeftink, R. M. Boom and W. J. Briels.** Repeated segregation and energy dissipation in an axially segregated granular bed. *Accepted for publication in Europhysics Letters.*

**M.M.H.D. Arntz, W.K. den Otter, H.H. Beeftink, P.J.T. Bussmann, W.J. Briels and R.M. Boom** Granular mixing and segregation in a horizontal rotating drum: a simulation study on the impact of rotational speed and fill level. *AIChE Journal*, 54 (12), 2008, p. 3133-3146

**J.L. van Roon, M.M.H.D. Arntz, Kalleberg A.I., Paasman M.A., Tramper J., Schroën C.G.P.H., and Beeftink H.H.** A multi-component reaction-diffusion model of a heterogeneously distributed immobilized enzyme, *Applied microbiology and biotechnology*, 72 (2), 2005, p. 263-278

**CONFERENCE PROCEEDINGS**

**M.M.H.D. Arntz et al.** The Mechanism behind Axial Segregation of Granules in a Horizontal Rotating Drum, *Proceedings of the 2007 AIChE Annual Meeting*, 2007

**M.M.H.D. Arntz et al.** Modelling Radial Mixing and Segregation in Rotating Drums: Effects of Process Parameters, *Proceedings of the 2006 AIChE Annual Meeting*, 2006

## Nawoord

Eindelijk. Ik ben in het stadium dat ik het nawoord kan typen! Dit hoofdstuk is natuurlijk bedoeld om mensen te bedanken. Ik wil dat graag doen op de manier waarop je een artikel hoort te schrijven: je beperken tot één heldere, duidelijke boodschap. In de praktijk betekent dit dat ik een ieder voor één ding bedank, namelijk datgene, waar ik het meest dankbaar voor ben, met andere woorden, hetgeen het meeste opviel. Maar ik ben iedereen natuurlijk voor veel meer dankbaar.

*Remko*, wat ik bijzonder waardeerde aan onze samenwerking was het vertrouwen dat je in me had. Door dit vertrouwen voelde ik mij vrij in het uitvoeren van mijn onderzoek. Ook leerde ik om zelf te vertrouwen op de resultaten uit mijn eigen onderzoek, zoals bijvoorbeeld de oscillaties in de ordeparameters in hoofdstuk 4. Jij geloofde meteen in de toegevoegde waarde van deze oscillaties, wat mij de energie gaf om er meteen in te duiken om verder te onderzoeken wat er nu precies aan de hand was.

*Wim*, wat ik hier niet onvermeld kan laten is natuurlijk het feit dat je me opgenomen hebt in de groep. Ik kwam voor een paar weken om te leren modeleren, maar ik bleef maar terugkomen, en steeds voor langere periodes! Die gastvrijheid was natuurlijk fantastisch en daar ben ik je erg dankbaar voor. Ik wijk voor deze ene keer toch af van het geven van één boodschap, maar dat zijn jullie inmiddels van me gewend. In dit stukje moet namelijk ook energiedissipatie genoemd worden. Zonder jou, *Wim*, zou ik nooit de energiedissipatie uitgerekend hebben. Deze resultaten hebben ons heel wat voor voor discussie geleverd!

*Wouter*, ik heb een ongelooflijke hekel aan het maken van plaatjes en aan het taaltechnisch verbeteren van artikelen. Jij wist me hierin echter erg goed aan te

vullen. Jouw nooit-aflatende consciëntieusheid zorgde er altijd voor dat ik inzag dat het bijvoorbeeld toch nodig was om nog een middag aan een plaatje te knutselen. Ook hier moet ik nog een aanvulling geven. Jij was namelijk degene die me thuis heeft gemaakt in het modeleren op zich en de DEM-methode. Ook kon ik altijd met mijn vragen bij je terecht. Hartstikke bedankt hiervoor.

*Rik*, mijn dank en bewondering gaan met name uit naar het feit dat je me altijd bent blijven steunen. Als ik links wilde en jij vond dat ik rechts moest gaan, ben ik meer dan eens toch links gegaan. Dat bleek dan soms dus de verkeerde keuze, en je hebt daarvan nooit achteraf gezegd: “Zie je nu wel.” In plaats daarvan was je net als daarvoor nog even bereid om te helpen; om te kijken wat een voor mij acceptabele manier was om alsnog naar rechts te gaan. Ik vind het erg prettig dat je nooit een oordeel hebt geveld over mijn besluiten.

*Marieke*, bedankt voor het altijd actief betrekken van mij bij de rest van de groep. Ook heb ik onze gesprekken altijd erg gewaardeerd. Ik hoop dat het je goed gaat in je nieuwe carrière!

*Coen, Floor en Paul*, bedankt voor jullie enthousiasme en kritische houding. Ik heb met veel plezier voortgangspresentaties gegeven en meegedacht over de experimenten en resultaten, die bij jullie in Apeldoorn plaatsvonden.

*Arjen*, bedankt dat je mij hebt voorgedragen voor dit promotieproject en voor het vertrouwen dat je daarmee in mij stelde.

*Ron en Jan-Harm*, ik vond het erg leerzaam én leuk om jullie te mogen begeleiden. Ik hoop dat jullie er met net zoveel plezier aan terugdenken als ik. Bedankt voor jullie interesse en inzet.

*Pieter en Gerrit*, bedankt voor het oplossen van alle PC-problemen. *Gerrit*, het feit dat je dit nawoord kunt lezen betekent dat het boekje af is, maar ook dat je waarschijnlijk al je externe harde schijven terughebt!

*Hedy, Joyce en Mirande*, dankzij jullie behulpzaamheid en gezelligheid werden zelfs vervelende klusjes aangenaam.

*Sebastiaan*, bedankt voor het begeleiden van de experimenten van *Ron* en alle probeersels, die ik wel eens heb willen uittesten op het lab.

Ook zijn er een aantal mensen, die ik lastig heb gevallen met Linux- of Matlab-vragen. Het is fijn dat ik bij al deze mensen terecht kon en graag zou ik ze hierbij dan ook willen bedanken: *Gerben, Hylke, Olivier, Koen* bedankt.

Ik heb aan mijn promotietijd natuurlijk ook nog vele andere leuke herinneringen overgehouden. Uiteraard wil ik al mijn kamergenoten (*Cynthia, Sandra, Hylke, Sebastiaan* en *Jasper*) en mijn andere Wageningse en Enschedese collega's waaronder uiteraard *Gerben, Alessandra, Amol, Nur* en *Rene* bedanken voor de leuke tijd: de spelletjesavonden, verjaardagsfeesten, congressen, carnavalsfeesten, etentjes of gewoon het wegtikken van wat biertjes. En niet te vergeten de lunchwandelingen. Deze zorgden niet alleen voor ontspanning, maar ik heb tijdens deze wandelingen ook collega's beter leren kennen. *Dione*, bedankt voor je vriendschap. Ik hoop dat ondanks de afstand onze vriendschap zal blijven voortduren.

Een belangrijke groep mensen wordt gevormd door mijn familie. Hun steun en de afleiding, waarvoor met name mijn neefjes (*Ruben, Julian* en later ook *Bjorn*) zorgden, maakten mijn promotietijd extra plezierig. Ook hier zou ik graag een voorbeeld willen noemen van de steun, die mijn familie mij heeft gegeven: het ziekbed van mijn paard *Marouschka*. Helaas is aan het einde van mijn promotie mijn paard, die erg belangrijk voor me is, ernstig ziek geworden. Gedurende het verblijf in een paardenkliniek heeft haar leven aan een zijden draadje gehangen. Nadat ze weer naar huis mocht, had ze nog steeds erg veel verzorging nodig, zoals zes tot acht keer per dag tien minuten met haar wandelen. Maar probeer maar eens een boekje te schrijven als je acht keer per dag naar je paard moet om te wandelen! Dit heen en weer gereis kostte mij erg veel tijd. Gelukkig stond mijn familie voor me klaar. *Mijn moeder*, ondanks dat ze doodsbang is voor paarden, heeft toch zeker drie wandelingen per dag op zich genomen. Ook mijn zussen *Esther* en *Judith*, *mijn vader* en *Frans* hebben, zodra ze in de gelegenheid waren, met haar gewandeld of haar verzorgd. *Mijn vader* heeft ons vaak naar Utrecht of Arnhem moeten brengen. Bedankt hiervoor *pap. Peter* ook jij bedankt voor het begeleiden van *Marouschka* naar de dierenarts in Arnhem.

Na dit paardenrelaas is het tijd om weer een duidelijker verband met de inhoud van dit boekje op te zoeken. *Esther* en *Judith*, ik vind het fantastisch dat jullie het podium met mij willen delen, bedankt dat jullie mijn paranimfen willen zijn. *Jos*, bedankt voor het ontwerpen van de kaft van het boekje. Deze is erg mooi

geworden. *Kris*, bedankt voor het lay-outen en *Rik* voor je hulp aan *Kris* bij het lay-outen.

*Kris*, ik weet dat je meer dan alleen het lay-outen van me hebt overgenomen. Jij hebt huishoudelijke taken uit mijn handen genomen en ons huis in Maastricht vrijwel in je eentje opgeknapt. Dankjewel voor de tijd, die hierdoor voor mij ontstond om aan mijn boekje te werken, maar vooral ook voor de tijd om samen leuke dingen te doen. Voor jou betekent het afronden van dit boekje denk ik bijna net zoveel als voor mij. Het afronden van dit boekje betekent een nieuwe periode voor ons, waarbij we ineens tijd over hebben. Haha, ik denk niet dat dat ooit bij ons het geval zal zijn. Jij hebt ons waarschijnlijk al voor een cursus Spaans opgegeven en weet ik veel wat nog meer. Ik heb er in ieder geval nu al zin in.

*Marleen*

## Curriculum vitae

Marleen Maria Helena Desiree Arntz was born July 2 1980 in Nijmegen, the Netherlands. In 1998 she successfully completed her secondary education at the Canisius College Mater Dei. Subsequently she commenced studying Chemical Engineering at the University of Twente, where she specialised in Process Technology. As part of this specialization she completed an internship on ammonium carbonate production with BASF AG in Ludwigshafen, Germany. After further specializing into Bioprocess Engineering, she concluded her MSc education in 2004 with a thesis on the enzymatic production of cefalexin, which was executed in close collaboration with the Wageningen University. Within a week she started a PhD project at the Food Process engineering group of Wageningen University in collaboration with the computational Biophysics group of the University of Twente on the subject of modelling particles segregation in a rotating drum, of which this dissertation is the result. Mid 2008 she accepted a research position at DSM in Geleen to develop new production processes for the manufacturing of super strong Dyneema<sup>®</sup> fibres. As of September 2010 she pursued her DSM career as scientist separation technology on the down stream processing of industrially produced antibiotics in Delft.

Marleen Maria Helena Desiree Arntz is op 2 juli 1980 geboren te Nijmegen. In 1998 heeft zij haar Atheneumdiploma behaald aan het Nijmeegse Canisius College Mater Dei. Vervolgens is zij Chemische Technologie gaan studeren aan de Universiteit Twente, waar zij zich specialiseerde in de Proceskunde. Als onderdeel van deze specialisatie heeft zij in 2002 een stage voltooid op het gebied van ammoniumcarbonaatproductie bij BASF AG te Ludwigshafen in Duitsland. Na een verdere specialisatie in de Bioproceskunde en een afstudeeropdracht over enzymatische cefalexineproductie, in samenwerking met de Wageningen Universiteit, heeft zij in 2004 haar ingenieursdiploma behaald.

Nog geen week later is zij begonnen aan een promotie-onderzoek bij de vakgroep Levensmiddelenproceeskunde van de Wageningen Universiteit, in samenwerking met de Computational Biophysics vakgroep van de Universiteit Twente, op het gebied van modellering van deeltjesontmenging in een roterende drum; dit proefschrift is daarvan het resultaat. Halverwege 2008 heeft zij een onderzoeksfunctie in Geleen geaccepteerd als procesontwerper voor de productie van de supersterke vezel Dyneema<sup>®</sup> van DSM. Sinds september 2010 heeft zij haar DSM carrière voortgezet als scheidingstechnoloog op het gebied van *down stream processing* in de industriële antibioticaproductie te Delft.



## Overview of completed training activities

### DISCIPLINE SPECIFIC ACTIVITIES

#### COURSES

- Granular Matter (JMBC, 2005)
- Bioreactor Design and Operation (VLAG, BSDL, 2004)
- A Unified approach to mass transfer (OSPT, 2004)
- Physical chemistry (Han-Sur-Less Winterschool, 2005, 2006)
- Reaction Kinetics in Food Science (VLAG, 2005)
- Particle based modeling of transport phenomena (OSPT, 2004)

#### CONGRESSES AND SYMPOSIA

- EUROTHERM Seminar 77 (2005)
- American Institute of Chemical Engineers Annual Meeting (2006,2007)
- Netherlands Process Technology Symposium (2004,2005,2006)

### GENERAL COURSES

- Cambridge Advanced English (CENTA,2005)
- Supervising and guiding a BSc/MSc thesis (OWU,2005)
- Vlag PhD week (VLAG, 2004)
- Career perspectives (WGS, 2007)
- Personal efficacy (WGS, 2006)
- PhD competence assessment (WGS, 2006)

### OPTIONALS

- PhD trip Process Engineering (WUR, 2004, 2006)





The research described in this thesis was financially supported through a grant from the Program Economy, Ecology and Technology (E.E.T.) by The Netherlands' Department of Economic Affairs, the Department of Public Housing, Spatial Planning and Environmental Protection, and the Department of Education, Cultural Affairs and Sciences.